Abstract

RAYE, JULIE KNOWLES. An electromagnetic interrogation technique utilizing pressure-dependent polarization. (Under the direction of H. T. Banks.)

This dissertation focuses on an interrogation technique that uses traveling acoustic wavefronts as a virtual reflector for an oncoming electromagnetic wave. Electromagnetic interrogation techniques in general have the potential for wide applicability in practical problems and this technique in particular enjoys that potential.

We begin by developing a viable model for pressure-dependent orientational (Debye) polarization. We then incorporate it into a one-dimensional Maxwell system to describe the electromagnetic/acoustic interaction.

This system may be generalized to include a wider class of electromagnetic behavior; we establish well-posedness, enhanced regularity, and convergence results for this general system.

Under the framework provided by the mathematical theory, we obtain computational results for sample forward and inverse problems relating to the interrogation technique. Our numerical algorithms for the forward problem involve finite difference approximations in time and finite element approximations with piecewise linear basis elements in space. Solving the inverse problem entails least squares minimization using a gradient-free Nelder Mead optimization routine.

Finally, as a first step in developing a model in which the pressure wave may be

modulated by the electromagnetic wave (unlike the one-way coupling in the model presented here), we consider the system describing an acoustic wave propagating through a layered medium. We derive a weak formulation for this system and present computational findings.

AN ELECTROMAGNETIC INTERROGATION TECHNIQUE UTILIZING PRESSURE-DEPENDENT POLARIZATION

BY

Julie Knowles Raye

A THESIS SUBMITTED TO THE GRADUATE FACULTY OF

NORTH CAROLINA STATE UNIVERSITY

IN PARTIAL FULFILLMENT OF THE

REQUIREMENTS FOR THE DEGREE OF

DOCTOR OF PHILOSOPHY

APPLIED MATHEMATICS

RALEIGH, NORTH CAROLINA

May 2002

APPROVED BY:

H. T. Banks	Kazufumi Ito
CHAIR OF ADVISORY COMMITTEE	
Michael Shearer	Hien T. Tran

To Kevin M. Short,
for at times knowing me better
than I know myself.

Biography

The author was born in Melrose, Massachusetts and grew up in the Monadnock Region of New Hampshire, attending Surry School, Cutler School, and Monadnock Regional High School. She graduated summa cum laude from the University of New Hampshire in 1997 with a bachelor of science degree in mathematics with University Honors. She then attended North Carolina State University in Raleigh where she received a PhD in applied mathematics in August of 2002. She has accepted a tenure-track assistant professor position in mathematics on the faculty at Virginia Commonwealth University in Richmond to start in the Fall of 2002.

Acknowlegements

This thesis is brought to you by the letters E and M.

One of the most gratifying aspects to finishing this dissertation is having the occasion to thank those who have helped make the work possible. I certainly could not have done it alone.

My advisor, Dr. H. T. Banks, has given enthusiasm, energy, and experience to this project, and the field of applied mathematics in general, from the beginning. He has provided me with countless professional opportunities that would have otherwise been unavailable. Moreover, he and his wife Sue Banks have provided a mathematical family for me and the rest of his students that has been a wonderful support system.

Dr. Richard Albanese, our colleague at Brooks Air Force base, has been a driving force behind this project. His zeal, curiosity, and expertise have enhanced this work in many ways, and I have been honored to work with him.

My committe members, Dr. Hien Tran, Dr. Kazi Ito, and Dr. Michael Shearer, have each taught me a great deal, both in the classroom and within the context of this research. I appreciate the time, effort, and interest they have expended on my behalf.

Over the course of the past five years, I have enjoyed funding from the Department of Education in the form of a GAANN Computational Science Fellowship and from the Air Force Office of Scientific Research under grants AFOSR F49620-98-1-0430 and AFOSR F49620-01-1-0026.

While completing his degree at NC State, Dr. Mike Buksas cleared the path for me and this research. I am grateful to him for the trail of bread (brownie?) crumbs he left behind, and for his continued support, sense of humor, and yes, cynicism.

While I was a student at UNH, Dr. Kevin Short and Dr. Kelly Black introduced me to the world of applied mathematics. If it weren't for their encouragement and attention, coupled with Kevin's telepathic powers, I am certain I would be on an entirely different, and likely less fulfilling, life path.

Dr. Ralph Smith has been invaluable as a teaching mentor, mathematical sounding board, and willing dog-walker. It would be difficult to find time for research if I had to make two trips around Johnson Lake, one for each dog.

Some of my closest friends, Amy Croteau, Emily Aldrich, Sherry Frost, Susann Westlake, and Elizabeth Robinson, have been very supportive of this undertaking, even though they don't quite comprehend my fascination with this "scary math" [Sherry]. Meanwhile, my colleagues-turned-friends who share and understand my interest in the subject, David Bortz, Mike Zager, Rebecca Segal, Jim Nealis, Brian Adams, Karen Klein, Cammey Cole, Laura Potter, Michele Joyner, and John Noland, have made this process fun (a word not normally associated with graduate school). I thank them all for their friendship.

My grandparents have been an almost incessant source of pride and generosity. I am appreciative of all that they do. They, and all of my family and friends, have been very understanding of the distance between North Carolina and New England; this patience has made my life much easier.

Throughout my life, my parents have been supportive of all of the choices I have made. Whether I had chosen to go to graduate school or join the circus, I would have had their unconditional love and pride and for that I am grateful.

Last but not least, I must thank Taliesin and Sidney for not eating this homework.

Table of Contents

List of Tables

List of Figures

Chapter 1

Introduction

Electromagnetic interrogation techniques have many potentially useful applications, especially in the fields of military and medicine. It might be possible to detect undergound mines and bunkers from the surface. Tanks and planes on the ground may be able to be "seen" from the air despite the presence of foliage. Tumorous tissue might be identifiable without surgery.

In [7], the authors focus on two different electromagnetic interrogation techniques. The first method relies on the assumption that the object of interrogation has a perfectly conductive (metal) backing. This backing can be an original part of the object, or it can be added for the purpose of interrogation. For example, in using the composition of an airplane's paint to determine its country of origin, the paint is the subject of interrogation and the plane shell acts as the metal backing. Alternatively, in the instance of tumor detection, a metal-tipped catheter could be inserted to serve as the perfect conductor. This perfectly conductive backing acts as a reflector for the interrogating electromagnetic waves. An electromagnetic wave pulse is launched through the object under interrogation. When the wave pulse makes contact with the perfectly conductive backing, the wave is reflected and travels back toward the point of initiation. Data is collected from the reflected waves and is used to identify

dielectric and geometric characteristics of the interrogated object.

Often it is not practical, or even possible, for a perfect conductor to be situated behind the interrogated object. In these cases another approach is needed. In this technique, the second described in [7], one requires that a standing acoustic wave (one that varies only in time) is present behind the object. This wave can occur naturally, such as a pressure wave in the human body, or can be introduced as part of the method, for example by creating a subsurface explosion in the context of underground interrogation. Experimental observation has shown that this standing wave can act as a virtual reflector for the electromagnetic wave pulse. Thus this approach is similar to the previous one; here the acoustic wave replaces the backing. The assumption that the standing wave is confined to one spatial position at the back boundary of the object limits this method. To overcome this limitation, one can use a traveling acoustic wave that varies both temporally and spatially. This is advantageous because the reflecting interface can be moved back and forth in the material. The variable positioning facilitates the assessment of material uniformity [7].

This thesis treats an electromagnetic interrogation technique that uses a traveling acoustic wave as a virtual reflector for the interrogating electromagnetic wave pulse. We begin with the basic electromagnetic model formulated in [7] and incorporate a model that describes the electromagnetic/acoustic interaction. In the development of the model, we discuss interaction models found in the literature, including those found in [39] and [22]; we then proffer a new model for the interaction of the electromagnetic and acoustic waves. This model features modulation of the material polarization by the pressure wave and thus the behavior of the electromagnetic pulse. This assumption is based on ideas found in [2], [42], and [23] among others, and incorporated into our system via a pressure-dependent Debye model for orientational polarization. The model for the pressure-dependent electromagnetic system is motivated and described

in Chapter 2.

Once a model has been formulated to describe the physical dynamics of the system, it must be investigated from a mathematical perspective, both theoretically and computationally. In Chapter 4, we detail the numerical methods used to compute approximate solutions for the system, present sample numerical solutions, and discuss the behavior of the solutions relative to the pressure-dependent polarization parameters. In order to trust these numerical approximations, we need to know that the underlying mathematical system is well-posed. That is, a unique solution to the system exists and depends continuously on initial data. These issues are addressed in Chapter 3.

For the electromagnetic interrogation technique to be successful, we must be able to identify dielectric properties of the interrogated material from the observed wave reflections. In Chapter 5, we discuss a proof of concept parameter estimation problem in which we estimate model parameters from simulated data. Eventually, we will attempt to approximate the values of these parameters from actual experimental data. As a first step, we use data consisting of numerical simulations from the mathematical model with added random noise. If we have excessive difficulties estimating the parameter values from this data directly related to our model, we do not expect to be able to estimate them from experimental data.

Since the work presented in this thesis relies on the electromagenetic/acoustic interaction, it is imperative that the pressure-dependence of our model be significant. In Chapter 6, we examine the significance of the pressure-dependent terms in our model from a statistical perspective.

The work presented in Chapters 2-6 assumes that the acoustic pressure wave is specified *a priori*. In some contexts, especially if we were to assume modification of the pressure wave by the electromagnetic field, it may be useful to solve the acoustic wave equation to obtain the pressure dynamics. Solutions of these type are discussed in

Chapter 7.

Finally we offer some concluding remarks and directions for future work in Chapter 8.

Chapter 2

The model

2.1 Problem formulation

In this section, we specify the electromagnetic interrogation problem under consideration. The geometry of the problem is shown in Figure 2.1. We consider a region $\tilde{\Omega}$ divided in two by an interface Γ; one region Ω_0 is comprised of air and the other Ω is comprised of a dielectric material (mud or living tissue, for example). We launch a right-traveling electromagnetic wave pulse into the air at the boundary Γ_0. As it travels, the pulse crosses the interface Γ and passes into the dielectric medium in the region Ω. At the air/dielectric interface some of the pulse may be reflected back into the region Ω_0, but most of the wave is transmitted into the dielectric. Meanwhile, an acoustic pressure wave is traveling toward the electromagnetic wave in Ω but in the opposite direction. We note that the pressure wave travels at a much slower speed than the electromagnetic wave. In the dielectric material Ω, the two oncoming waves meet. This wave interaction causes some electromagnetic waves to be reflected back to the left, but the majority continue to travel toward the right boundary Γ_1. We assume that the effect of the interaction on the pressure wave is negligible (page 810, [39]). The right-traveling electromagnetic waves pass through the dielectric until

they reach the boundary Γ_1 which is assumed to be perfectly conductive. At the same time, the electromagnetic waves traveling in the opposite direction propagate through the dielectric, cross the air/dielectric interface Γ (where again some of the energy is transmitted and some is reflected), and passes through the air in the region Ω_0 until they are absorbed at the boundary Γ_0. We infer information about the dielectric and its properties from these wave reflections that reach Γ_0.

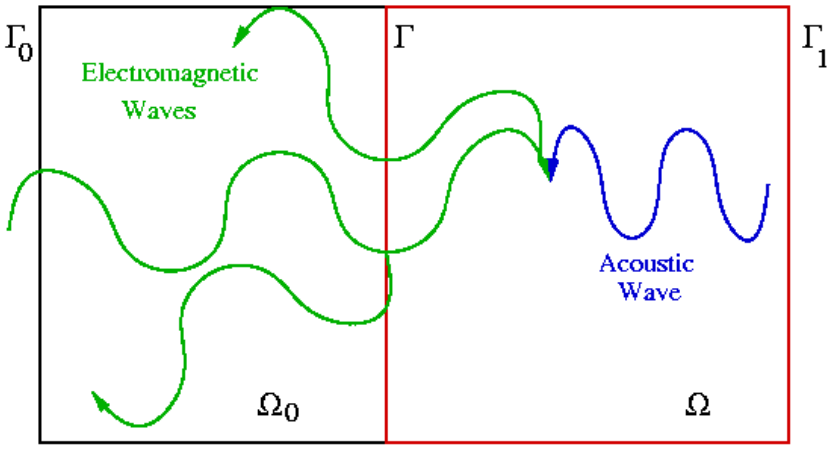

Figure 2.1: Schematic diagram of general geometry

In order to formulate this problem mathematically, we must make some further assumptions. We assume that the electromagnetic fields within the entire region $\tilde{\Omega}$ are governed by Maxwell's equations. For a vector $\vec{x} \in \tilde{\Omega}$, we have

$$\begin{aligned} \nabla \times \vec{E} &= -\tfrac{\partial}{\partial t}\vec{B} \\ \nabla \times \vec{H} &= \tfrac{\partial}{\partial t}\vec{D} + \vec{J} \\ \nabla \cdot \vec{D} &= 0 \\ \nabla \cdot \vec{B} &= 0 \end{aligned} \qquad \begin{aligned} \vec{D} &= \epsilon_0 \vec{E} + \vec{P} \\ \vec{B} &= \mu_0 \vec{H} + \mu_0 \vec{M} \\ \vec{J} &= \vec{J}_c + \vec{J}_s. \end{aligned}$$

In these equations, $\vec{E}$ and $\vec{H}$ denote the electric and magnetic field strengths, while the electric and magnetic flux densities are denoted by $\vec{D}$ and $\vec{B}$, and the electric and magnetic polarizations are denoted by $\vec{P}$ and $\vec{M}$. The function $\vec{J}$ represents the total current, comprised of both the conduction current $\vec{J}_c$ and the source current $\vec{J}_s$.
The polarizations and the conduction current describe the material response to the electromagnetic fields; thus the quantities $\vec{P}, \vec{M}$, and $\vec{J}_c$ depend on $\vec{E}$ and $\vec{H}$. These relationships are defined by constitutive laws. We assume that the region containing air, Ω_0, has zero conductivity and polarization, i.e., $\vec{J}_c = 0$, $\vec{M} = 0$, and $\vec{P} = 0$ in Ω_0, and that the source current $\vec{J}_s$ is zero in this region as well. Meanwhile, we suppose that the dielectric material in Ω is such that we can ignore any magnetic effects and assume Ohmic conductivity. That is, for $\vec{x} \in \Omega$

$$\begin{aligned} \vec{M}(\vec{x}) &= 0 \\ \vec{J}_c(\vec{x}) &= \sigma \vec{E}(\vec{x}). \end{aligned}$$

One way [26] to model the electric polarization $\vec{P}$ is with a general integral equation so that the polarization is precisely dependent on the past behavior of the electric field. This type of equation can be used to model such behavior as orientational polarization, atomic polarization, and electronic polarization, as well as other polarization mechanisms that depend on frequency [7]. The equation is given by

$$\vec{P}(t,\vec{x}) = \int_0^t g(t-s,\vec{x})\vec{E}(s,\vec{x})\ ds, \tag{2.1}$$

where the function g is the polarization susceptibility kernel. The kernel function g may take many forms depending on the type of polarization modeled. We discuss the kernel in more detail, as well as its relation to the electromagnetic/acoustic interaction, in Section 2.3. We note that the general model automatically yields the initial condition $\vec{P}(0,\vec{x}) = 0$. To account for instantaneous polarization which depends on the immediate strength of the electric field, the kernel g must include a delta function. To avoid the resulting mathematical complications, we instead use an equivalent formulation. We assume that the polarization has two components, the instantaneous component $\vec{P_i}$ and the history-dependent component $\vec{P}$. We let the history-dependent component be as given in (2.1), and we assume that the instantaneous component is proportional to the electric field

$$\vec{P_i} = \epsilon_0 \chi \vec{E},$$

where χ is a constant of proportionality. Thus

$$\begin{aligned} \vec{D} &= \epsilon_0\vec{E} + \epsilon_0\chi\vec{E} + \vec{P} \\ \vec{D} &= \epsilon_0(1+\chi)\vec{E} + \vec{P} \\ \vec{D} &= \epsilon_0\epsilon_r\vec{E} + \vec{P} \end{aligned} \tag{2.2}$$

where $\epsilon_r = 1 + \chi$ is the relative permittivity and $\vec{P}$ is given by (2.1). We point out that ϵ_r can vary spatially to account for different instantaneous polarization effects in different locations.

It is worthwhile to note that not all polarization models can be written in the form of equation (2.1). In Section 2.3, we introduce some polarization models that cannot

be expressed in this form.

2.2 The electromagnetic wave

In this section, we state additional assumptions about the system and discuss the implications.

In the description of the problem in Section 2.1, we do not discuss the source current $\vec{J}_s$ in detail. However, the choice of source current can have significant impact on the problem formulation. For this problem, we choose to use a windowed microwave pulse emitted from an exterior attenna in Ω_0. We specify that this pulse consists of a polarized plane wave so that the signal produced has nontrivial components of $\vec{E}$ and $\vec{H}$ in only one dimension in Ω_0. Moreover, we assume that the entire region $\tilde{\Omega}$ is infinite and homogeneous in the planes orthogonal to the direction of wave propogation. In particular, we suppose that the signal is normally incident to faces in the xy-plane and that an infinite (in the x and y directions) slab of air lies between $z = 0$ and $z = z_1$ and an infinite slab of dielectric material lies between $z = z_1$ and $z = 1$. Under these assumptions, we may conclude that the electric and magnetic fields are parallel to the $\hat{i}$ and $\hat{j}$ axes respectively at all points in Ω_0, and both fields are homogeneous in x and y in Ω_0. For this problem, these properties of the electric field apply to $\vec{P}$ and $\vec{D}$ via their dependence on $\vec{E}$. Moreover, the uniformity of the dielectric material in x and y implies that these conclusions hold throughout $\tilde{\Omega}$. So for any $\vec{x} \in \tilde{\Omega}$, the notation

$$\begin{aligned} \vec{E}(t,\vec{x}) &= \hat{i}E(t,z) \\ \vec{H}(t,\vec{x}) &= \hat{j}H(t,z) \\ \vec{P}(t,\vec{x}) &= \hat{i}P(t,z) \\ \vec{D}(t,\vec{x}) &= \hat{i}D(t,z). \end{aligned} \tag{2.3}$$

applies.

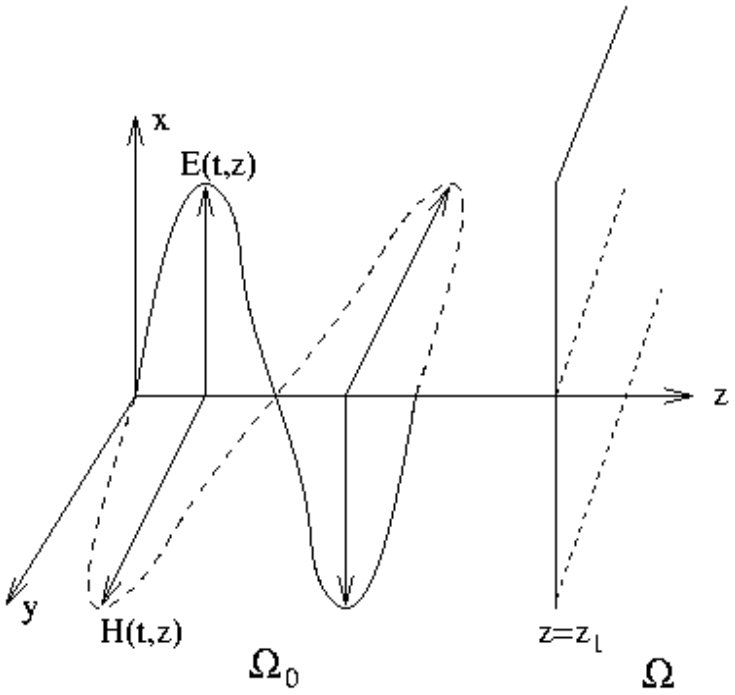

Figure 2.2: Schematic diagram of simplified geometry

These assumptions allow us to profoundly simplify the Maxwell's equations given in Section 2.1. For a vector function dependent only on z, i.e., $\vec{F}(\vec{x}) = \vec{F}(z)$, we have

$$\nabla \times \vec{F} = -\frac{\partial}{\partial z} F_y \hat{i} + \frac{\partial}{\partial z} F_x \hat{j}.$$

Using this simplification as well as the aforementioned assumptions, the first two of Maxwell's equations become

$$\frac{\partial}{\partial z} E = -\mu_0 \frac{\partial}{\partial t} H \tag{2.4}$$

$$-\frac{\partial}{\partial z} H = \frac{\partial}{\partial t} D + \sigma E + J_s. \tag{2.5}$$

Moreover, we note that the functions D and $B = \mu_0 H$, written in the form (2.3), automatically satisfy the final two Maxwell's two equations. By taking a spatial derivative of (2.4) and a time derivative of (2.5), we can remove the magnetic field from the equations. In addition, we can use the relationship

$$D = \epsilon_0(1 + (\epsilon_r - 1)I_\Omega)E + P = \epsilon_0 \tilde{\epsilon}_r E + P,$$

with $\tilde{\epsilon}_r \equiv 1 + (\epsilon_r - 1)I_\Omega$ where I_S is the indicator function for a set S. We note that this expression for D agrees with (2.2) for points in Ω. These steps lead to the equation

$$\mu_0 \epsilon_0 \tilde{\epsilon}_r \ddot{E} + \mu_0 \ddot{P} + \mu_0 \sigma \dot{E} - E'' = -\mu_0 \dot{J}_s, \tag{2.6}$$

which will be our primary focus. Here and throughout, we use $\dot{E}$ to denote $\frac{\partial}{\partial t} E$ and E' to denote $\frac{\partial}{\partial z} E$.

We assume that initially the system is at rest, i.e.,

$$\begin{aligned} E(0,z) &= 0 & P(0,z) &= 0 \\ \dot{E}(0,z) &= 0 & \dot{P}(0,z) &= 0. \end{aligned}$$

We next formulate our boundary conditions. No reflections occur at $z = 0$; we express this with the equation

$$\dot{E}(t,0) - cE'(t,0) = 0$$

where $c^2 \equiv \frac{1}{\epsilon_0 \mu_0}$. At the boundary $z = 1$, we assume there is a perfectly conductive backing. This assumption is made primarily to facilitate computations; the physical implication of such a boundary condition will not be exploited. In three dimensions, a perfectly conductive boundary is modeled by the two equations

$$\begin{aligned} \vec{E} \times \hat{n}|_{\vec{x} \in \Gamma_1} &= 0 \\ \vec{B} \cdot \hat{n}|_{\vec{x} \in \Gamma_1} &= 0. \end{aligned}$$

With the simplified geometry of our problem, these boundary conditions simplify as well. The unit normal is given by $\hat{n} = \hat{k}$, so that $\vec{B} \cdot \hat{n} = B(t,z)\hat{j} \cdot \hat{k} = 0$ is automatically satisfied. Moreover, $\vec{E} \times \hat{n} = E(t,z)\hat{i} \times \hat{k} = -E(t,z)\hat{j}$, so that $\vec{E} \times \hat{n} = 0$ at $z = 1$ becomes $E(t,1) = 0$.

Finally we again consider the source current. We assume previously that the source current is a windowed microwave pulse consisting of a polarized plane wave and that the emitted signal is incident normal to the xy plane. As in [7], we choose a windowed sine wave that is launched at $z = 0$. The form of this wave is given by

$$J_s(t,z) = \delta(z) g_s(t) I_{(0,t_f)} = \delta(z) \sin(\omega t) I_{(0,t_f)},$$

where ω is the frequency of the input signal and $\delta(z)$ is the usual Dirac delta function centered at $z = 0$. To guarantee continuity in t of J_s, we choose t_f so that $g_s(t_f) = \sin(\omega t_f) = 0$. If more smoothness is desired in J_s, the windowing indicator function $I_{(0,t_f)}$ can be replaced by a smoother function.

By choosing a windowed sine wave, we ensure that the pulse has a finite duration. This allows us to distinguish between reflections from the air/dielectric interface $z = z_1$, reflections from the pressure wave, and reflections from the back boundary.

2.3 The electromagnetic/acoustic interaction

The previous two sections deal with the electromagnetic wave and the acoustic pressure wave individually as separate entities. However, our electromagnetic interrogation technique relies on the assumption that the two systems interact – and that the interaction results in the reflection of the electromagnetic wave. In this section, we develop a model for the electromagnetic/acoustic wave interaction. We begin by discussing several interaction models found in the literature. We then discuss the polarization model on which our interaction model is based and finally present our model.

2.3.1 A survey of interaction models found in the literature

We begin our survey of electromagnetic/acoustic interaction models found in the literature by noting that there are various ways to address this issue and not all are equivalent. We use interchangeably the notation used by the original authors (e. g., $\ddot{E}$ and $\frac{\partial^2 E}{\partial t^2}$ are the same) to facilitate cross-referencing. We first consider the model in [7]. The authors assume that the dielectric material obeys the generalized pressure-dependent polarization rule

$$\frac{1}{\epsilon_0}\frac{\partial^2 P}{\partial t^2} = f_0(p)E + f_1(p)\frac{\delta E}{\delta t} + f_2(t)\frac{\delta^2 E}{\delta t^2}$$

and make the simplification

$$f_0(p) = 0, \quad f_1(p) = 0, \quad f_2(p) = \chi_0 + \kappa p(t, z).$$

This reduces the model to

$$\frac{1}{\epsilon_0}\frac{\partial^2 P}{\delta t^2} = (\chi_0 + \kappa p(t, z))\,\frac{\partial^2 E}{\delta t^2} \tag{2.7}$$

which is used with standing acoustic waves in both [7] and [13].

We point out that this model is a model of instantaneous polarization, and not of the form of (2.1) described in Section 2.1. Nonetheless, the model (2.7) can be used to replace $\ddot{P}$ in (2.6) to create a pressure-dependent electromagnetic system.

Next, we look at an alternate approach to modeling the electromagnetic/acoustic interaction. The authors of [39] begin with the electromagnetic wave equation

$$\nabla^2 \vec{E} - \frac{1}{c^2}\frac{\partial^2}{\partial t^2}\vec{E} = 0.$$

We note that in one dimension this is equivalent to (2.6) with $\tilde{\epsilon}_r = 1$, and no polarization, conduction, or source terms. They then suggest that a change in pressure will produce a change in the index of refraction; they describe this perturbation in the refraction index in terms of a variation in the dielectric constant $\delta\epsilon/\epsilon_0$. This leads to the following equation

$$\nabla^2 \vec{E} - \frac{1}{c^2}\frac{\partial^2}{\partial t^2}\vec{E} = \frac{\delta\epsilon/\epsilon_0}{c^2}\frac{\partial^2}{\partial t^2}\vec{E}. \tag{2.8}$$

Reducing equation (2.8) to one dimension, we see that it can also be written in the form of (2.6), this time with $\tilde{\epsilon}_r = 1$, no conduction or source terms and

$$\mu_0 \ddot{P} = \frac{\delta\epsilon}{\epsilon_0}\ddot{E}.$$

The dielectric constant ϵ can be thought of as a function of the pressure and entropy of the system, $\tilde{P}$ and S respectively. Thus

$$\delta\epsilon = \frac{\partial\epsilon}{\partial\tilde{P}}\delta\tilde{P} + \frac{\partial\epsilon}{\partial S}\delta S.$$

If the system is assumed to be at constant entropy, this reduces to

$$\delta\epsilon = \frac{\partial\epsilon}{\partial\tilde{P}}\delta\tilde{P}.$$

which can then be used in (2.8) to obtain

$$\nabla^2\vec{E} - \frac{1}{c^2}\frac{\partial^2}{\partial t^2}\vec{E} = \frac{1}{c^2}\frac{1}{\epsilon_0}\frac{\partial\epsilon}{\partial\tilde{P}}p\frac{\partial^2}{\partial t^2}\vec{E}, \tag{2.9}$$

where $p = \delta\tilde{P}$ is the pressure variation. We note that if $\frac{\partial\epsilon}{\partial\tilde{P}}$ is constant, the polarization model in (2.9) is of the same form as (2.7) with $\chi_0 = 0$. This implies that this too is a model of instantaneous polarization.

An approach similar to that in [39] is found in [22]. The author considers the case where light is scattered due to fluctuations in the dielectric constant and assumes that these fluctuations are the result of fluctuations in thermodynamic variables, such as pressure, within the system. We follow his arguments to present a macroscopic view of the problem. This begins with the assumption that the scattered field $\vec{E}$ is described by the equation (after conversion from gaussian to MKS units)

$$\nabla^2\vec{E} - \frac{n^2}{c^2}\ddot{\vec{E}} = \frac{\epsilon_0}{c^2}\ddot{\vec{P}}, \tag{2.10}$$

where n is the index of refraction. We note that in one dimension this can be written as

$$\frac{n^2}{c^2}\ddot{E} - E'' = -\frac{\epsilon_0}{c^2}\ddot{P}, \tag{2.11}$$

which is equivalent to equation (2.6) with $\tilde{\epsilon}_r = n^2$ and no conduction or source terms. We then let $\Delta\epsilon$ be a fluctuation in the dielectric constant and $\Delta\chi$ be a fluctuation in electric susceptibility. Since

$$\epsilon = \epsilon_0(1 + \chi),$$

it follows that

$$\Delta\chi = \frac{1}{\epsilon_0}\Delta\epsilon.$$

We next suppose that the polarization due to the fluctuation is given by

$$\vec{P} = \Delta\chi\vec{E}_0 = \frac{1}{\epsilon_0}\Delta\epsilon\vec{E}_0, \tag{2.12}$$

where $\vec{E}_0$ is the incident optical field.

We further assume that density and temperature, ρ and T, are the independent thermodynamic variables in order to represent the dielectric constant fluctuation as

$$\Delta\epsilon = \left(\frac{\partial\epsilon}{\partial\rho}\right)\Delta\rho + \left(\frac{\partial\epsilon}{\partial T}\right)\Delta T.$$

Under assumption that the dielectric constant has a stronger dependence on density than on temperature [22], we can approximate this relationship by

$$\Delta\epsilon = \left(\frac{\partial\epsilon}{\partial\rho}\right)\Delta\rho. \tag{2.13}$$

If we then treat the density as dependent on pressure and entropy, p and s (which are now the independent thermodynamic variables), we find that the fluctuation in density can be written

$$\Delta\rho = \left(\frac{\partial\rho}{\partial p}\right)\Delta p + \left(\frac{\partial\rho}{\partial s}\right)\Delta s.$$

Finally since our main interest is the scattering due to variations in acoustic pressure, as opposed to entropy, we neglect the second term and consider the relationship

$$\Delta\rho = \left(\frac{\partial\rho}{\partial p}\right)\Delta p. \tag{2.14}$$

Using relations (2.13) and (2.14) in equation (2.12), we obtain

$$\vec{P} = \frac{1}{\epsilon_0}\frac{\partial\epsilon}{\partial\rho}\frac{\partial\rho}{\partial p}\Delta p\vec{E}_0,$$

which can then be used in equations (2.10) or (2.11). We note that this results in an equation very similar to (2.9).

2.3.2 Our pressure-dependent polarization model

Before we introduce our model for pressure-dependent polarization, we provide the motivation behind it. We begin by discussing polarization in general and then explain how it pertains to our problem.

Mechanisms of polarization

Electric polarization is by definition the electric dipole moment per unit volume. The formation of these electric dipoles can be caused by several mechanisms [2], [4] which we briefly summarize here.

Electronic polarization/ Optical polarization/ Induced polarization An applied field displaces the electron cloud center of an atom with respect to its nucleus. This induces a dipole moment. Electronic polarization is found in both materials that possess molecules with large dipole moments (polar materials) and those that do not (nonpolar materials).

Atomic polarization/ Ionic polarization/ Molecular polarization An applied electric field may displace the atoms in the molecules, changing the

distance between the atoms, and thus changing the dipole moment. Atomic polarization only occurs in polar materials.

Orientational polarization/ Dipole polarization Without an applied field, a polar material possesses permanent dipole moments that are randomly oriented. When a field is applied, these dipoles align themselves with the field. Since orientational polarization is reliant upon the existence of permanent dipole moments, it only is found in polar materials.

Interfacial polarization The impurities and defects in crystal can impede the flow of charge created by an applied field. The resulting charge accumulation can result in a dipole moment. This type of polarization is found only in crystals.

The multiple names for each type of polarization can be confusing, especially when comparing the research of different contributors. We attempt to refer to each mechanism by the first name given above. We point out that in addition to this terminology both atomic and electronic polarization are sometimes referred to as distortional polarization [2].

In a given material, polarization can be the result of one or more of these four mechanisms. We are primarily interested in materials that contain a high water-content, such as living tissue or mud, so here we focus on polar liquids. The polarization in this class of liquids tends to depend mostly on the orientation of permanent electric dipoles in the molecules (orientational polarization) and the distortion of the molecules by an applied electric field (electronic and atomic polarization) [29]. With this in mind, we focus on these polarization mechanisms in the remainder of our discussions.

In the presence of most applied electric fields, the polarization of a high water-content liquid is both distortional and orientational. At high (optical) frequencies however, the electric field oscillates so rapidly that it does not hold any orientation long enough

for the dipoles to align with it. Thus, the orientational polarization is virtually insignificant [42]. This implies that at sufficiently high frequencies, the only contribution to the dielectric constant or optical index of refraction is from electrical distortion [29].

Since the polarization of a polar liquid has multiple mechanisms, we expect that a complete model must incorporate them all. Orientational polarization is suggestive of a mechanism with an exponential decay factor, such as the one in the model proposed by Debye [2]. However, a system rarely conforms exactly to the model described by the Debye dispersion equations due to the fact that the polarizational decay may not be represented accurately by a mechanism with one relaxation time [30]. On the other hand, distortional polarization causes charges to behave somewhat like linear harmonic oscillators; thus it is reasonable to model them as such (the Lorentz model is an example). Neither of these types of models alone will be sufficient to completely describe the polarization of a polar liquid. Nonetheless as a first step and to illustrate our ideas, we base our model on the Debye model for orientational polarization. Future modeling attempts will require systems of more complexity.

The Debye model

The Debye model [7] can be represented by the first order ordinary differential equation

$$\tau \dot{P} + P = \epsilon_0(\epsilon_s - \epsilon_\infty)E, \tag{2.15}$$

or by

$$P(t,z) = \int_0^t g(t-s,z)E(s,z)\, ds$$

with kernel

$$g(t) = \exp\left(\frac{-t}{\tau}\right)\frac{\epsilon_0(\epsilon_s - \epsilon_\infty)}{\tau}.$$

In these equations, ϵ_s is the static relative permitivitty and ϵ_∞ is the value of permittivity for an extremely high ($\approx$ infinite) frequency field. In this model, the value of the relative permittivity ϵ_r of (2.2) in the dielectric is given by ϵ_∞; that is, $\epsilon_r = 1$ in $[0, z_1]$ and $\epsilon_r = \epsilon_\infty$ in $(z_1, 1]$. The variable τ is the relaxation time of the dielectric.

In [2], Anderson describes a potential double well formulation for an atomic model that leads to the Debye polarization model. In this model, the dielectric is made up of independent noninteracting particles; each particle has two equilibrium positions separated by a barrier of high potential. One considers a charged particle with two equilibrium positions A and B located a distance d from each other. Between them is a potential barrier W such that $W \gg k_B T$ where k_B is the Boltzmann constant and T is the temperature. (See Figure 2.3.) If there is no electromagnetic field present, one assumes that the particle oscillates about either equilibrium, and on occassion, obtains enough energy to cross the potential barrier and jump into the other well. Over time, for constant temperature, the particle is near A as often as near B and the probability of finding the particle near a given well is $\frac{1}{2}$.

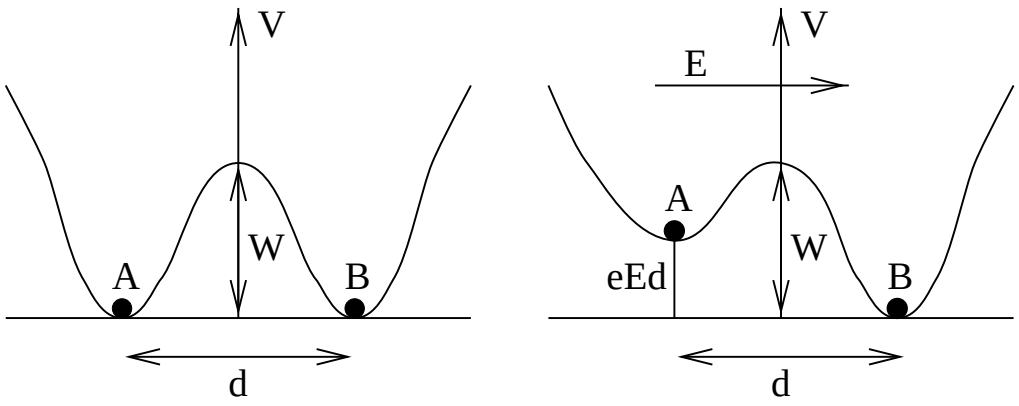

Figure 2.3: Potential double well model with and without an applied field

When an electric field E is applied in the direction from A to B, the potentials at each equilibrium are no longer equal, for instance $V_A > V_B$, and

$$V_A - V_B = edE,$$

where e is the charge of the particle. (See Figure 2.3.) A result from Boltzmann statistics implies that the probability that a particle has potential V is proportional to $\exp(-\frac{V}{k_B T})$, so that now it is more likely to find the particle near equilibrium B. As before, a particle can jump from one equilibrium to the other if it acquires enough energy. For a potential barrier W, the probability that a particle can cross this barrier in the direction from B to A is proportional to $\exp(-\frac{W}{k_B T})$, with proportionality constant $\frac{w_0}{2\pi}$, the assumed frequency of oscillation due to thermal agitation of the particle about the equilibrium. Likewise, the probability that the particle can cross the barrier in the direction from A to B is given by $\frac{w_0}{2\pi}\exp(-\frac{W-edE}{k_B T})$. Using these probabilities and the fact that the total number $N = N_A + N_B$ of particles is constant, one can derive [2] (see also page 387 of [26]) a linear first order differential equation to describe the difference $N_B(t) - N_A(t)$ in the number of particles in wells B and A at any time t

$$\frac{d}{dt}(N_B(t) - N_A(t)) =$$

$$\frac{w_0}{\pi}\exp\left(-\frac{W}{k_B T}\right)\left(-(N_B(t) - N_A(t)) + \frac{ed}{2k_B T}NE\right).$$

The polarization $P(t)$ due to the applied electromagnetic field is proportional to $N_B(t) - N_A(t)$. By relating τ with $\frac{w_0}{\pi}\exp\left(-\frac{W}{k_B T}\right)$ and $\epsilon_s - \epsilon_\infty$ with $\frac{w_0}{\pi}\exp\left(-\frac{W}{k_B T}\right)\frac{ed}{2k_B T}N$, one thus arrives at the Debye model (2.15) from atomic considerations.

There is substantial reason to believe that the behavior described by the Debye model is pressure-dependent. One approach to understand this pressure-dependence is to

extend the above arguments and consider the polarization from a non-equilibrium thermodynamics perspective. A discussion of this nature is given in [35].

We however take a different approach to incorporating pressure-dependence into the Debye model. We present the model here and provide motivation in Section 2.3.2. We begin by assuming that the material-dependent parameters in the differential equation (2.15) depend on pressure, i.e.,

$$\tau(p)\dot{P} + P = \epsilon_0(\epsilon_s(p) - \epsilon_\infty(p))E = \epsilon_0(\gamma(p) - \zeta(p))E.$$

We suppose as a first approximation that each of the pressure-dependent parameters can be represented as a mean value plus a perturbation that is proportional to the pressure

$$\begin{aligned} \tau(p) &= \tau_0 + \tilde{\tau} = \tau_0 + \kappa_\tau p \\ \gamma(p) &= \gamma_0 + \tilde{\gamma} = \gamma_0 + \kappa_\gamma p \\ \zeta(p) &= \zeta_0 + \tilde{\zeta} = \zeta_0 + \kappa_\zeta p. \end{aligned}$$

Then the equation

$$\tau(p)\dot{P} + P = \epsilon_0(\gamma(p) - \zeta(p))E$$

can be written

$$(\tau_0 + \kappa_\tau p)\,\dot{P} + P = \epsilon_0\,(\gamma_0 - \zeta_0 + (\kappa_\gamma - \kappa_\zeta)p)\,E. \tag{2.16}$$

We recall that the polarization term in (2.6) involves second-order time derivatives. To express (2.16) in a compatible form, we take the time derivative of both sides to obtain

$$\ddot{P} = -\frac{(1+\kappa_\tau \dot{p})}{(\tau_0+\kappa_\tau p)}\dot{P} + \frac{\epsilon_0\left(\gamma_0-\zeta_0+(\kappa_\gamma-\kappa_\zeta)p\right)}{(\tau_0+\kappa_\tau p)}\dot{E} + \frac{\epsilon_0\left(\kappa_\gamma-\kappa_\zeta\right)\dot{p}}{(\tau_0+\kappa_\tau p)}E \tag{2.17}$$

with

$$\dot{P} = -\frac{1}{(\tau_0+\kappa_\tau p)}P + \frac{\epsilon_0\left(\gamma_0-\zeta_0+(\kappa_\gamma-\kappa_\zeta)p\right)}{(\tau_0+\kappa_\tau p)}E. \tag{2.18}$$

From here, we can use (2.18) in (2.17) and then replace $\ddot{P}$ in (2.6) with the expression given by (2.17).

Additionally, we should note that the relation $\epsilon_r = \epsilon_\infty$ in $(z_1, 1]$ becomes $\epsilon_r = \epsilon_\infty(p) = \zeta_0 + \kappa_\zeta p$ in $(z_1, 1]$.

Motivation for pressure-dependence of polarization

The polarization described by both the original and pressure-dependent Debye models is due to the alignment of permanent dipole moments with the applied field. This tendency to align is inhibited by the presence of centrifugal or gyroscopic forces. These forces are caused by molecular rotations and collisions [42]. The pressure in a polarizable medium influences and is influenced by the short range particle interaction in the medium, including these molecular rotations and collisions. This interaction between particles may serve to inhibit or facilitate the alignment of dipole moments with the applied field, resulting in the modification of the orientational polarization [23]. Figure 2.4 depicts this schematically.

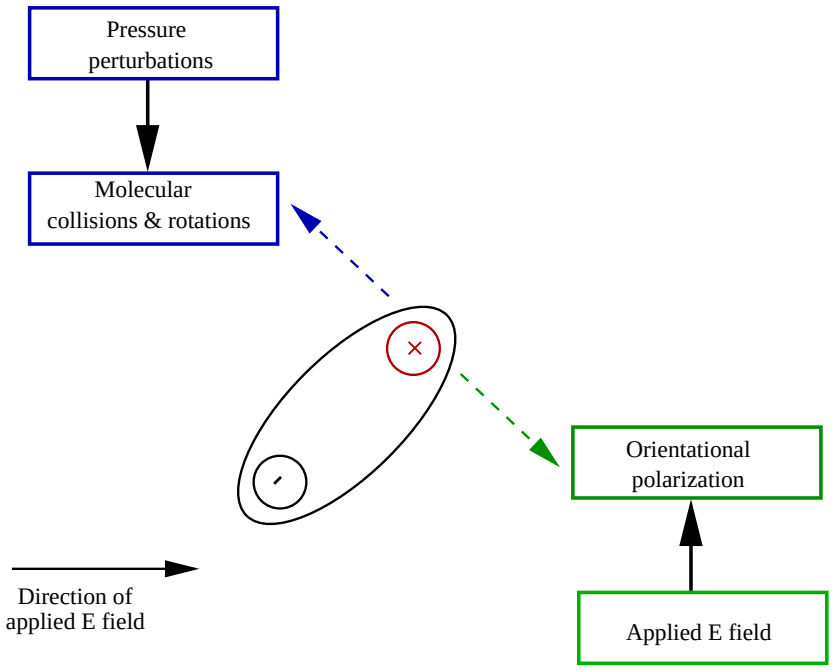

Figure 2.4: Pressure-dependence of orientational polarization

This interaction makes sense intuitively; however, we want to better understand the interaction mechanism. Specifically, we want to consider each polarization parameter individually and address its possible pressure-dependence.

We begin with the static permittivity ϵ_s, which is the electric permittivity of a dielectric in the presence of a constant applied electric field. In 1850 and 1879 respectively, Clausius and Mossitti independently discovered that for any given material, the quantity

$$\left(\frac{\epsilon_s}{\epsilon_0} - 1\right) / \left(\frac{\epsilon_s}{\epsilon_0} + 2\right)$$

is proportional to the material density (page 155, [32]; page 140, [41]). Pressure variations in the material cause changes in its density. These changes are reflected in the static permittivity of the material due to the law of Clausius and Mossitti. So the static permittivity can be expected to depend on pressure.

The pressure-dependence of ϵ_s does not necessarily suggest the pressure-dependence of ϵ_∞, the permittivity of a material under a very high frequency electric field. However in the interest of generality, we allow for the possibility that ϵ_∞ is pressure-dependent. Pressure-*independent* behavior of ϵ_∞ is just a special case of our model (see Section 2.1) with $\kappa_\zeta = 0$ so that $\epsilon_\infty(p) = \zeta_0$.

Lastly we examine the feasibility of the pressure-dependence of the relaxation parameter τ. To do so we consider a dipolar liquid which consists of freely moving molecules. If an individual dipole changes its orientation, the nearby dipoles shift to compensate and produce a new equilibrium position. Their collective motion can be viewed as a viscous frictional damping force that acts on the original dipole. When an electric field is applied, its force causes the dipole to align itself with the field. The rate of alignment depends on the amount of friction. However since the dipole is subject to the effects of Brownian motion, this rate also depends on thermal fluctuations. Taking this into account Debye derived the following expression for the relaxation (page 73, [2])

$$\tau = \frac{\xi}{2k_B T},$$

where ξ is the frictional constant. Dipoles arranged in smaller groups are less apt to resist reorientation [21]. This leads to diminished frictional effects. Variations in pressure likely alter the cohesion of dipole groupings and thus affect the friction. A specific example of this relationship is given in (page 63, [38]) for hard sphere fluids. In this case, the frictional viscosity constant is given by

$$\xi = \frac{k_B T}{mD},$$

where m is the particle mass and D is the self-diffusion coefficient. The self-diffusion coefficient is pressure-dependent; that is

$$D = \frac{1}{2} R \Big(\frac{\pi k_B T}{m} \Big)^{\frac{1}{2}} \Big(\frac{p}{\rho k_B T} - 1 \Big)^{-1},$$

where R is the hard sphere diameter, p is the pressure, and ρ is the liquid density. Clearly in this example the relaxation parameter τ is pressure-dependent.

Chapter 3

Theoretical results

The main purpose of this chapter is to provide a general theoretical foundation for a class of electromagnetic/acoustic interaction problems. This class includes the electromagnetic interrogation techniques described in [7] as well as the technique presented in this thesis. Specifically, in Section 3.1 we consider the well-posedness of a general variational form of the model. As in Chapter 2, we consider the equation in the domain $0 \leq z \leq 1$ and assume that the boundary conditions are absorbing on the left ($z = 0$) and perfectly conductive on the right ($z = 1$). We use general initial conditions for the electric field, but without loss of generality we assume that the polarization, present in the dielectric material region $(z_1, 1]$ with $0 < z_1 < 1$, and its first time derivative are initially zero. In Section 3.2, we show that with some additional asssumptions, our solutions have enhanced regularity. Finally, we use the results of the first two sections to establish a framework for the parameter estimation problem in Section 3.3. In each of these sections, we verify that the results in question are satisfied by the systems incorporating pressure-dependent Debye and Lorentz polarization.

3.1 Well-posedness

We begin by formulating the Gelfand triple $V \hookrightarrow H \hookrightarrow V^*$, where $H = L^2(0,1)$ and $V = H_R^1(0,1) \equiv \{\phi \in H^1(0,1) : \phi(1) = 0\}$. Specifically, we note that there is a value $k > 0$ such that for all $\phi \in V$, we have

$$|\phi|_H \leq k|\phi|_V.$$

The usual duality product is denoted by $< \cdot, \cdot >_{V^*,V}$; it is the extension by continuity of the H inner product from $H \times V$ to $V^* \times V$. Both inner products $< \cdot, \cdot >$ and norms $|\cdot|$ denoted without subscripts are assumed to be in H. A variational form of Maxwell's equation in second order form for a general polarization term is given in [7], Chapter 2, by

$$\begin{aligned} &< a\ddot{E}, \phi >_{V^*,V} + < b\dot{E}, \phi > + < e\ddot{P}, \phi > \\ &+c\dot{E}(t,0)\phi(0) + \sigma_1(E,\phi) =< F, \phi >_{V^*,V} \end{aligned} \tag{3.1}$$

for all $\phi \in V$. Here the sesquilinear form σ_1 is defined by

$$\sigma_1(\phi, \psi) = c^2 < \phi', \psi' >, \tag{3.2}$$

where $c^2 = \frac{1}{\epsilon_0 \mu_0}$ is a positive constant and the parameter functions a, b, and e depend on geometry as well as conductivity and the instantaneous polarization of the dielectric medium. The absorbing boundary condition $\dot{E} - cE' = 0$ at $z = 0$ is a natural condition and is thus incorporated into this variational formulation of the equation, but the superconductive boundary condition at $z = 1$ is an essential boundary condition and is imposed in the definition of V.

We note that σ_1 is V-continuous and V-elliptic, i.e., there exist positive constants c_1, c_2 such that

$$\sigma_1(\phi,\psi) = c^2 < \phi', \psi' > \leq c^2 |\phi'|_H |\psi'|_H \leq c_1 |\phi|_V |\psi|_V \tag{3.3}$$

$$\sigma_1(\phi,\phi) = c^2 < \phi', \phi' >= c^2 |\phi'|_H^2 \geq c_2 |\phi|_V^2, \tag{3.4}$$

since $|\phi|_V^2$ is equivalent to $|\phi'|_H^2 + |\phi(1)|^2 = |\phi'|_H^2$.

The model (3.1) is a very general Maxwell system that can be used with numerous polarization models. As an example, we show that (3.1) can be specialized to include a Debye polarization model with pressure-dependent coefficients. The pressure-dependent Debye polarization model we consider (see [16] and [2] for physics-based discussions) is given by

$$\dot{P} = -\frac{1}{(\tau_0 + \kappa_\tau p)} P + \frac{\epsilon_0 \left(\gamma_0 - \zeta_0 + (\kappa_\gamma - \kappa_\zeta) p\right)}{(\tau_0 + \kappa_\tau p)} E. \tag{3.5}$$

where $\tau = \tau(p) = \tau_0 + \kappa_\tau p$ is the pressure-dependent decay parameter, $\epsilon_s = \gamma(p) = \gamma_0 + \kappa_\gamma p$ and $\epsilon_\infty = \zeta(p) = \zeta_0 + \kappa_\zeta p$ are pressure-dependent dielectric parameters, and $p = p(t,z)$ is the acoustic pressure in the Debye material.

The solution to (3.5), for $P(0,z) = 0$, can be written

$$P(t,z) = \int_0^t \exp\left(\int_s^t \frac{-d\xi}{\tau_0 + \kappa_\tau p(\xi, z)} \right) \frac{\epsilon_0 \left(\gamma_0 - \zeta_0 + (\kappa_\gamma - \kappa_\zeta) p(s,z)\right)}{(\tau_0 + \kappa_\tau p(s,z))} E(s,z)\, ds.$$

We may use (3.5), its derivative, and its solution to replace $\ddot{P}$ in (3.1). These substitutions lead to the following variational form of the system

$$< a\ddot{E}, \phi >_{V^*,V} + < b\dot{E}, \phi > + < hE, \phi > + < \int_0^t G(t,s,\cdot) E(s,\cdot)\, ds, \phi >$$

$$+ c\dot{E}(t,0)\phi(0) + \sigma_1(E,\phi) =< F, \phi >_{V^*,V} \tag{3.6}$$

$$E(0,z) = E_0(z) \quad \dot{E}(0,z) = E_1(z) \quad P(0,z) = \dot{P}(0,z) = 0$$

where $E_0 \in V$ and $E_1 \in H$ with coefficients, kernel and forcing functions, and sesquilinear form defined by

$$\begin{aligned}
a(t,z) &= 1 + (\epsilon_\infty - 1) I_{(z_1,1)} = 1 + (\zeta_0 + \kappa_\zeta p(t,z) - 1) I_{(z_1,1)} \\
b(t,z) &= \left(\frac{\sigma}{\epsilon_0} + \frac{1}{\epsilon_0} \frac{\epsilon_0 \left(\gamma_0 - \zeta_0 + (\kappa_\gamma - \kappa_\zeta) p(t,z) \right)}{(\tau_0 + \kappa_\tau p(t,z))} \right) I_{(z_1,1)} \\
h(t,z) &= \frac{1}{\epsilon_0} \Big(\frac{\epsilon_0 (\kappa_\gamma - \kappa_\zeta) \dot{p}(t,z)}{(\tau_0 + \kappa_\tau p(t,z))} \\
&\quad - \frac{(1 + \kappa_\tau \dot{p}(t,z)) \, \epsilon_0 \left(\gamma_0 - \zeta_0 + (\kappa_\gamma - \kappa_\zeta) p(t,z) \right)}{(\tau_0 + \kappa_\tau p(t,z))^2} \Big) I_{(z_1,1)} \\
G(t,s,z) &= \frac{1}{\epsilon_0} \frac{(1 + \kappa_\tau \dot{p}(t,z)) \, \epsilon_0 \left(\gamma_0 - \zeta_0 + (\kappa_\gamma - \kappa_\zeta) p(s,z) \right)}{(\tau_0 + \kappa_\tau p(t,z))^2 \, (\tau_0 + \kappa_\tau p(s,z))} \\
&\quad \times \exp \left(\int_s^t \frac{-d\xi}{\tau_0 + \kappa_\tau p(\xi,z)} \right) I_{(z_1,1)} \\
c^2 &= \tfrac{1}{\epsilon_0 \mu_0} \\
F(t,z) &= -\tfrac{1}{\epsilon_0} \dot{J}_s(t) \\
\sigma_1(\phi,\psi) &= c^2 < \phi', \psi' > .
\end{aligned} \tag{3.7}$$

(Here I_Ω is the indicator or characteristic function for a set Ω.)
Moreover, we may consider the Lorentz model for polarization

$$\ddot{P} + \frac{1}{\tau} \dot{P} + \omega_0^2 P = \epsilon_0 \omega_0^2 (\epsilon_s - \epsilon_\infty) E$$

as the pressure-dependent equation

$$\ddot{P} + \frac{1}{\tau_0 + \kappa_\tau p} \dot{P} + (\alpha_0 + \kappa_\alpha p) P = \epsilon_0 (\alpha_0 + \kappa_\alpha p)(\gamma_0 - \zeta_0 + (\kappa_\gamma - \kappa_\zeta) p) E.$$

Coupling this polarization model with the Maxwell system formulated above leads to equation (3.6), where again $E_0 \in V$ and $E_1 \in H$. For this model, the coefficients, kernel and forcing functions, and sesquilinear form are given by

$$\begin{aligned}
a(t,z) &= 1 + (\epsilon_\infty - 1)I_{(z_1,1)} = 1 + (\zeta_0 + \kappa_\zeta p(t,z) - 1)I_{(z_1,1)} \\
b(t,z) &= \tfrac{\sigma}{\epsilon_0} I_{(z_1,1)} \\
h(t,z) &= \tfrac{1}{\epsilon_0}\left(\epsilon_0(\alpha_0 + \kappa_\alpha p(t,z))(\gamma_0 - \zeta_0 + (\kappa_\gamma - \kappa_\zeta)p(t,z))\right) I_{(z_1,1)} \\
G(t,s,z) &= \frac{-1}{\epsilon_0}\Big(\frac{1}{\tau_0 + \kappa_\tau p(t,z)}\Phi_{21}(t,s) + (\alpha_0 + \kappa_\alpha p(t,z))\Phi_{11}(t,s)\Big) \\
&\quad \times\Big(\epsilon_0(\alpha_0 + \kappa_\alpha p(s,z))(\gamma_0 - \zeta_0 + (\kappa_\gamma - \kappa_\zeta)p(s,z))\Big) I_{(z_1,1)} \\
c^2 &= \tfrac{1}{\epsilon_0\mu_0} \\
F(t,z) &= -\tfrac{1}{\epsilon_0}\dot{J}_s(t) \\
\sigma_1(\phi,\psi) &= c^2 < \phi', \psi' > .
\end{aligned} \tag{3.8}$$

Here the Φ_{ij} are the components of the state transition matrix corresponding to the system

$$\frac{d}{dt}\begin{bmatrix} P \\ \dot{P} \end{bmatrix} = \begin{bmatrix} 0 & 1 \\ -(\gamma_0 + \kappa_\gamma p) & \frac{-1}{\tau_0 + \kappa_\tau p} \end{bmatrix}\begin{bmatrix} P \\ \dot{P} \end{bmatrix}; \quad \begin{bmatrix} P \\ \dot{P} \end{bmatrix}(0) = 0. \tag{3.9}$$

Provided that $p \in C(0,T;C[0,1])$, the above stiffness matrix is continuous in each of the variables, t,γ_0,κ_γ,τ_0, and κ_τ. We may then conclude that the solutions P and $\dot{P}$ and the components of the state transition matrix are continuous in each of the variables, t, γ_0,κ_γ,τ_0, and κ_τ, as well [3].

We assume here, and throughout the entire thesis, that the material parameters may only be chosen from an admissible set Q (for the Debye model $Q \subset \mathbb{R}^7$, for

the Lorentz model $Q \subset \mathbb{R}^9$). This insures that our Debye and Lorentz coefficients are well-defined. First, because of the physical meaning of these parameters, the values of $\sigma, \gamma_0, \zeta_0$, τ_0,and α_0 must be positive. Then for a given pressure wave p with $\frac{d^k}{dt^k}p \in L^\infty(0,T;L^\infty(0,1))$ for $k = 0,1,2,3$ and a fixed $\delta > 0$, we admit only values of $\kappa_\gamma, \kappa_\zeta, \kappa_\tau$, and κ_α such that $\gamma_0+\kappa_\gamma p(t,z)$, $\zeta_0+\kappa_\zeta p(t,z)$, $\tau_0+\kappa_\tau p(t,z)$, and $\alpha_0+\kappa_\alpha p(t,z)$ are greater than δ for all $z \in [0,1]$ and $t \in [0,T]$. In addition to these requirements, we assume that the admissible parameter sets are closed and bounded in $\mathbb{R}^7$ and $\mathbb{R}^9$. As we shall see, under appropriate assumptions on the coefficients, kernels, and forcing functions in (3.7) and (3.8), we can give general arguments that establish the well-posedness of the Debye- and Lorentz-based systems, as well as any other system that satisfies the general assumptions listed in the next section for the generalized system (3.10) below. We remark that other models based on more general polarization models can also be shown to be special cases of (3.10).

3.1.1 Well-posedness of solutions to the general variational form

Motivated by the Debye and Lorentz examples and a wide range of applications, we consider the general variational form

$$\begin{gathered} < a\ddot{E}, \phi >_{V^*,V} + < b\dot{E}, \phi > + < hE, \phi > \\ + < \int_0^t G(t,s,\cdot)E(s,\cdot)\, ds, \phi > \\ +c\dot{E}(t,0)\phi(0) + c^2 < E', \phi' > =< F, \phi >_{V^*,V}, \quad \phi \in V \end{gathered} \tag{3.10}$$

$$E(0,z) = E_0(z) \quad \dot{E}(0,z) = E_1(z) \quad P(0,z) = \dot{P}(0,z) = 0,$$

where $E_0 \in V$ and $E_1 \in H$. As introduced previously, we take $H = L^2(0,1)$ and $V = H_R^1(0,1) \equiv \{\phi \in H^1(0,1) : \phi(1) = 0\}$ which, with V^*, are Hilbert spaces that

form a Gelfand triple $V \hookrightarrow H \hookrightarrow V^*$. We again note that there is a value $k > 0$ such that for all $\phi \in V$, we have

$$|\phi|_H \leq k|\phi|_V.$$

The usual duality product is denoted by $< \cdot, \cdot >_{V^*,V}$ and both inner products $< \cdot, \cdot >$ and norms $|\cdot|$ denoted without subscripts are assumed to be in H. In addition, motivated by (3.7), we make the following assumptions:

A1) The coefficient a along with its derivatives $\dot{a}$ and $\ddot{a}$ are in $L^\infty(0,T;L^\infty[0,1])$, and for all $z \in [0,1]$, $a(z) \geq a_0$, for some $1 \geq a_0 > 0$.

A2) The coefficient b and its time derivative $\dot{b}$ are in $L^\infty(0,T;L^\infty[0,1])$ and $b(t,z) \geq 0$ for all $(t,z) \in [0,T] \times [0,1]$.

A3) The coefficient h is in $L^\infty(0,T;L^\infty[0,1])$.

A4) The kernel function G is in $L^\infty([0,T] \times [0,T];L^\infty[0,1])$.

A5) The sequilinear form σ_1 is given by $\sigma_1(\phi,\psi) = c^2 < \phi', \psi' >$ for $\phi, \psi \in V$ with $c > 0$.

A6) The forcing function F is in $H^1(0,T,V^*)$.

We recall that the sesquilinear form $\sigma_1 : V \times V \to \mathbb{R}$ is V-continuous and V-elliptic, so that (3.3) and (3.4) are satisfied.

Under the above hypotheses, we seek solutions $t \to E(t)$ where $E(t) \in V$ and (3.10) is satisfied in the $L^2(0,T)$ sense for all $\phi \in V$. We begin by showing that such solutions exist.

To this end, we follow the arguments in [19], [7]. We choose a linearly independent subset $\{w_i\}_{i=0}^\infty$ that spans V which is dense in H. We let $V^m \equiv \text{span}\{w_0, w_1, \ldots, w_m\}$ and choose $E_{0m}, E_{1m} \in V^m$ such that as $m \to \infty$, $E_{0m} \to E_0$ in V, and $E_{1m} \to E_1$ in H. Then we let $E_m = \sum_{i=0}^m \eta_i(t) w_i(z)$ be the unique solution on $0 < t < T$ to the integrodifferential equation system (for existence we will use Theorems 1 and 2 of [5]

combined with the arguments below)

$$\begin{gathered} < a\ddot{E}_m(t), w_j >_{V^*,V} + < b\dot{E}_m(t), w_j > + < hE_m(t), w_j > \\ + < \int_0^t G(t,s,\cdot)E_m(s,\cdot)\, ds, w_j > + c\dot{E}_m(t,0)w_j(0) \\ + \sigma_1(E_m(t), w_j) =< F(t), w_j >_{V^*,V} \\ E_m(0) = E_{0m} \quad \dot{E}_m(0) = E_{1m}, \end{gathered} \tag{3.11}$$

where $j = 0, 1, \ldots, m$.

We note here that for any $i = 0, 1, \ldots, m$, $w_i \in V = H_R^1(0,1)$, and thus w_i is absolutely continuous. From this we also have that $w_i w_j \in C(0,1)$. Thus, all products involving E_m and its time derivatives are spatially continuous functions on the interval $[0,1]$. Moreover, inner product terms containing coefficients in L^∞, e.g., $< b(t,\cdot)\dot{E}_m(t,\cdot), w_j >$, are well-defined.

We may write (3.11) in the form

$$M_1(t)\ddot{\eta}(t) + M_2(t)\dot{\eta}(t) + M_3(t)\eta(t) + G_1(t,\eta(\cdot)) = D_1(t),$$

where

$$\begin{aligned} \eta(t) &= [\eta_0(t)\ \eta_1(t)\ \ldots\ \eta_m(t)]^T \\ [G_1(t,\eta(\cdot))]_j &= \textstyle\sum_{i=1}^m < \int_0^t G(t,s,\cdot)\eta_i(s)\ ds\ w_i, w_j > \\ [D_1(t)]_j &= < F(t), w_j > \\ [M_1(t)]_{ij} &= < a(t)w_j, w_i > \\ [M_2(t)]_{ij} &= < b(t)w_j, w_i > + c w_i(0) w_j(0) \\ [M_3(t)]_{ij} &= < h(t)w_j, w_i > + c^2 < w_i', w_j' > . \end{aligned}$$

Since the w_i are linearly-independent and a satisfies the lower bound of A1), $M_1(t)$ is positive definite for each t, hence invertible. Then the above linear system may be written

$$\begin{aligned} \dot{\mathcal{Y}}(t) &= \mathcal{M}(t)\left(\mathcal{A}(t)\mathcal{Y}(t) + \mathcal{G}(t, \mathcal{Y}(\cdot)) + \mathcal{D}(t)\right) \\ &= \mathcal{F}(t, \mathcal{Y}(\cdot)) + \mathcal{M}(t)\mathcal{D}(t) \end{aligned} \tag{3.12}$$

with

$$\mathcal{Y}(t) = \begin{bmatrix} \eta(t) \\ \dot{\eta}(t) \end{bmatrix}$$

$$\mathcal{M}(t) = \begin{bmatrix} I & 0 \\ 0 & M_1(t) \end{bmatrix}^{-1}$$

$$\mathcal{A}(t) = \begin{bmatrix} 0 & I \\ -M_3(t) & -M_2(t) \end{bmatrix}$$

$$[\mathcal{G}(t, \mathcal{Y}(\cdot))]_j = \begin{cases} 0, & j = 0, \ldots, m \\ -\left[G(t, \eta(\cdot))\right]_j, & j = m+1, \ldots, 2m+1 \end{cases}$$

$$[\mathcal{D}(t)]_j = \begin{cases} 0, & j = 0, \ldots, m \\ [D_1(t)]_j, & j = m+1, \ldots, 2m+1. \end{cases}$$

We point out that the notation $\mathcal{F}(t, \mathcal{Y}(\cdot))$ implies that for each $t \in [0, T]$, $\mathcal{F}$ depends on t and on the past history of $\mathcal{Y}$ in an interval $[0, t]$. We now want to argue that (3.12) does, in fact, have a unique solution that is continuous in t in $[0, T]$. To this end, we argue that (3.12) satisfies the following conditions:

Y1) For a fixed $\mathcal{Y}$, $\mathcal{F}$ is measurable in t.

Y2) For almost every fixed $t \in [0, T]$, $\mathcal{F}$ is continuous in $\mathcal{Y}$.

Y3) There is an $L^1(0,T)$ function m_F such that

$$|\mathcal{F}(t,\mathcal{Y}(\cdot))| \leq m_F(t) \sup_{s\in[0,T]} |\mathcal{Y}(s)| \qquad (t,\mathcal{Y}) \in [0,T]\times C[0,T]. \tag{3.13}$$

Y4) There is an $L^1(0,T)$ function k such that

$$\begin{gathered} |\mathcal{F}(t,\mathcal{Y}(\cdot)) - \mathcal{F}(t,\mathcal{X}(\cdot))| \leq k(t)\sup_{s\in[0,T]} |\mathcal{Y}(s)-\mathcal{X}(s)| \\ \text{for } (t,\mathcal{Y}),(t,\mathcal{X}) \in [0,T]\times C[0,T]. \end{gathered} \tag{3.14}$$

Y5) The function $\mathcal{D}$ is in $L^1(0,T)$.

Since the components of $\mathcal{M},\mathcal{A}$ and $\mathcal{G}(\cdot,\mathcal{Y}(\cdot))$ are in $L^\infty(0,T)$, we have that $\mathcal{F}(\cdot,\mathcal{Y}(\cdot))$ is measurable in t for a fixed $\mathcal{Y}$ and Y1) holds.

In order to verify Y2), we must show that both $\mathcal{M}(t)\mathcal{A}(t)\mathcal{Y}$ and $\mathcal{M}(t)\mathcal{G}(t,\mathcal{Y})$ are continuous in $\mathcal{Y}$. It is clear that this is true for $\mathcal{M}(t)\mathcal{A}(t)\mathcal{Y}$, but we now give a more formal argument to show the continuity of $\mathcal{G}(t,\mathcal{Y})$.

Let $\epsilon > 0$ be given. Choose $\delta > 0$ such that

$$\delta^2 = \epsilon^2 / \left(|G|^2_{L^\infty} T^2 \sum_{j=0}^{m} \left(\sum_{i=0}^{m} \int_0^1 |w_i||w_j| \, dz \right)^2 \right).$$

Since $w_i, w_j \in V$, the integral $\int_0^1 |w_i||w_j| \, dz$ is finite.

Then

$$|\mathcal{Y}-\mathcal{X}| < \delta \quad \Rightarrow \quad \sum_{i=0}^{m} (\eta_i - x_i)^2 < \delta^2 \quad \Rightarrow \quad |\eta_i - x_i| < \delta \text{ for any } i = 0,\ldots,m.$$

Thus we have, for all $\mathcal{Y},\mathcal{X}$ with $|\mathcal{Y}-\mathcal{X}| < \delta$,

$$
\begin{aligned}
& |\mathcal{G}(t,\mathcal{Y}) - \mathcal{G}(t,\mathcal{X})|^2 \\
= \;& \textstyle\sum_{j=0}^{m} \left(\sum_{i=0}^{m} \int_0^1 \int_0^t G(t,s,z)(\eta_i - x_i)\; ds\; w_i w_j\; dz \right)^2 \\
\leq \;& \textstyle\sum_{j=0}^{m} \left(\int_0^1 \int_0^t |G(t,s,z)| \sum_{i=0}^{m} |\eta_i - x_i||w_i||w_j|\; ds\; dz \right)^2 \\
\leq \;& |G|_{L^\infty}^2 \delta^2 T^2 \textstyle\sum_{j=0}^{m} \left(\sum_{i=0}^{m} \int_0^1 |w_i||w_j|\; dz \right)^2 \\
= \;& \epsilon^2.
\end{aligned}
$$

Hence, $\mathcal{G}(t,\mathcal{Y})$ is continuous in $\mathcal{Y}$, and $\mathcal{M}(t)\mathcal{G}(t,\mathcal{Y})$ is continuous in $\mathcal{Y}$.

Thus we have that Y2) holds.

We next show that there is an $L^1(0,T)$ function m_F such that (3.13) holds. For this, we choose an arbitrary $(t,\mathcal{Y}) \in [0,T] \times C[0,T]$. We let

$$\bar{w} = \max_{i,j=0,\ldots,m} | < w_i, w_j > |^2.$$

Then we note that

$$|\mathcal{F}(t,\mathcal{Y}(\cdot))| \leq |\mathcal{M}(t)||\mathcal{A}(t)| \sup_{s\in[0,T]} |\mathcal{Y}(s)| + |\mathcal{M}(t)||\mathcal{G}(t,\mathcal{Y}(\cdot))|.$$

Since the components of $\mathcal{M}$ and $\mathcal{A}$ are in $L^\infty(0,T)$ and hence

$$|\mathcal{M}| \leq \bar{M} \quad \text{and} \quad |\mathcal{A}(t)| \leq \bar{A}$$

for any $t \in [0,T]$, we need only show that there is a function $m_G \in L^1(0,T)$ such that

$$|\mathcal{G}(t,\mathcal{Y}(\cdot))| \leq m_G(t) \sup_{s\in[0,T]} |\mathcal{Y}(s)|.$$

We have

$$
\begin{aligned}
|\mathcal{G}(t,\mathcal{Y}(\cdot))|^2 &\leq \sum_{j=0}^{m}\left(\sum_{i=0}^{m} < \int_0^t G(t,s,\cdot)\eta_i(s)\ dsw_i, w_j >\right)^2 \\
&\leq |G|^2_{L^\infty}\sum_{j=0}^{m}\left(\sum_{i=0}^{m} < \int_0^t \eta_i(s)\ dsw_i, w_j >\right)^2 \\
&\leq |G|^2_{L^\infty}\bar{w}\sum_{j=0}^{m}\left(\sum_{i=0}^{m}\int_0^t \eta_i(s)\ ds\right)^2 \\
&\leq |G|^2_{L^\infty}\bar{w}m\left(\int_0^t \sum_{i=0}^{m}|\eta_i(s)|\ ds\right)^2 \\
&\leq |G|^2_{L^\infty}\bar{w}m^2T^2\sup_{s\in[0,T]}|\mathcal{Y}(s)|^2.
\end{aligned}
$$

If we let

$$m_G(t) = |G|_{L^\infty}\sqrt{\bar{w}}mT,$$

we have

$$|\mathcal{G}(t,\mathcal{Y}(\cdot))| \leq m_G(t)\sup_{s\in[0,T]}|\mathcal{Y}(s)|.$$

Therefore, equation (3.13), and thus Y3), hold.

In order to verify Y4), we note that the mapping $\mathcal{Y}\to\mathcal{F}(t,\mathcal{Y}(\cdot))$ is linear. Then the verification of Y4) follows immediately from Y3).

In verifying Y5), we need only note that the components of $\mathcal{D}$ are in $H^1(0,T)$.

Having argued that assumptions Y1)-Y5) hold, we may use Theorem 2 in [5] to conclude that (3.12) and hence (3.11) has a unique, continuous solution E_m for which we next derive *a priori* bounds.

We then multiply (3.11) by $\dot{\eta}_j(t)$ and sum over j to obtain

$$
\begin{gathered}
< a\ddot{E}_m, \dot{E}_m >_{V^*,V} + < b\dot{E}_m, \dot{E}_m > + < hE_m, \dot{E}_m > \\
+ < \int_0^t G(t,s,\cdot)E_m(s,\cdot)\, ds, \dot{E}_m > \\
+c\dot{E}_m(t,0)\dot{E}_m(t,0) + \sigma_1(E_m, \dot{E}_m) =< F, \dot{E}_m >_{V^*,V} \\
E_m(0) = E_{0m} \quad \dot{E}_m(0) = E_{1m}.
\end{gathered}
\tag{3.15}
$$

We note that

$$
\begin{aligned}
2 < a\ddot{E}_m, \dot{E}_m >_{V^*,V} &= \tfrac{d}{dt} < a\dot{E}_m, \dot{E}_m > - < \dot{a}\dot{E}_m, \dot{E}_m > \\
&= \tfrac{d}{dt}|\sqrt{a}\dot{E}_m|_H^2 - < \dot{a}\dot{E}_m, \dot{E}_m >
\end{aligned}
$$

and

$$
\frac{d}{dt}\sigma_1(E_m, E_m) = 2\sigma_1(E_m, \dot{E}_m),
$$

so that (3.15) becomes

$$
\begin{gathered}
\tfrac{d}{dt}\left(|\sqrt{a}\dot{E}_m|_H^2 + \sigma_1(E_m, E_m)\right) + < (2b - \dot{a})\dot{E}_m, \dot{E}_m > +2 < hE_m, \dot{E}_m > \\
+2 < \int_0^t GE_m(s,\cdot)\, ds, \dot{E}_m > +2c|\dot{E}_m(t,0)|^2 = 2 < F, \dot{E}_m >_{V^*,V} .
\end{gathered}
$$

Then

$$
\begin{gathered}
|\sqrt{a}\dot{E}_m(t)|_H^2 + \sigma_1(E_m(t), E_m(t)) + \int_0^t < (2b - \dot{a})\dot{E}_m, \dot{E}_m > \; d\xi \\
+ \int_0^t 2 < hE_m, \dot{E}_m > \; d\xi + \int_0^t 2 < \int_0^\xi GE_m(s,\cdot)\, ds, \dot{E}_m(\xi,\cdot) > \; d\xi \\
+ \int_0^t 2c|\dot{E}_m(\xi,0)|^2 \, d\xi \\
= |\sqrt{a}(0)\dot{E}_m(0)|_H^2 + \sigma_1(E_m(0), E_m(0)) + \int_0^t 2 < F, \dot{E}_m >_{V^*,V} \; d\xi.
\end{gathered}
\tag{3.16}
$$

Using the V-continuity and V-ellipticity of σ_1 and the fact that $2ab \leq a^2 + b^2$, we have

$$
\begin{aligned}
&|\sqrt{a}\dot{E}_m(t)|_H^2 + c_2|E_m(t)|_V^2 + \int_0^t 2c|\dot{E}_m(\xi,0)|^2 \, d\xi \\
&\leq \int_0^t 2 < -hE_m, \dot{E}_m > \, d\xi + \int_0^t < (\dot{a} - 2b)\dot{E}_m, \dot{E}_m > \, d\xi \\
&\quad + \int_0^t 2 < -\int_0^\xi GE_m(s,\cdot)\, ds, \dot{E}_m(\xi,\cdot) > \, d\xi \\
&\quad + |\sqrt{a}\dot{E}_m(0)|_H^2 + \sigma_1(E_m(0), E_m(0)) + \int_0^t 2 < F, \dot{E}_m >_{V^*,V} \, d\xi \\
&\leq \int_0^t \left\{ |hE_m|_H^2 + |\dot{E}_m|_H^2 \right\} \, d\xi + \int_0^t \left\{ \tfrac{1}{2}|\dot{E}_m|_H^2 + \tfrac{1}{2}|(\dot{a} - 2b)\dot{E}_m|_H^2 \right\} \, d\xi \\
&\quad + \int_0^t \left\{ |\int_0^\xi GE_m(s,\cdot)\, ds|_H^2 + |\dot{E}_m|_H^2 \right\} \, d\xi \\
&\quad + |\sqrt{a}(0)\dot{E}_m(0)|_H^2 + c_1|E_m(0)|_V^2 + |\int_0^t 2 < F, \dot{E}_m >_{V^*,V} \, d\xi|.
\end{aligned}
$$

For $F \in H^1(0,T;V^*)$, we find

$$
\begin{aligned}
&|\int_0^t 2 < F, \dot{E}_m >_{V^*,V} \, d\xi| \\
&= |\int_0^t \left(2\tfrac{d}{d\xi} < F, E_m >_{V^*,V} - 2 < \dot{F}, E_m >_{V^*,V} \right) \, d\xi| \\
&= |2 < F(t), E_m(t) >_{V^*,V} - 2 < F(0), E_m(0) >_{V^*,V} - \int_0^t 2 < \dot{F}, E_m >_{V^*,V} \, d\xi| \\
&\leq 2| < F(t), E_m(t) >_{V^*,V} | + 2| < F(0), E_m(0) >_{V^*,V} | \\
&\quad + \int_0^t 2| < \dot{F}, E_m >_{V^*,V} | \, d\xi \\
&\leq \tfrac{1}{\epsilon}|F(t)|_{V*}^2 + \epsilon|E_m(t)|_V^2 + |F(0)|_{V*}^2 + |E_m(0)|_V^2 + \int_0^t \left\{ |\dot{F}|_{V*}^2 + |E_m|_V^2 \right\} \, d\xi.
\end{aligned}
$$

Thus, from (3.16) we find

$$
\begin{aligned}
&|\sqrt{a}\dot{E}_m(t)|_H^2 + c_2|E_m(t)|_V^2 + \textstyle\int_0^t 2c|\dot{E}_m(\xi,0)|^2\ d\xi \\
&\leq \textstyle\int_0^t \left\{|hE_m|_H^2 + |\dot{E}_m|_H^2\right\}\ d\xi + \int_0^t \left\{\frac{1}{2}|\dot{E}_m|_H^2 + \frac{1}{2}|(\dot{a}-2b)\dot{E}_m|_H^2\right\}\ d\xi \\
&\quad + \textstyle\int_0^t \left\{|\int_0^\xi GE_m(s,\cdot)\ ds|_H^2 + |\dot{E}_m|_H^2\right\}\ d\xi \\
&\quad + |\sqrt{a}(0)\dot{E}_m(0)|_H^2 + c_1|E_m(0)|_V^2 + \tfrac{1}{\epsilon}|F(t)|_{V*}^2 + \epsilon|E_m(t)|_V^2 + |F(0)|_{V*}^2 + |E_m(0)|_V^2 \\
&\quad + \textstyle\int_0^t \left\{|\dot{F}|_{V*}^2 + |E_m|_V^2\right\}\ d\xi.
\end{aligned}
$$

Using the fact that $E_m(0) = E_{0m}$ and $\dot{E}_m(0) = E_{1m}$ and combining like terms, we have finally

$$
\begin{aligned}
&|\sqrt{a}\dot{E}_m(t)|_H^2 + (c_2-\epsilon)|E_m(t)|_V^2 + \textstyle\int_0^t 2c|\dot{E}_m(\xi,0)|^2\ d\xi \\
\leq\ & \int_0^t \left\{|hE_m|_H^2 + \frac{5}{2}|\dot{E}_m|_H^2 + \frac{1}{2}|(\dot{a}-2b)\dot{E}_m|_H^2\right. \\
&\left. + |\int_0^\xi GE_m(s,\cdot)\ ds|_H^2 + |\dot{F}|_{V*}^2 + |E_m|_V^2\right\}\ d\xi \\
&+ |\sqrt{a}(0)E_{1m}|_H^2 + (c_1+1)|E_{0m}|_V^2 + \tfrac{1}{\epsilon}|F(t)|_{V*}^2 + |F(0)|_{V*}^2.
\end{aligned}
$$

We next use the assumptions on the coefficients and kernel function to establish some bounds.

Hypothesis A1) implies that there exists $\bar{a} > 1$ such that

$$|\sqrt{a(0,\cdot)}E_{1m}(\cdot)|_H^2 \leq \bar{a}|E_{1m}(\cdot)|_H^2.$$

Moreover, there exists $a_0 > 0$ such that

$$a_0|\dot{E}_m(t,\cdot)|_H^2 \leq |\sqrt{a(\cdot)}\dot{E}_m(t,\cdot)|_H^2.$$

Hypotheses A1) and A2) allow us to show that there exists $\bar{b} > 0$ such that

$$\begin{aligned}
&\textstyle\int_0^t \frac{1}{2}|(\dot{a}(\xi,\cdot) - 2b(\xi,\cdot))\dot{E}_m(\xi,\cdot)|_H^2 \, d\xi \\
&\leq \textstyle\frac{1}{2}\int_0^t \int_0^1 |\dot{a}(\xi,z) - 2b(\xi,z)|^2 |\dot{E}_m(\xi,z)|^2 \, dz \, d\xi \\
&\leq \textstyle\frac{1}{2}|\dot{a} - 2b|_{L^\infty}^2 \int_0^t \int_0^1 |\dot{E}_m(\xi,z)|^2 \, dz \, d\xi \\
&\leq \bar{b} \textstyle\int_0^t |\dot{E}_m(\xi,\cdot)|_H^2 \, d\xi.
\end{aligned}$$

We use hypothesis A3) to claim that there exists $\bar{h} \geq 0$ such that

$$\begin{aligned}
\textstyle\int_0^t |h(\xi,\cdot)E_m(\xi,\cdot)|_H^2 \, d\xi &\leq \textstyle\int_0^t \int_0^1 |h(\xi,z)|^2 |E_m(\xi,z)|^2 \, dz \, d\xi \\
&= |h|_{L^\infty}^2 \textstyle\int_0^t |E_m(\xi,\cdot)|_H^2 \, d\xi \\
&\leq \bar{h} \textstyle\int_0^t |E_m(\xi,\cdot)|_H^2 \, d\xi.
\end{aligned}$$

Using A4), we have that there exists $\bar{G} \geq 0$ such that

$$\begin{aligned}
&\textstyle\int_0^t |\int_0^\xi G(\xi,s,\cdot)E_m(s,\cdot) \, ds|_H^2 \, d\xi \\
&= \textstyle\int_0^t \int_0^1 |\int_0^\xi G(\xi,s,z)E_m(s,z) \, ds|^2 \, dz \, d\xi \\
&= |G|_{L^\infty}^2 \textstyle\int_0^t \int_0^1 \left(\int_0^\xi |E_m(s,z)| \, ds\right)^2 \, dz \, d\xi \\
&\leq |G|_{L^\infty}^2 \textstyle\int_0^t \int_0^1 \left(T^{\frac{1}{2}}|E_m(z)|_{L^2(0,\xi)}\right)^2 \, dz \, d\xi \\
&\leq T|G|_{L^\infty}^2 \textstyle\int_0^t \int_0^1 \int_0^t |E_m(s,z)|^2 \, ds \, dz \, d\xi \\
&= T^2\bar{G} \textstyle\int_0^t |E_m(\xi,\cdot)|_H^2 \, d\xi.
\end{aligned}$$

Using these bounds, we have

$$a_0|\dot{E}_m(t)|_H^2 + (c_2-\epsilon)|E_m(t)|_V^2 + 2c\int_0^t |\dot{E}_m(\xi,0)|^2\ d\xi$$

$$\leq \int_0^t \left\{(\bar{h}+T^2\bar{G})|E_m|_H^2 + (\tfrac{5}{2}+\bar{b})|\dot{E}_m|_H^2 + |\dot{F}|_{V*}^2 + |E_m|_V^2\right\}\ d\xi$$

$$+\bar{a}|E_{1m}|_H^2 + (c_1+1)|E_{0m}|_V^2 + \tfrac{1}{\epsilon}|F(t)|_{V*}^2 + |F(0)|_{V*}^2.$$

Letting

$$H(t) = \bar{a}|E_{1m}|_H^2 + (c_1+1)|E_{0m}|_V^2 + \frac{1}{\epsilon}|F(t)|_{V*}^2 + |F(0)|_{V*}^2 + \int_0^t |\dot{F}|_{V*}^2\ d\xi,$$

and using the definitions of the V and H norms to obtain

$$|E_m|_V^2 \geq |E_m|_H^2,$$

we find

$$a_0|\dot{E}_m(t)|_H^2 + (c_2-\epsilon)|E_m(t)|_V^2 + 2c\int_0^t |\dot{E}_m(\xi,0)|^2\ d\xi$$

$$\leq H(t) + \int_0^t \left\{(1+\bar{h}+T^2\bar{G})|E_m|_V^2 + (\tfrac{5}{2}+\bar{b})|\dot{E}_m|_H^2\right\}\ d\xi.$$

We note that $\left(1+\bar{h}+T^2\bar{G}\right) \geq 1$. Moreover, we can choose ϵ such that $0 < c_2-\epsilon \leq 1$, and

$$\frac{1+\bar{h}+T^2\bar{G}}{c_2-\epsilon} \geq 1.$$

Similarly, $\frac{5}{2}+\bar{b} > 1$ and $a_0 \leq 1$ so that

$$\frac{\frac{5}{2}+\bar{b}}{a_0} > 1.$$

Then,

$$\begin{aligned}
& a_0|\dot{E}_m(t)|_H^2 + (c_2-\epsilon)|E_m(t)|_V^2 + 2c\int_0^t |\dot{E}_m(\xi,0)|^2 \, d\xi \\
\leq \;& H(t) + \int_0^t \left(1+\bar{h}+T^2\bar{G}\right)|E_m|_V^2 + (\tfrac{5}{2}+\bar{b})|\dot{E}_m|_H^2 \, d\xi \\
\leq \;& H(t) + \int_0^t \tfrac{\frac{5}{2}+\bar{b}}{a_0}\left(1+\bar{h}+T^2\bar{G}\right)|E_m|_V^2 + \left(\tfrac{1+\bar{h}+T^2\bar{G}}{c_2-\epsilon}\right)(\tfrac{5}{2}+\bar{b})|\dot{E}_m|_H^2 \, d\xi \\
\leq \;& H(t) + \int_0^t \tfrac{(\frac{5}{2}+\bar{b})\left(1+\bar{h}+T^2\bar{G}\right)}{a_0(c_2-\epsilon)}\left((c_2-\epsilon)\,|E_m|_V^2 + a_0|\dot{E}_m|_H^2\right) \, d\xi.
\end{aligned} \tag{3.17}$$

We recall that the convergence of E_{0m} in V and the convergence of E_{1m} in H imply the boundedness of the sequences in their respective spaces. This, along with A6), yields that $H(t)$ is bounded. Hence we can use Gronwall's inequality to show that $\{E_m\}$ is bounded in $C(0,T;V)$ and $\{\dot{E}_m\}$ is bounded in $C(0,T;H)$. We can thus conclude that $\{\dot{E}_m(\cdot,0)\}$ is bounded in $L^2(0,T)$. It follows that there exist a subsequence $\{E_{m_k}\}$ and limits $E \in L^2(0,T;V)$, $\tilde{E} \in L^2(0,T;H)$, and $E_L \in L^2(0,T)$ such that

$$\begin{aligned}
E_{m_k} &\rightarrow E \text{ weakly in } L^2(0,T;V) \\
\dot{E}_{m_k} &\rightarrow \tilde{E} \text{ weakly in } L^2(0,T;H) \\
\dot{E}_{m_k}(\cdot,0) &\rightarrow E_L \text{ weakly in } L^2(0,T).
\end{aligned}$$

Since $E_{m_k} \in C(0,T;V)$ and $\dot{E}_{m_k} \in C(0,T;V)$, we have

$$E_{m_k}(t) - E_{m_k}(0) - \int_0^t \dot{E}_{m_k}(\xi)\, d\xi = 0$$

in the V norm for all $t \in [0,T)$, and we note that this, of course, holds in the H norm as well.

We also have

$$E_{m_k}(0) = E_{0m_k} \rightarrow E_0$$

in the V sense, and

$$\int_0^t \dot{E}_{m_k}(\xi)\ d\xi \to \int_0^t \tilde{E}(\xi)\ d\xi$$

weakly in H for each $t \in [0,T)$.

We take weak limits in H to obtain

$$\begin{aligned} E(t) &= E_0 + \textstyle\int_0^t \tilde{E}(\xi)\ d\xi \\ E(t,0) &= E_0(0) + \textstyle\int_0^t E_L(\xi)\ d\xi \end{aligned}$$

in the H sense. Thus $\dot{E}(t)$ exists almost everywhere in H with $\dot{E} = \tilde{E} \in L^2(0,T;H)$, while $E(0) = E_0$ and $\dot{E}(t,0) = E_L(t)$ almost everywhere.

We must show that E is in fact a solution to our weak equation. We let $\psi \in C^1(0,T)$ with $\psi(T) = 0$ be arbitrary and let $\psi_j = \psi(t)w_j$ where the $\{w_i\}_{i=0}^{\infty}$ are selected as before. For a fixed j, we have

$$\begin{aligned} &\int_0^T \Big\{ < a\ddot{E}_m, \psi_j >_{V^*,V} + < b\dot{E}_m, \psi_j > + < hE, \psi_j > \\ &+ < \textstyle\int_0^t G(t,s,\cdot)E_m(s,\cdot)\ ds, \psi_j > + c\dot{E}_m(t,0)\psi_j(0) + \sigma_1(E_m,\psi_j) \Big\}\ dt \\ &= \textstyle\int_0^T < F, \psi_j >_{V^*,V}\ dt. \end{aligned}$$

Then we integrate by parts in the first term to obtain

$$\begin{aligned} &\int_0^T \Big\{ - < \dot{E}_m, a\dot{\psi}_j + \dot{a}\psi_j >_{V^*,V} + < b\dot{E}_m, \psi_j > + < hE_m, \psi_j > \\ &+ < \textstyle\int_0^t G(t,s,\cdot)E_m(s,\cdot)\ ds, \psi_j > + c\dot{E}_m(t,0)\psi_j(0) + \sigma_1(E_m,\psi_j) \Big\}\ dt \\ &= \textstyle\int_0^T < F, \psi_j >_{V^*,V}\ dt + < a(0)E_{1m}, \psi_j(0) > \end{aligned}$$

for each ψ_j.

We would like to be able to take weak limits as $m \to \infty$ in the previous equation, but first we must verify that this is possible, particularly in the integral term. We know that $E_m \to E$ weakly in $L^2(0,T;V)$ and $\psi \in C^1(0,T)$. Then for a function $g \in L^\infty(0,T;L^\infty(0,1))$ and any function $w \in V$, we have $g(s,\cdot)w(\cdot) \in H \subset V$ and $g(\cdot,z) \in L^2(0,T)$. So we may conclude that for each t

$$\int_0^T < g(s,\cdot)E_m(s), \psi(t)w > \ ds \to \int_0^T < g(s,\cdot)E(s), \psi(t)w > \ ds.$$

We next consider $G \in L^\infty([0,T] \times [0,T]; L^\infty[0,1])$. Since $E_m \to E$ weakly in $L^2(0,T;V)$, we have that for any $t \in [0,T]$

$$\int_0^T < G(t,s,\cdot)I_{(0,t)}(s)E_m(s), \psi(t)w > \ ds \to$$

$$\int_0^T < G(t,s,\cdot)I_{(0,t)}(s)E(s), \psi(t)w > \ ds.$$

This implies

$$\begin{aligned}
< \textstyle\int_0^t G(t,s,\cdot)E_m(s)\ ds, \psi(t)w > &= \int_0^t < G(t,s,\cdot)E_m(s), \psi(t)w > \ ds \\
&= \int_0^T < G(t,s,\cdot)I_{(0,t)}(s)E_m(s), \psi(t)w > \ ds \\
&\to \int_0^T < G(t,s,\cdot)I_{(0,t)}(s)E(s), \psi(t)w > \ ds \\
&= < \textstyle\int_0^t G(t,s,\cdot)E(s)\ ds, \psi(t)w >
\end{aligned}$$

for each $t \in [0,T]$ and thus by boundedness we have convergence in $L^1(0,T)$.
This convergence, as well as the fact that $\sigma_1(\cdot, \psi_j(t)) \in V^*$, show that we are indeed able to take weak limits in the previous equation. As $m \to \infty$, we have for each j

$$\int_0^T \{- < \dot{E}, a\dot{\psi}_j + \dot{a}\psi_j >_{V^*,V} + < b\dot{E}, \psi_j > + < hE, \psi_j >$$

$$+ < \int_0^t G(t,s,\cdot)E(s,\cdot)\ ds, \psi_j > + c\dot{E}_m(t,0)\psi_j(0) \tag{3.18}$$

$$+\sigma_1(E,\psi_j)\}\ dt = \int_0^T < F, \psi_j >_{V^*,V}\ \ dt + < a(0)E_1, \psi_j(0) > .$$

We restrict ψ to lie in $C_0^\infty(0,T)$ and write

$$\int_0^T -\dot{\psi} < a\dot{E}, w_j >_{V^*,V} -\psi < \dot{a}\dot{E}, w_j > dt + \int_0^T \Big\{ < b\dot{E}, w_j > + < hE, w_j >$$

$$+ < \int_0^t G(t,s,\cdot)E(s,\cdot)\ ds, w_j >$$

$$+ c\dot{E}(t,0)w_j(0) + \sigma_1(E,w_j)\Big\}\ \psi\ dt = \int_0^T < F, w_j >_{V^*,V}\ \psi\ dt$$

for each w_j.

Then we can interpret the first term in the sense of distributions as follows

$$\int_0^T \psi \tfrac{d}{dt} < a\dot{E}, w_j >\ \ dt + \int_0^T \Big\{ - < \dot{a}\dot{E}, w_j > + < b\dot{E}, w_j > + < hE, w_j >$$

$$+ < \int_0^t G(t,s,\cdot)E(s,\cdot)\ ds, w_j >$$

$$+ c\dot{E}(t,0)w_j(0) + \sigma_1(E,w_j)\Big\}\ \psi\ dt = \int_0^T < F, w_j >_{V^*,V}\ \psi\ dt$$

for each w_j.

Thus for each j, the equation

$$\tfrac{d}{dt} < a\dot{E}, w_j > - < \dot{a}\dot{E}, w_j > + < b\dot{E}, w_j > + < hE, w_j >$$

$$+ < \int_0^t G(t,s,\cdot)E(s,\cdot)\ ds, w_j > + c\dot{E}(t,0)w_j(0) + \sigma_1(E,w_j) \tag{3.19}$$

$$= < F, w_j >_{V^*,V}$$

holds in the $L^2(0,T)$ sense.

Since $\{w_j\}$ is total in V, this implies that $\ddot{E} \in L^2(0,T;V^*)$. Furthermore, upon observing that

$$< a\ddot{E}, \phi >= \frac{d}{dt} < a\dot{E}, \phi > - < \dot{a}\dot{E}, \phi >,$$

we have for all $\phi \in V$

$$< a\ddot{E}, \phi >_{V^*,V} + < b\dot{E}, \phi > + < hE, \phi > + < \int_0^t G(t,s,\cdot)E(s,\cdot)\, ds, \phi >$$

$$+c\dot{E}(t,0)\phi(0) + \sigma_1(E,\phi) =< F, \phi >_{V^*,V}$$

which is our original equation (3.10).

Now we have that $E(0,z) = E_0(z)$, but we need to show $\dot{E}(0,z) = E_1(z)$. We recall that (3.18) holds for all $\psi_j = \psi w_j$ with $\psi \in C^1(0,T)$ and $\psi(T) = 0$. Then if we integrate by parts in the first term, we have

$$\int_0^T < a\ddot{E}, \psi_j > \; dt - < a\dot{E}, \psi_j > |_{t=0}^{t=T} + \int_0^T \Big\{ < b\dot{E}, \psi_j > + < hE, \psi_j >$$

$$+ < \int_0^t G(t,s,\cdot)E(s,\cdot)\, ds, \psi_j > + c\dot{E}(t,0)\phi_j(0) + \sigma_1(E,\psi_j) \Big\} \; dt$$

$$= \int_0^T < F, \psi_j >_{V^*,V} \; dt + < a(0)E_1, \psi_j(0) > .$$

Recalling (3.19), we can thus conclude that

$$- < a\dot{E}, \psi_j > |_{t=0}^{t=T} =< a(0)E_1, \psi_j(0) >,$$

or, since $a(z) \geq a_0 > 0$ and $\psi_j(T) = 0$,

$$< \dot{E}(0), \psi_j(0) > \;\; = \;\; < E_1, \psi_j(0) > \;\; \text{or}$$

$$< \dot{E}(0), w_j > \psi(0) \;\; = \;\; < E_1, w_j(0) > \psi(0).$$

Since this holds for all j and $\psi(0)$ is arbitrary, we have $\dot{E}(0) = E_1$, and E is in fact a solution of the system (3.10).

The next step is to show that our solution is unique. It suffices to show that $E = 0$ is the only solution that corresponds to the zero initial conditions $E_0 = E_1 = 0$ and zero forcing function $F = 0$. We begin by assuming E is a solution corresponding to zero initial data and zero forcing function. For all $\phi \in V$, this solution E satisfies

$$< a\ddot{E}, \phi >_{V^*,V} + < b\dot{E}, \phi > + < hE, \phi >$$

$$+ < \int_0^t G(t,s,\cdot)E(s,\cdot)\ ds, \phi > + c\dot{E}(t,0)\phi(0) + \sigma_1(E,\phi) = 0.$$

We define $\psi_s(t)$ for $t, s \in [0,T]$ by

$$\psi_s(t) = \begin{cases} -\int_t^s E(\xi)\ d\xi, & t < s \\ 0, & t \geq s \end{cases}$$

and note that $\dot{\psi}_s(t) = E(t)$ and $\psi_s(T) = \psi_s(s) = 0$. Since $\psi_s(t) \in V$, we can choose $\phi = \psi_s(t)$ to obtain

$$\begin{aligned} &< a\ddot{E}, \psi_s >_{V^*,V} + < b\dot{E}, \psi_s > + < hE, \psi_s > \\ &+ < \int_0^t G(t,\xi,\cdot)E(\xi,\cdot)\ d\xi, \psi_s > + c\dot{E}(t,0)\psi_s(t)(0) + \sigma_1(E,\psi_s) = 0. \end{aligned} \tag{3.20}$$

Integrating this equation and considering some of the terms separately, we find

$$
\begin{aligned}
2\int_0^s < a\ddot{E}, \psi_s > \ dt &= -2\int_0^s \left(< a\dot{E}, E > + < \dot{a}\dot{E}, \psi_s > \right) \ dt \\
&= \int_0^s \left(-\tfrac{d}{dt}|\sqrt{a}E|_H^2 + < \dot{a}E, E > -2 < \dot{a}\dot{E}, \psi_s > \right) \ dt \\
&= -|\sqrt{a}(s)E(s)|_H^2 + \int_0^s \left(< \dot{a}E, E > +2 < E, \tfrac{d}{dt}(\dot{a}\psi_s) > \right) \ dt \\
&= -|\sqrt{a}(s)E(s)|_H^2 \\
&\quad + \int_0^s (< \dot{a}E, E > +2 < \ddot{a}E, \psi_s > +2 < \dot{a}E, E >) \ dt \\
&= -|\sqrt{a}(s)E(s)|_H^2 + \int_0^s (3 < \dot{a}E, E > +2 < \ddot{a}E, \psi_s >) \ dt,
\end{aligned}
$$

$$
2\int_0^s \sigma_1(E, \psi_s) \ dt = \int_0^s \frac{d}{dt}\sigma_1(\psi_s, \psi_s) \ dt = -\sigma_1(\psi_s(0), \psi_s(0)),
$$

$$
\int_0^s \left(\dot{E}(t,0)\psi_s(t)(0) + |E(t,0)|^2 \right) \ dt = \int_0^s \frac{d}{dt} \left(E(t,0)\psi_s(t)(0) \right) = 0,
$$

and

$$
\begin{aligned}
\int_0^s \tfrac{d}{dt} < bE, \psi_s > \ dt &= \int_0^s \left(< b\dot{E}, \psi_s > + < \dot{b}E, \psi_s > + < bE, E > \right) \ dt \\
&= \int_0^s \left(< b\dot{E}, \psi_s > + < \dot{b}E, \psi_s > + |\sqrt{b}E|_H^2 \right) \ dt \\
&= 0.
\end{aligned}
$$

Using these relationships, we obtain from the integrated form of (3.20)

$$
\begin{aligned}
&|\sqrt{a}E(s)|_H^2 + \sigma_1(\psi_s(0), \psi_s(0)) + \int_0^s 2c|E(t,0)|^2 \ dt = \\
&\int_0^s \Big(3 < \dot{a}E, E > +2 < \ddot{a}E, \psi_s > +2 < -\dot{b}E, \psi_s > -2|\sqrt{b}E|_H^2 \\
&+2 < hE, \psi_s > +2 < \int_0^t G(t, \xi, \cdot)E(\xi, \cdot) \ d\xi, \psi_s > \Big) \ dt.
\end{aligned} \tag{3.21}
$$

We may next use some of the previous assumptions on our coefficients to make the following estimates.

We note that

$$\int_0^s 3 < \dot{a}E, E > \ dt \leq 3|\dot{a}|_{L^\infty} \int_0^s |E|_H^2 \ dt$$

and

$$\int_0^s 2 < \ddot{a}E, \psi_s > \ dt \leq |\ddot{a}|_{L^\infty}^2 \int_0^s |E|_H^2 \ dt + \int_0^s |\psi_s|_H^2 \ dt.$$

Thus from Hypothesis A1), we have that there exists an $\alpha > 0$ such that for $s < T$

$$\int_0^s 3 < \dot{a}E, E > +2 < \ddot{a}E, \psi_s > \ dt \leq \int_0^s \left\{\alpha |E|_H^2 + |\psi_s|_H^2\right\} \ dt.$$

Moreover, we note that

$$\int_0^s -2|\sqrt{b(t,\cdot)}E(t,\cdot)|_H^2 \ dt \leq 2|b|_{L^\infty} \int_0^s |E(t,\cdot)|_H^2 \ dt$$

and

$$\int_0^s 2 < -\dot{b}E, \psi_s > \ dt \leq |\dot{b}|_{L^\infty}^2 \int_0^s |E(t,\cdot)|_H^2 \ dt + \int_0^s |\psi_s|_H^2 \ dt.$$

Then, as a consequence of A2), there exists a $\beta > 0$ such that for $s \leq T$ we have

$$\int_0^s \left\{-2|\sqrt{b(t,\cdot)}E(t,\cdot)|_H^2 + 2 < -\dot{b}E, \psi_s >\right\} \ dt \leq \int_0^s \beta |E(t,\cdot)|_H^2 + |\psi_s|_H^2 \ dt.$$

We next substitute these bounds, as well as some of those established previously, into (3.21) to obtain the inequality

$$|\sqrt{a}E(s)|_H^2 + \sigma_1(\psi_s(0), \psi_s(0)) \leq \int_0^s \left\{(\alpha + \beta + \bar{h} + T^2\bar{G})|E|_H^2 + 4|\psi_s|_H^2\right\} \ dt.$$

Furthermore, we note that

$$\begin{aligned}
\int_0^s |\psi_s|_H^2 \, dt &= \int_0^s \int_0^1 \left(\int_t^s E(\xi, z) \, d\xi \right)^2 \, dz \, dt \\
&\leq \int_0^s \int_0^1 \left(T^{\frac{1}{2}} |E(\cdot, z)|_{L^2(t,s)} \right)^2 \, dz \, dt \\
&\leq T \int_0^s \int_0^1 \int_0^s |E(\xi, z)|^2 \, d\xi \, dz \, dt \\
&\leq T^2 \int_0^s |E(t)|_H^2 \, dt.
\end{aligned}$$

Then, we have

$$|\sqrt{a} E(s)|_H^2 + \sigma_1(\psi_s(0), \psi_s(0)) \leq \int_0^s (\alpha + \beta + \bar{h} + T^2 \bar{G} + 4T^2) |E(t)|_H^2 \, dt,$$

from which it follows that

$$a_0 |E(s)|_H^2 \leq \int_0^s (\alpha + \beta + \bar{h} + T^2 \bar{G} + 4T^2) |E(t)|_H^2 \, dt.$$

Finally, using Gronwall's inequality, we have $|E(s)|_H^2 = 0$ for all $s \in [0, T]$.

This establishes uniqueness of solutions.

The final step is to establish that the solution depends continuously on the initial conditions and forcing function. To begin, we let

$$H_m = \bar{a} |E_{1m}|_H^2 + (c_1 + 1) |E_{0m}|_V^2 + \frac{1}{\epsilon} |F|_{L^\infty(0,T;V^*)}^2 + |F(0)|_{V^*}^2 + |\dot{F}|_{L^2(0,T;V^*)}^2.$$

Then from (3.17) we have

$$\begin{aligned}
&a_0 |\dot{E}_m(t)|_H^2 + (c_2 - \epsilon) |E_m(t)|_V^2 \\
&\leq H_m + \frac{(\frac{5}{2} + \bar{b})(1 + \bar{h} + T^2 \bar{G})}{a_0 (c_2 - \epsilon)} \int_0^t \left((c_2 - \epsilon) |E_m|_V^2 + a_0 |\dot{E}_m|_H^2 \right) \, d\xi.
\end{aligned}$$

By use of Gronwall's inequality, we have

$$a_0|\dot{E}_m(t)|_H^2 + (c_2-\epsilon)|E_m(t)|_V^2 \leq H_m \exp\left(\frac{(\frac{5}{2}+\bar{b})\left(1+\bar{h}+T^2\bar{G}\right)}{a_0\,(c_2-\epsilon)}T\right) = H_m K_1.$$

If we integrate over the interval $(0,T)$, we have

$$a_0|\dot{E}_m|_{L^2(0,T;H)}^2 + (c_2-\epsilon)|E_m|_{L^2(0,T;V)}^2 \leq H_m K_2.$$

We next use the fact that as $m \to \infty$, $E_{0m} \to E_0$ and $E_{1m} \to E_1$, the weak convergences established previously, and the weak lower semicontinuity of norms to conclude that

$$a_0|\dot{E}|_{L^2(0,T;H)}^2 + (c_2-\epsilon)|E|_{L^2(0,T;V)}^2$$

$$\leq \left(\bar{a}|E_1|_H^2 + (c_1+1)|E_0|_V^2 + (1+\tfrac{1}{\epsilon})|F|_{L^\infty(0,T;V^*)}^2 + |\dot{F}|_{L^2(0,T;V^*)}^2\right) K_2.$$

Since the mapping $(E_0, E_1, F, \dot{F}) \to (E, \dot{E})$ is linear, we thus have continuous dependence on the initial data and forcing function. Summarizing, we have proven the result:

Theorem 1: Under assumptions A1)-A6), the system (3.10) possesses a unique solution and $(E, \dot{E})$ depends continuously on initial data (E_0, E_1) and forcing function F from

$(E_0, E_1, F) \in V \times H \times H^1(0,T;V^*)$ to $(E, \dot{E}) \in L^2(0,T;V) \times L^2(0,T;H)$.

Remark: If we restrict the form of the forcing function F so that $F(t,z) = \delta(z)g(t)$ (see Chapter 2), where $\delta(z)$ is the usual Dirac delta function, we may relax the smoothness condition on F from $F \in H^1(0,T;V^*)$ to $F \in L^2(0,T;V^*)$. That is, if we replace A6) with the assumption

A6′) The forcing functions F is of the form $F(t,z) = \delta(z)g(t)$, where $\delta(z)$ is the usual Dirac delta function and $g \in L^2(0,T)$.

we may prove the following result:

Theorem 1(a): Under assumptions A1)-A6′), the system (3.10) possesses a unique solution and $(E, \dot{E})$ depends continuously on initial data (E_0, E_1) and forcing function F from
$(E_0, E_1, F) \in V \times H \times L^2(0,T;V^*)$ to $(E, \dot{E}) \in L^2(0,T;V) \times L^2(0,T;H)$.

3.1.2 Well-posedness of solutions to the system with pressure-dependent Debye polarization

In this section we apply the results of Section 3.1 to establish the well-posedness of the Debye polarization model with pressure-dependent coefficients. We consider (3.6) and (3.7) using the definitions of V, H, V^* and σ_1 given in Section 1. We recall that V,H, and V^* form a Gelfand triple as described in Section 2. Moreover, we note that σ_1 as defined in (3.2) is V-continuous and V-elliptic. The following discussion establishes the validity of hypotheses A1)-A6).

We first outline some assumptions about our pressure wave.

P1) The pressure wave p in (3.5) is in $H^1(0,T;V)$ so that p is in the space
$C(0,T;C[0,1])$ and hence in $L^\infty(0,T;L^\infty[0,1])$.

P2) The derivatives of the pressure wave, $\dot{p}$ and $\ddot{p}$, are in $L^\infty(0,T;L^\infty[0,1])$. (See [18] and [17] for details regarding the regularity of p.)

We use these assumptions and the conditions on the admissible parameter set Q to verify that A1)-A6) hold for the Debye example.

A1) The coefficient a is in $L^\infty(0,T;L^\infty[0,1])$, as are its derivatives $\dot{a}$ and $\ddot{a}$, and for all $(t,z) \in [0,T] \times [0,1]$, $a(t,z) \geq a_0$, for some $a_0 > 0$.

Proof: Recall that

$$a(t,z) = 1 + (\epsilon_\infty - 1)I_{(z_1,1)} = 1 + (\zeta_0 + \kappa_\zeta p(t,z) - 1)I_{(z_1,1)}.$$

We note that p, $\dot{p}$, and $\ddot{p}$ are all assumed to be $L^\infty(0,T;L^\infty[0,1])$ functions. From the form of a, we therefore have a, $\dot{a}$, and $\ddot{a}$ in $L^\infty(0,T;L^\infty[0,1])$.

We also have for $(t,z) \in [0,T] \times [0,z_1)$, $a(t,z) = 1 > 0$. Moreover, for $(t,z) \in [0,T] \times [z_1,1]$, $a(t,z) = \zeta_0 + \kappa_\zeta p(t,z) > \delta > 0$.

A2) The coefficient b is in $L^\infty(0,T;L^\infty[0,1])$ and $b(t,z) \geq 0$ for all $(t,z) \in [0,T]\times[0,1]$. Additionally, the time derivative of b, $\dot{b}$, exists and is in $L^\infty(0,T;L^\infty[0,1])$.

Proof: Again recall

$$b(t,z) = \left(\frac{\sigma}{\epsilon_0} + \frac{(\gamma_0 - \zeta_0 + (\kappa_\gamma - \kappa_\zeta)p(t,z))}{(\tau_0 + \kappa_\tau p(t,z))} \right) I_{(z_1,1)}.$$

We recall the restrictions placed on $\kappa_\gamma, \kappa_\zeta$, and κ_τ and conclude that b is strictly positive in $[0,T] \times (z_1,1]$. Thus, $b(t,z) \geq 0$ for all $(t,z) \in [0,T] \times [0,1]$.

Since $p \in L^\infty(0,T;L^\infty[0,1])$, we have that $\gamma_0 - \zeta_0 + (\kappa_\gamma - \kappa_\zeta)p \in L^\infty(0,T;L^\infty[0,1])$. Moreover, since $\tau_0 + \kappa_\tau p > \delta$ for all $(t,z) \in [0,T] \times [0,1]$, we know $(\tau_0 + \kappa_\tau p)^{-1} \in L^\infty(0,T;L^\infty[0,1])$.

Hence b is bounded, and $b \in L^\infty(0,T;L^\infty[0,1])$.

Next, we have

$$\dot{b}(t,z) =$$

$$\left(\frac{((\kappa_\gamma - \kappa_\zeta)\dot{p}(t,z))\,(\tau_0 + \kappa_\tau p(t,z)) - (\gamma_0 - \zeta_0 + (\kappa_\gamma - \kappa_\zeta)p(t,z))\,(\kappa_\tau \dot{p}(t,z))}{(\tau_0 + \kappa_\tau p(t,z))^2} \right) I_{(z_1,1)}$$

Since $(\tau_0 + \kappa_\tau p)^{-2}$, $\tau_0 + \kappa_\tau p, \gamma_0 - \zeta_0 + (\kappa_\gamma - \kappa_\zeta)p, (\kappa_\gamma - \kappa_\zeta)\dot{p}$, and $\kappa_\tau \dot{p}$ are all in $L^\infty(0,T;L^\infty[0,1])$, we can conclude that $\dot{b} \in L^\infty(0,T;L^\infty[0,1])$.

A3) The coefficient h is in $L^\infty(0,T;L^\infty[0,1])$.

Proof: From the definition

$$h(t,z) = \left(\frac{(\kappa_\gamma - \kappa_\zeta)\dot{p}(t,z)}{(\tau_0 + \kappa_\tau p(t,z))} - \frac{(1 + \kappa_\tau \dot{p}(t,z))\,(\gamma_0 - \zeta_0 + (\kappa_\gamma - \kappa_\zeta)p(t,z))}{(\tau_0 + \kappa_\tau p(t,z))^2} \right) I_{(z_1,1)}.$$

Since $(\tau_0 + \kappa_\tau p)^{-1}$ and $(\kappa_\gamma - \kappa_\zeta)\dot{p}$ are in $L^\infty(0,T;L^\infty[0,1])$, we have $(\kappa_\gamma - \kappa_\zeta)\dot{p}\,(\tau_0 + \kappa_\tau p)^{-1}$ is in $L^\infty(0,T;L^\infty[0,1])$.

In the same way, since $\gamma_0 - \zeta_0 + (\kappa_\gamma - \kappa_\zeta)p$ and $\kappa_\tau \dot{p}$ are in $L^\infty(0,T;L^\infty[0,1])$, and $(\tau_0 + \kappa_\tau p)^{-2} < \delta^{-2}$, we have $(1 + \kappa_\tau \dot{p})\,(\gamma_0 - \zeta_0 + (\kappa_\gamma - \kappa_\zeta)p)\,(\tau_0 + \kappa_\tau p)^{-2}$ is in $L^\infty(0,T;L^\infty[0,1])$. Therefore, we have h in $L^\infty(0,T;L^\infty[0,1])$.

A4) The kernel function G is in $L^\infty([0,T]\times[0,T];L^\infty[0,1])$.

Proof: The Debye kernel is given by

$$G(t,s,z) =$$

$$\frac{(1+\kappa_\tau \dot{p}(t,z))\,(\gamma_0 - \zeta_0 + (\kappa_\gamma - \kappa_\zeta)p(s,z))}{(\tau_0 + \kappa_\tau p(t,z))^2\,(\tau_0 + \kappa_\tau p(s,z))} \exp\left(\int_s^t \frac{-d\xi}{\tau_0 + \kappa_\tau p(\xi,z)}\right) I_{(z_1,1)}.$$

First, we note that

$$\frac{(1+\kappa_\tau \dot{p}(t,z))\,(\gamma_0 - \zeta_0 + (\kappa_\gamma - \kappa_\zeta)p(s,z))}{(\tau_0 + \kappa_\tau p(t,z))^2\,(\tau_0 + \kappa_\tau p(s,z))} \in L^\infty([0,T]\times[0,T];L^\infty[0,1]).$$

Since $(\tau_0 + \kappa_\tau p(\cdot,z))^{-1} \in C(0,T)$, we know that

$$\int_s^t \frac{-d\xi}{\tau_0 + \kappa_\tau p(\xi,z)}$$

is absolutely continuous in t and in s, hence

$$\exp\left(\int_s^t \frac{-d\xi}{\tau_0 + \kappa_\tau p(\xi,z)}\right)$$

is in $L^\infty([0,T]\times[0,T])$.

Hence we may conclude that $G \in L^\infty([0,T]\times[0,T];L^\infty[0,1])$.

It is clear from the definition $c^2 = 1/\epsilon_0\mu_0$ that c^2 satisfies A5). Furthermore, by an appropriate choice of the source current J_s, we may guarantee that A6) holds and the forcing function defined by $F(t,z) = -\frac{1}{\epsilon_0}\dot{J}_s(t)$ is in $H^1(0,T,V^*)$.

With A1)-A6) satisfied by the pressure-dependent Debye polarization model, we may apply the theory in Section 3.1 and conclude that the system is well-posed.

3.1.3 Well-posedness of solutions to the system with pressure-dependent Lorentz polarization

In this section, we address the assumptions outlined in Section 3.1 in the context of the well-posedness of the Lorentz polarization model with pressure-dependent coefficients. Here we consider (3.6) with the functions given in (3.7). Again, we use the definitions of V, H, V^*, which form a Gelfand triple, and the V-continuous and V-elliptic σ_1 given in Section 3.1. We assume that assumptions P1)-P2) in Section 3.1.2 hold and our admissible parameter set Q is as defined previously.

We verify that A1)-A6) hold for the Lorentz example under these assumptions.

A1) The coefficient a is in $L^\infty(0,T;L^\infty[0,1])$, as are its derivatives $\dot{a}$ and $\ddot{a}$, and for all $(t,z) \in [0,T] \times [0,1]$, $a(t,z) \geq a_0$, for some $a_0 > 0$.

Proof: Since the coefficient a is the same in (3.7) and (3.8), we know that A1) holds.

A2) The coefficient b is in $L^\infty(0,T;L^\infty[0,1])$ and $b(t,z) \geq 0$ for all $(t,z) \in [0,T]\times[0,1]$. Additionally, the time derivative of b, $\dot{b}$, exists and is in $L^\infty(0,T;L^\infty[0,1])$.

Proof: Since

$$b(t,z) = \frac{\sigma}{\epsilon_0} I_{(z_1,1)}$$

is piecewise constant, it is clear that b and $\dot{b}$ are $L^\infty(0,T;L^\infty[0,1])$ functions.

A3) The coefficient h is in $L^\infty(0,T;L^\infty[0,1])$.

Proof: We recall that

$$h(t,z) = \frac{1}{\epsilon_0}\left(\epsilon_0(\alpha_0 + \kappa_\alpha p(t,z))(\gamma_0 - \zeta_0 + (\kappa_\gamma - \kappa_\varsigma)p(t,z))\right) I_{(z_1,1)}.$$

Since $\alpha_0 + \kappa_\alpha p$ and $\gamma_0 - \zeta_0 + (\kappa_\gamma - \kappa_\zeta)p$ are in $L^\infty(0,T;L^\infty[0,1])$, we know that $h \in L^\infty(0,T;L^\infty[0,1])$.

A4) The kernel function G is in $L^\infty([0,T]\times[0,T];L^\infty[0,1])$.

Proof: The Lorentz kernel is given by

$$\begin{aligned} G(t,s,z) &= \frac{-1}{\epsilon_0}\Big(\frac{1}{\tau_0+\kappa_\tau p(t,z)}\Phi_{21}(t,s) + (\alpha_0+\kappa_\alpha p(t,z))\Phi_{11}(t,s)\Big) \\ &\quad \times\Big(\epsilon_0(\alpha_0+\kappa_\alpha p(s,z))(\gamma_0-\zeta_0+(\kappa_\gamma-\kappa_\zeta)p(s,z))\Big)I_{(z_1,1)}. \end{aligned}$$

We recall that ordinary differential equations theory coupled with the continuity of p guarantees the continuity of Φ_{11} and $\Phi 21$. Moreover we have that $(\tau_0+\kappa_\tau p)^{-1} < \delta^{-1}$ and $(\alpha_0+\kappa_\alpha p)$ and $(\gamma_0-\zeta_0+(\kappa_\gamma-\kappa_\zeta)p)$ are continuous functions. We may conclude from this that G is a $L^\infty([0,T]\times[0,T];L^\infty[0,1])$ function.

We note that the definitions of c^2 and $F(t,z)$ are unchanged from Section 3.1.2, so we may conclude that A5)-A6) are satisfied.

We now know that A1)-A6) are satisfied by the pressure-dependent Lorentz polarization model; thus we may conclude that the system is well-posed based on the theory in Section 3.1.

3.2 Enhanced regularity of solutions

In Section 3.1, we show that unique solutions $E \in L^2(0,T;V)$ and $\dot{E} \in L^2(0,T;H)$ exist for the variational form

$$\begin{gathered} < a\ddot{E}(t), \phi >_{V^*,V} + < b\dot{E}(t), \phi > + < hE(t), \phi > \\ + < \int_0^t G(t,s,\cdot)E(s,\cdot)\, ds, \phi > \\ +c\dot{E}(t,0)\phi(0) + \sigma_1(E(t),\phi) =< F(t), \phi >_{V^*,V}, \\ E(0,z) = E_0(z) \quad \dot{E}(0,z) = E_1(z) \end{gathered} \tag{3.22}$$

for all $\phi \in V$ where $V = H_R^1(0,1) \equiv \{\phi \in H^1(0,1) : \phi(1) = 0\}$ and $H = L^2(0,1)$. This existence holds provided that $E_0 \in V$ and $E_1 \in H$, Assumptions A1)-A6) given in Section 3.1 are satisfied, and the sesquilinear form σ_1 is V-elliptic and V-continuous. This theory not only establishes well-posedness for a class of partial differential equations, but it provides a foundation for the parameter estimation problem described in Chapter 5. The ability to estimate parameters is critical to the success of interrogation techniques. As we shall see in Section 3.3 however, the theoretical results on which the parameter estimation problem is based rely on the assumption that the solution to (3.22) has enhanced regularity, namely that $\ddot{E} \in L^2(0,T;H)$ or $E \in H^2(0,T;H)$. This improved regularity can be readily established under some additional assumptions.

In this section, we develop arguments for the enhanced regularity of the system (3.22). We begin by describing the additional assumptions required. We then proceed to use these assumptions and those detailed in Section 3.1 to demonstrate the enhanced regularity of the solution. Finally, we discuss the additional assumptions in the context of the Debye and Lorentz-based systems in Sections 3.2.2-3.2.3.

3.2.1 Enhanced regularity of solutions to general variational form

The arguments presented in this section follow those given in [7] and [20]. As in Section 3.1, we take $H = L^2(0,1)$ and $V = H_R^1(0,1) \equiv \{\phi \in H^1(0,1) : \phi(1) = 0\}$ to be Hilbert spaces that form a Gelfand triple $V \hookrightarrow H \hookrightarrow V^*$ with the dual space V^*. We denote the usual duality product by $< \cdot, \cdot >_{V^*,V}$. Inner products $< \cdot, \cdot >$ and norms $| \cdot |$ written without subscripts are assumed to be in H. Moreover, we assume that A1)-A6) hold and that the sesquilinear form σ_1 is V-continuous and V-elliptic. In addition to Assumptions A1)-A6) we make some further assumptions about the coefficients:

A7) The second time derivative, $\ddot{b}$, of b is in $L^\infty(0,T;L^\infty[0,1])$.

A8) The first and second time derivatives, $\dot{h}$ and $\ddot{h}$, of h are in $L^\infty(0,T;L^\infty[0,1])$.

A9) The first and second derivatives with respect to the first temporal variable, $\frac{d}{dt}G$ and $\frac{d^2}{dt^2}G$, of the kernel function G are in $L^\infty((0,T)\times(0,T);L^\infty[0,1])$.

A10) The forcing function F is in $H^2(0,T,V^*)$ and is of the form $F(t,z) = \tilde{g}(t)\delta(z)$ with $\tilde{g}(t) \in H^2(0,T)$ and $\tilde{g}(0) = \dot{\tilde{g}}(0) = 0$. (This assumption may replace A6).)

In addition, we assume that $E_0 \in H_R^3(0,1)$ and $E_1 \in H_R^2(0,1)$, with the consistency conditions $E_1(0) = cE_0'(0)$ and $E_1'(0) = cE_0''(0)$. (We note that these conditions are satisfied trivially by the initial conditions used in our computations, $E_0 = E_1 = 0$.)

In order to show that the solutions to (3.22) have enhanced regularity under the additional assumptions and restrictions, we smooth the given data, E_0, E_1, and F, and argue that the solutions corresponding to the new system possess the desired regularity. We then show that as the smoothing parameter tends to zero, the solutions corresponding to the smoothed system tend to the solutions of the original system.

We let our smoothing parameter Δ be arbitrary in $(0, z_1)$. Using the previous assumptions for E_0, E_1 and $\tilde{g}$, we may define functions $\tilde{g}_\Delta \in H^3(0,T)$, $E_{\Delta 0} \in H_R^3(0,1)$, and

$E_{\Delta 1} \in H^2_R(0,1)$ such that

$$\begin{aligned} \tilde{g}_\Delta(0) &= \tilde{g}(0), \qquad E_{\Delta 1}(0) = E_1(0), \qquad E_{\Delta 0}(0) = E_0(0), \\ \dot{\tilde{g}}_\Delta(0) &= \dot{\tilde{g}}(0), \qquad E'_{\Delta 1}(0) = E'_1(0), \qquad E'_{\Delta 0}(0) = E'_0(0), \end{aligned}$$

with

$$|\tilde{g}_\Delta - \tilde{g}|_{H^2(0,T)} \leq \Delta, \qquad |E_{\Delta 0} - E_0|_{H^2(0,1)} \leq \Delta, \qquad |E_{\Delta 1} - E_1|_{H^1(0,1)} \leq \Delta.$$

We approximate the forcing function by

$$F_\Delta(t,z) = \begin{cases} \frac{2(\Delta - z)}{\Delta^2} \tilde{g}_\Delta(t), & z \in [0, \Delta] \\ 0, & z \in (\Delta, 1], \end{cases}$$

and note that

$$|F - F_\Delta|_{H^2(0,T;V^*)} \to 0 \text{ as } \Delta \to 0.$$

We now consider the resulting smoothed problem, which is analogous to equation (3.22). From the theory in Section 3.1, we know that there exists a unique solution $E_\Delta \in H^2(0,T;V^*) \cap H^1(0,T;H) \cap L^2(0,T;V)$ such that

$$\begin{aligned} &< a\ddot{E}_\Delta(t), \phi >_{V^*,V} + < b\dot{E}_\Delta(t), \phi > + < hE_\Delta(t), \phi > \\ &+ < \textstyle\int_0^t G(t,s,\cdot) E_\Delta(s,\cdot)\, ds, \phi > + c\dot{E}_\Delta(t,0)\phi(0) + \sigma_1(E_\Delta(t), \phi) \\ &=< F_\Delta(t), \phi >_{V^*,V} \end{aligned} \tag{3.23}$$

holds for all $\phi \in V$ and almost every $t \in (0,T)$. Moreover the initial conditions

$$E_\Delta(0,z) = E_{\Delta 0}(z) \quad \dot{E}_\Delta(0,z) = E_{\Delta 1}(z) \tag{3.24}$$

are satisfied for z in $(0,1)$.

We now show that this solution has the additional smoothness

$$E_\Delta \in H^3(0,T;V^*) \cap H^2(0,T;H) \cap H^1(0,T;V).$$

We first differentiate (3.23) with respect to t. We express the new equation in terms of u_Δ, where $u_\Delta = \dot{E}_\Delta$. Subsequently

$$E_\Delta(t) = E_{\Delta 0} + \int_0^t u_\Delta(s)\ ds.$$

The resulting equation is

$$\begin{aligned}
&< a\ddot{u}_\Delta(t), \phi > + < (\dot{a}+b)\dot{u}_\Delta(t), \phi > + < (\dot{b}+h)u_\Delta(t), \phi > \\
&+ < (\dot{h} + G(t,t)) \textstyle\int_0^t u_\Delta(s)\ ds, \phi > \\
&+ < \textstyle\int_0^t \frac{d}{dt}G(t,s,\cdot) \int_0^s u_\Delta(\xi,\cdot)\ d\xi\ ds, \phi > \\
&+ < \left(\dot{h} + G(t,t) + \textstyle\int_0^t \frac{d}{dt}G(t,s,\cdot)\ ds\right) E_{\Delta 0}, \phi > + c\dot{u}_\Delta(t,0)\phi(0) \\
&+ \sigma_1(u_\Delta(t), \phi) = < \dot{F}_\Delta(t), \phi >
\end{aligned} \tag{3.25}$$

with the corresponding initial conditions

$$
\begin{aligned}
u_\Delta(0,z) &= E_{\Delta 1}(z) \\
\dot{u}_\Delta(0,z) &= \frac{1}{a(0,z)}\Big(- b(0,z)\dot{E}_\Delta(0,z) - h(0,z)E_\Delta(0,z) - c\dot{E}_\Delta(0,0) \\
&\quad + c^2 E''_\Delta(0,z) - c^2 E'_\Delta(0,z)|_{z=0}^{z=1}\Big) \\
&= \frac{1}{a(0,z)}\Big(- b(0,z)E_{\Delta 1}(z) - h(0,z)E_{\Delta 0}(z) - cE_{\Delta 1}(0) \\
&\quad + c^2 E''_{\Delta 0}(z) - c^2 E'_{\Delta 0}(1) + c^2 E'_{\Delta 0}(0)\Big) \qquad (3.26) \\
&= \frac{1}{a(0,z)}\Big(- b(0,z)E_{\Delta 1}(z) - h(0,z)E_{\Delta 0}(z) - c^2 E'_{\Delta 0}(0) \\
&\quad + c^2 E''_{\Delta 0}(z) + c^2 E'_{\Delta 0}(0)\Big) \\
&= \frac{1}{a(0,z)}\Big(- b(0,z)E_{\Delta 1}(z) - h(0,z)E_{\Delta 0}(z) + c^2 E''_{\Delta 0}(z)\Big) \\
&\equiv Z_\Delta(z).
\end{aligned}
$$

We note that these conditions are derived using the consistency conditions and the fact that $a(0,z) > 0$ and $F_\Delta(0,z) = 0$.

We mention that, except for the term

$$< \int_0^t \frac{d}{dt} G(t,s,\cdot) \int_0^s u_\Delta(\xi,\cdot)\, d\xi\, ds, \phi >, \qquad (3.27)$$

equation (3.25) is in the same form as (3.22), for which we have well-posedness results. Using Assumptions A1)-A9) and arguments similar to those behind Theorem 1 in Section 3.1 one can show that (3.25)-(3.26) is well-posed despite the inclusion of the term (3.27). Thus there exists a unique solution $u_\Delta \in H^2(0,T;V^*) \cap H^1(0,T;H) \cap L^2(0,T;V)$ such that equations (3.25)-(3.26) are satisfied.

We now must verify that the solution u_Δ to (3.25)-(3.26) is, in fact, $\dot{E}_\Delta$. We first integrate (3.25) with respect to t to obtain

$$\begin{aligned}
&< \textstyle\int_0^t a\ddot{u}_\Delta(s)\ ds, \phi > + < \int_0^t (\dot{a}+b)\dot{u}_\Delta(s)\ ds, \phi > \\
&+ < \textstyle\int_0^t (\dot{b}+h)u_\Delta(s)\ ds, \phi > + < \int_0^t (\dot{h}+G(s,s)) \int_0^s u_\Delta(\xi)\ d\xi\ ds, \phi > \\
&+ < \textstyle\int_0^t \int_0^s \frac{d}{ds}G(s,\xi,\cdot) \int_0^\xi u_\Delta(r,\cdot)\ dr\ d\xi\ ds, \phi > \\
&+ < \textstyle\int_0^t \left(\dot{h} + G(s,s) + \int_0^s \frac{d}{ds}G(s,\xi,\cdot)\ d\xi\right)\ ds\ E_{\Delta 0}, \phi > \\
&+c \textstyle\int_0^t \dot{u}_\Delta(s,0)\ ds\ \phi(0) + \sigma_1(\int_0^t u_\Delta(s)\ ds, \phi) =< F_\Delta(t), \phi > .
\end{aligned} \tag{3.28}$$

We define a function v_Δ by

$$\begin{aligned}
v_\Delta(t) &= E_{\Delta 0} + \textstyle\int_0^t u_\Delta(s)\ ds \\
\dot{v}_\Delta(t) &= \textstyle\frac{d}{dt}\int_0^t u_\Delta(s)\ ds = u_\Delta(t) \\
\ddot{v}_\Delta(t) &= \dot{u}_\Delta(t) \\
v_\Delta(0) &= E_{\Delta 0} \\
\dot{v}_\Delta(0) &= E_{\Delta 1}
\end{aligned} \tag{3.29}$$

so that we may write equation (3.28) in the form

$$
\begin{aligned}
&< a\ddot{v}_\Delta(t), \phi > + < b\dot{v}_\Delta(t), \phi > + < hv_\Delta(t), \phi > \\
&+ < \textstyle\int_0^t G(s,s) v_\Delta(s)\ ds, \phi > + < \int_0^t \int_0^s \frac{d}{ds} G(s,\xi,\cdot) v_\Delta(\xi)\ d\xi\ ds, \phi > \\
&+ c\dot{v}_\Delta(t,0)\ \phi(0) + \sigma_1(v_\Delta, \phi) \qquad (3.30) \\
&- < a(0)\ddot{v}_\Delta(0), \phi > - < b(0) E_{\Delta 1}, \phi > - < h(0) E_{\Delta 0}, \phi > \\
&- cE_{\Delta 1}(0)\ \phi(0) - \sigma_1(E_{\Delta 0}, \phi) =< F_\Delta(t), \phi > .
\end{aligned}
$$

We note that (3.26) and the definitions of σ_1 and v_Δ imply

$$
\begin{aligned}
- < a(0,z)\ddot{v}_\Delta(0,z), \phi > - < b(0,z) E_{\Delta 1}(z), \phi > - < h(0,z) E_{\Delta 0}(z), \phi > & \\
- cE_{\Delta 1}(0)\phi(0) - \sigma_1(E_{\Delta 0}, \phi) &= \\
- < a(0,z)\ddot{v}_\Delta(0,z), \phi > - < b(0,z) E_{\Delta 1}(z), \phi > - < h(0,z) E_{\Delta 0}(z), \phi > & \\
- cE_{\Delta 1}(0)\phi(0) + < c^2 E''_{\Delta 0}(z), \phi > + c^2 E'_{\Delta 0}(0)\phi(0) &= \\
- < a(0,z)\ddot{v}_\Delta(0,z), \phi > + < a(0,z) Z_\Delta, \phi > & \\
- cE_{\Delta 1}(0)\phi(0) + c^2 E'_{\Delta 0}(0)\phi(0) &= \\
- < a(0,z)\dot{u}_\Delta(0,z), \phi > + < a(0,z) Z_\Delta, \phi > & \\
- cE_{\Delta 1}(0)\phi(0) + c^2 E'_{\Delta 0}(0)\phi(0) &= \\
- cE_{\Delta 1}(0)\phi(0) + c^2 E'_{\Delta 0}(0)\phi(0) &= 0.
\end{aligned}
$$

Thus equation (3.30) is equivalent to

$$
\begin{aligned}
&< a\ddot{v}_\Delta(t), \phi > + < b\dot{v}_\Delta(t), \phi > + < hv_\Delta(t), \phi > \\
&+ < \textstyle\int_0^t G(s,s)v_\Delta(s)\ ds, \phi > + < \int_0^t \int_0^s \frac{d}{ds}G(s,\xi,\cdot)v_\Delta(\xi)\ d\xi\ ds, \phi > \\
&+c\dot{v}_\Delta(t,0)\ \phi(0) + \sigma_1(v_\Delta, \phi) =< F_\Delta(t), \phi > .
\end{aligned}
\tag{3.31}
$$

If we compare equations (3.29),(3.31) with equations (3.24)-(3.23), we see that

$$v_\Delta(t) = E_\Delta(t) \ \text{ and } \ u_\Delta(t) = \dot{E}_\Delta(t).$$

We may then conclude that $\dot{E}_\Delta$ has the same regularity as u_Δ; that is, $\dot{E}_\Delta \in H^2(0,T;V^*) \cap H^1(0,T;H) \cap L^2(0,T;V)$.

We next want to establish the regularity $\ddot{E}_\Delta \in H^2(0,T;V^*) \cap H^1(0,T;H) \cap L^2(0,T;V)$. In order to do this, we differentiate (3.25) with respect to t and introduce the variable $w_\Delta = \dot{u}_\Delta$. This results in the equation

$$
\begin{aligned}
&< a\ddot{w}_\Delta, \phi > + < (2\dot{a} + b)\dot{w}_\Delta, \phi > + < (\ddot{a} + 2\dot{b} + h)w_\Delta, \phi > \\
&+ < (\ddot{b} + 2\dot{h} + G(t,t)) \textstyle\int_0^t w_\Delta(s)\ ds, \phi > \\
&+ < (\ddot{h} + 2\frac{d}{dt}G(t,t)) \int_0^t \int_0^s w_\Delta(\xi)\ d\xi\ ds, \phi > \\
&+ < \textstyle\int_0^t \frac{d^2}{dt^2}G(t,s) \int_0^s \int_0^\xi w_\Delta(r)\ dr\ d\xi\ ds, \phi > \\
&+ < (\ddot{b} + 2\dot{h} + G(t,t))E_{\Delta 1}, \phi > \\
&+ < (\ddot{h} + 2\frac{d}{dt}G(t,t)) \textstyle\int_0^t E_{\Delta 1}\ ds, \phi > + < \int_0^t \frac{d^2}{dt^2}G(t,s) \int_0^s E_{\Delta 1}\ d\xi\ ds, \phi > \\
&+ < (\ddot{h} + \textstyle\int_0^t \frac{d^2}{dt^2}G(t,s)\ ds + 2\frac{d}{dt}G(t,t))E_{\Delta 0}, \phi > \\
&+c\dot{w}_\Delta(t,0)\phi(0) + \sigma_1(w_\Delta, \phi) =< \ddot{F}_\Delta, \phi >
\end{aligned}
\tag{3.32}
$$

with initial conditions

$$\begin{aligned} w_\Delta(0,z) &= Z_\Delta(z) \\ \dot{w}_\Delta(0,z) &= \tfrac{1}{a(0,z)}\Big(-(\dot{a}(0,z)+b(0,z))Z_\Delta(z) - (\dot{b}(0,z)+h(0,z))E_{\Delta 1}(z) \\ &\quad -(\dot{h}(0,z)+G(0,0,z))E_{\Delta 0}(z) + c^2 E''_{\Delta 1}(z)\Big). \end{aligned} \tag{3.33}$$

Although (3.32) is not quite of the same form as (3.22) for which Theorem 1 guarantees well-posedness, its well-posedness may be established using the same methodology and the additional Assumptions A8) and A9). We thus assume the existence of a unique solution w_Δ to (3.32)-(3.33), with $w_\Delta \in H^2(0,T;V^*) \cap H^1(0,T;H) \cap L^2(0,T;V)$. We now argue that the solution w_Δ to (3.32)-(3.33) is $\dot{u}_\Delta$. We use the technique employed previously and begin by integrating (3.32) over t to obtain

$$< \textstyle\int_0^t a\ddot{w}_\Delta \; ds, \phi > + < \int_0^t (2\dot{a}+b)\dot{w}_\Delta \; ds, \phi > + < \int_0^t (\ddot{a}+2\dot{b}+h) w_\Delta \; ds, \phi >$$

$$+ < \textstyle\int_0^t (\ddot{b}+2\dot{h}+G(s,s)) \int_0^s w_\Delta(\xi) \; d\xi \; ds, \phi >$$

$$+ < \textstyle\int_0^t (\ddot{h}+2\frac{d}{ds}G(s,s)) \int_0^s \int_0^\xi w_\Delta(r) \; dr \; d\xi \; ds, \phi >$$

$$+ < \textstyle\int_0^t \int_0^s \frac{d^2}{ds^2}G(s,\xi) \int_0^\xi \int_0^r w_\Delta(x) \; dx \; dr \; d\xi \; ds, \phi >$$

$$+ < \textstyle\int_0^t (\ddot{b}+2\dot{h}+G(s,s)) \; ds E_{\Delta 1}, \phi >$$

$$+ < \textstyle\int_0^t (\ddot{h}+2\frac{d}{ds}G(s,s)) \int_0^s E_{\Delta 1} \; d\xi \; ds, \phi >$$

$$+ < \textstyle\int_0^t \int_0^s \frac{d^2}{ds^2}G(s,\xi) \int_0^\xi E_{\Delta 1} \; dr \; d\xi \; ds, \phi >$$

$$+ < \textstyle\int_0^t (\ddot{h} + \int_0^s \frac{d^2}{ds^2}G(s,\xi) \; d\xi + 2\frac{d}{ds}G(s,s)) \; ds \; E_{\Delta 0}, \phi >$$

$$+c \textstyle\int_0^t \dot{w}_\Delta(s,0) \; ds\phi(0) + \sigma_1(\int_0^t w_\Delta \; ds, \phi) =< \dot{F}_\Delta, \phi > .$$

We define a new variable

$$y_\Delta = E_{\Delta 1} + \int_0^t w_\Delta \, ds,$$

and rewrite the above equation, using integration by parts and Leibnitz' rule, as

$$\begin{gathered}
< a(t)\ddot{y}_\Delta(t), \phi > - < a(0)\ddot{y}_\Delta(0), \phi > \\
+ < (\dot{a}(t) + b(t))\dot{y}_\Delta(t), \phi > - < (\dot{a}(0) + b(0))\dot{y}_\Delta(0), \phi > \\
+ < (\dot{b}(t) + h(t))y_\Delta(t), \phi > + < (\dot{h}(t) + G(t,t)) \textstyle\int_0^t y_\Delta \, ds, \phi > \\
+ < \textstyle\int_0^t \frac{d}{dt} G(t,s) \int_0^s y_\Delta \, d\xi \, ds, \phi > \\
< (\dot{h}(t) - \dot{h}(0) + G(t,t) - G(0,0))E_{\Delta 0}, \phi > + < \textstyle\int_0^t \frac{d}{dt} G(t,s) \, ds E_{\Delta 0}, \phi > \\
< (-\dot{b}(0) - h(0))E_{\Delta 1}, \phi > \\
+ c\dot{y}_\Delta(t,0)\phi(0) - cE_{\Delta 1}(0)\phi(0) + \sigma_1(y_\Delta, \phi) - \sigma_1(E_{\Delta 1}, \phi) \\
=< \dot{F}_\Delta, \phi > .
\end{gathered}$$

Finally, the initial and consistency conditions yield

$$\begin{gathered}
< a\ddot{y}_\Delta(t), \phi > + < (\dot{a} + b)\dot{y}_\Delta(t), \phi > + < (\dot{b}(t) + h(t))y_\Delta(t), \phi > \\
+ < (\dot{h}(t) + G(t,t)) \textstyle\int_0^t y_\Delta \, ds, \phi > + < \textstyle\int_0^t \frac{d}{dt} G(t,s) \int_0^s y_\Delta \, d\xi \, ds, \phi > \\
< (\dot{h}(t) + G(t,t))E_{\Delta 0}, \phi > + < \textstyle\int_0^t \frac{d}{dt} G(t,s) \, ds E_{\Delta 0}, \phi > \\
+ c\dot{y}_\Delta(t,0)\phi(0) + \sigma_1(y_\Delta, \phi) =< \dot{F}_\Delta, \phi > .
\end{gathered} \tag{3.34}$$

If we compare equation (3.34) with (3.25), we see that $y_\Delta = u_\Delta = \dot{E}_\Delta$ and $\ddot{E}_\Delta = \dot{u}_\Delta = w_\Delta$. We may then conclude that $\ddot{E}_\Delta \in H^2(0,T;V^*) \cap H^1(0,T;H) \cap L^2(0,T;V)$.

The next step is to bound the solutions $E_\Delta, \dot{E}_\Delta$, and $\ddot{E}_\Delta$ with respect to Δ so that we may argue the convergence of these solutions to $E, \dot{E}$, and $\ddot{E}$ as Δ tends to zero. To construct these bounds, we make judicious choices for the test function ϕ in equations (3.23) and (3.25) and establish appropriate inequalities. We give the details for obtaining the desired result from (3.25) and remark that the process is analagous for (3.23). We begin by considering (3.25) with the choice of test function $\phi = \dot{u}_\Delta \in V$

$$\begin{aligned}
&< a\ddot{u}_\Delta(t), \dot{u}_\Delta(t) > + < (\dot{a}+b)\dot{u}_\Delta(t), \dot{u}_\Delta(t) > + < (\dot{b}+h)u_\Delta(t), \dot{u}_\Delta(t) > \\
&+ < (\dot{h} + G(t,t)) \textstyle\int_0^t u_\Delta(s)\ ds, \dot{u}_\Delta(t) > \\
&+ < \textstyle\int_0^t \frac{d}{dt}G(t,s,\cdot) \int_0^s u_\Delta(\xi,\cdot)\ d\xi\ ds, \dot{u}_\Delta(t) > \\
&+ < \left(\dot{h} + G(t,t) + \textstyle\int_0^t \frac{d}{dt}G(t,s,\cdot)\ ds\right) E_{\Delta 0}, \dot{u}_\Delta(t) > \\
&+ c\dot{u}_\Delta^2(t,0) + \sigma_1(u_\Delta(t), \dot{u}_\Delta(t)) =< \dot{F}_\Delta(t), \dot{u}_\Delta(t) > .
\end{aligned} \tag{3.35}$$

We next integrate (3.35) with respect to t to obtain

$$\begin{aligned}
&< a(t)\dot{u}_\Delta(t), \dot{u}_\Delta(t) > + \sigma_1(u_\Delta(t), u_\Delta(t)) + 2\textstyle\int_0^t c\dot{u}_\Delta^2(s,0)\ ds \\
&= \textstyle\int_0^t \Big\{ - < (\dot{a}+2b)\dot{u}_\Delta(s), \dot{u}_\Delta(s) > -2 < (\dot{b}+h)u_\Delta(s), \dot{u}_\Delta(s) > \\
&-2 < (\dot{h} + G(s,s)) \textstyle\int_0^s u_\Delta(\xi)\ d\xi, \dot{u}_\Delta(s) > \\
&-2 < \textstyle\int_0^s \frac{d}{ds}G(s,\xi,\cdot) \int_0^\xi u_\Delta(r,\cdot)\ dr\ d\xi, \dot{u}_\Delta(s) > \\
&-2 < \left(\dot{h} + G(s,s) + \textstyle\int_0^s \frac{d}{ds}G(s,\xi,\cdot)\ d\xi\right) E_{\Delta 0}, \dot{u}_\Delta(s) > + 2 < \dot{F}_\Delta(s), \dot{u}_\Delta(s) > \Big\}\ ds \\
&+ < a(0)\dot{u}_\Delta(0), \dot{u}_\Delta(0) > + \sigma_1(u_\Delta(0), u_\Delta(0)).
\end{aligned}$$

Using the Hölder inequality and the fact that $2ab < a^2 + b^2$, we may establish the

inequality

$$
\begin{aligned}
&< a(t)\dot{u}_\Delta(t), \dot{u}_\Delta(t) > + \sigma_1(u_\Delta(t), u_\Delta(t)) + 2\int_0^t c\dot{u}_\Delta^2(s,0)\ ds \\
&\leq \int_0^t \Big\{ |(\tfrac{1}{2}\dot{a} + b)\dot{u}_\Delta(s)|^2 + |(\dot{b} + h)u_\Delta(s)|^2 + |(\dot{h} + G(s,s))\int_0^s u_\Delta(\xi)\ d\xi|^2 \\
&\qquad + |\int_0^s \tfrac{d}{ds}G(s,\xi,\cdot)\int_0^\xi u_\Delta(r,\cdot)\ dr\ d\xi|^2 \\
&\qquad + |\left(\dot{h} + G(s,s) + \int_0^s \tfrac{d}{ds}G(s,\xi,\cdot)\ d\xi\right) E_{\Delta 0}|^2 + 5|\dot{u}_\Delta(s)|^2 \\
&\quad + 2 < \dot{F}_\Delta(s), \dot{u}_\Delta(s) > \Big\}\ ds + < a\dot{u}_\Delta(0), \dot{u}_\Delta(0) > + \sigma_1(u_\Delta(0), u_\Delta(0)).
\end{aligned}
\tag{3.36}
$$

We note that

$$
\begin{aligned}
\int_0^t 2 < \dot{F}_\Delta(s), \dot{u}_\Delta(s) >\ ds &= \\
-\int_0^t 2 < \ddot{F}_\Delta(s), u_\Delta(s) >\ ds + 2 < \dot{F}_\Delta(t), u_\Delta(t) > &\leq \\
\int_0^t \tfrac{2}{c_2}|\ddot{F}_\Delta(s)|_{V^*}^2 + \tfrac{c_2}{2}|u_\Delta(s)|_V^2\ ds + \tfrac{2}{c_2}|\dot{F}_\Delta(t)|_{V^*}^2 + \tfrac{c_2}{2}|u_\Delta(t)|_V^2 &\leq \\
K_1|F_\Delta|_{H^2(0,T;V^*)}^2 + \int_0^t \tfrac{c_2}{2}|u_\Delta(s)|_V^2\ ds + \tfrac{c_2}{2}|u_\Delta(t)|_V^2.&
\end{aligned}
$$

We use this inequality and the properties of σ_1 to write (3.36) as

$$
\begin{aligned}
&|\sqrt{a(t)}\dot{u}_\Delta(t)|^2 + \tfrac{c_2}{2}|u_\Delta(t)|_V^2 + 2\int_0^t c\dot{u}_\Delta^2(s,0)\ ds \\
&\leq \int_0^t \Big\{ |(\tfrac{1}{2}\dot{a}+b)\dot{u}_\Delta(s)|^2 + |(\dot{b}+h)u_\Delta(s)|^2 + |(\dot{h}+G(s,s))\int_0^s u_\Delta(\xi)\ d\xi|^2 \\
&\qquad + |\int_0^s \tfrac{d}{ds}G(s,\xi,\cdot)\int_0^\xi u_\Delta(r,\cdot)\ dr\ d\xi|^2 \\
&\qquad + |\left(\dot{h} + G(s,s) + \int_0^s \tfrac{d}{ds}G(s,\xi,\cdot)\ d\xi\right) E_{\Delta 0}|^2 \\
&\qquad + 5|\dot{u}_\Delta(s)|^2 + \tfrac{c_2}{2}|u_\Delta(s)|_V^2\ ds\Big\}\ ds \\
&\qquad + K_1|F_\Delta|^2_{H^2(0,T;V^*)} + |\sqrt{a(0)}Z_\Delta|^2 + c_1|E_{\Delta 1}|^2_{H^1(0,1)}.
\end{aligned}
\tag{3.37}
$$

We may write (3.37) in the simplified form

$$
\begin{aligned}
&a_0|\dot{u}_\Delta(t)|^2 + \tfrac{c_2}{2}|u_\Delta(t)|_V^2 + 2\int_0^t c\dot{u}_\Delta^2(s,0)\ ds \\
&\leq \int_0^t \{K_2|\dot{u}_\Delta(s)|^2 + K_3|u_\Delta(s)|_V^2\ ds\}\ ds \\
&\qquad + K_1|F_\Delta|^2_{H^2(0,T;V^*)} + K_4|E_{\Delta 1}|^2_{H^1(0,1)} + K_5|E_{\Delta 0}|^2_{H^2(0,1)}
\end{aligned}
\tag{3.38}
$$

with the use of Assumptions A1)-A10), the definition of Z_Δ, and norm properties. The convergence of the sequences $\{F_\Delta\}, \{E_{\Delta 1}\}$, and $\{E_{\Delta 0}\}$ implies boundedness and thus

$$
\begin{aligned}
&a_0|\dot{u}_\Delta(t)|^2 + \tfrac{c_2}{2}|u_\Delta(t)|_V^2 + 2\int_0^t c\dot{u}_\Delta^2(s,0)\ ds \\
&\leq K_6 + \int_0^t \{K_2|\dot{u}_\Delta(s)|^2 + K_3|u_\Delta(s)|_V^2\ ds\}\ ds.
\end{aligned}
\tag{3.39}
$$

(We note that the constants K_2, K_3, and K_6 are all independent of Δ and t.) We may now use Gronwall's inequality to conclude that $u_\Delta = \dot{E}_\Delta$ is bounded in $C(0,T;V)$, $\dot{u}_\Delta = \ddot{E}_\Delta$ is bounded in $C(0,T;H)$, and $\dot{u}_\Delta(\cdot,0) = \ddot{E}_\Delta(\cdot,0)$ is bounded in $L^2(0,T)$. In order to claim that E_Δ is bounded in $C(0,T;V)$ we assert that similar arguments can be used to establish the inequality

$$|\dot{E}_\Delta(t)|_H^2 + \tfrac{c_2}{2}|E_\Delta(t)|_V^2 + 2\int_0^t c\dot{E}_\Delta^2(s,0)\ ds \leq$$
$$C_1 + \int_0^t \left\{ C_2|\dot{E}_\Delta|_H^2 + C_3|E_\Delta|_V^2 \right\}\ ds \tag{3.40}$$

from equation (3.23). (Again, the constants C_1, C_2, and C_3 are independent of Δ and t.) The desired boundedness follows from Gronwall's inequality.

These results imply that there exist subsequences (also denoted by the subscript Δ) such that as Δ tends to zero

$$E_\Delta \ \rightarrow_{weakly}\ E_a \text{ in } L^2(0,T;V)$$

$$\dot{E}_\Delta \ \rightarrow_{weakly}\ E_b \text{ in } L^2(0,T;V)$$

$$\ddot{E}_\Delta \ \rightarrow_{weakly}\ E_c \text{ in } L^2(0,T;H)$$

$$\ddot{E}_\Delta(\cdot,0) \ \rightarrow_{weakly}\ E_d \text{ in } L^2(0,T).$$

With repeated applications of the Fundamental Theorem of Calculus, we may argue that $E_b = \dot{E}_a, E_c = \ddot{E}_a$, and $E_d = \ddot{E}_a(\cdot,0)$.

Lastly, we take weak limits as $\Delta \rightarrow 0$ in (3.23) and conclude that E_a is a solution to (3.22), i.e., $E_a = E$. The theory outlined in Section 3.1 guarantees that this solution is unique and depends continuously on the initial data and forcing function. The results are summarized in the following theorem.

Theorem 2: We assume that Assumptions A1)-A10) hold and the initial conditions $E_0 \in H_R^3(0,1), E_1 \in H_R^2(0,1)$ satisfy the consistency requirements $E_1(0) = cE_0'(0)$ and $E_1'(0) = cE_0''(0)$. Then the unique solution E to (3.22) has the enhanced regularity $E \in H^3(0,T;V^*) \cap H^2(0,T;H) \cap H^1(0,T;V)$.

3.2.2 Enhanced regularity of solutions to the Debye-based system

In this section, we want to show that the enhanced regularity results established in Section 3.2.1 can be applied to the solutions of the system with Debye-based pressure-dependent polarization (3.7). We have already shown that, under the conditions P1)-P2) and the assumptions on our admissible parameter set Q, Theorem 1 guarantees the well-posedness of the Debye solutions. Now we wish to use Theorem 2 to show that these solutions have additional smoothness, $E \in H^3(0,T;V^*) \cap H^2(0,T;H) \cap H^1(0,T;V)$, by demonstrating that the Debye coefficients satisfy Assumptions A7)-A10). First we must replace the condition P2) with a more restrictive condition P2′):

P2′) The derivatives of the pressure wave, $\dot{p}, \ddot{p}$, and $\frac{d^3}{dt^3}p$ are in $L^\infty(0,T;L^\infty[0,1])$. (See [18] and [17] and Chapter 7 for details regarding the regularity of p.)

Then we verify that A7)-A10) are satisfied by (3.7) provided that the conditions P1)-P2′) hold and that our admissible set of parameters Q is as described in Section 3.1.

A7) The second time derivative of b, $\ddot{b}$, is in $L^\infty(0,T;L^\infty[0,1])$.

Proof: The first derivative of b is given by

$$\dot{b}(t,z) =$$

$$\left(\frac{(\kappa_\gamma - \kappa_\zeta)\dot{p}(t,z)\left(\tau_0 + \kappa_\tau p(t,z)\right) - \left(\gamma_0 - \zeta_0 + (\kappa_\gamma - \kappa_\zeta)p(t,z)\right)\kappa_\tau \dot{p}(t,z)}{\left(\tau_0 + \kappa_\tau p(t,z)\right)^2} \right) I_{(z_1,1)}.$$

This can be written equivalently as

$$\dot{b}(t,z) =$$

$$\left(\frac{\Big(\dot{\gamma}(p(t,z)) - \dot{\zeta}(p(t,z))\Big)\tau(p(t,z)) - \Big(\gamma(p(t,z)) - \zeta(p(t,z))\Big)\dot{\tau}(p(t,z))}{\tau(p(t,z))^2} \right) I_{(z_1,1)},$$

where, for example, $\dot{\tau}(p(t,z))$ denotes the time derivative of $\tau(p(t,z))$ which must be computed using the chain rule, i.e., $\dot{\tau}(p(t,z)) = \frac{d}{dp}\tau(p)\dot{p}(t,z)$.

Thus

$$\begin{aligned} \ddot{b}(t,z) &= \Big\{ \frac{1}{\tau(p(t,z))}(\ddot{\gamma}(p(t,z)) - \ddot{\zeta}(p(t,z))) - \frac{2\dot{\tau}(p(t,z))}{\tau(p(t,z))^2}(\dot{\gamma}(p(t,z)) - \dot{\zeta}(p(t,z))) \\ &\quad + \frac{2\dot{\tau}(p(t,z))^2}{\tau(p(t,z))^3}(\gamma(p(t,z)) - \zeta(p(t,z)))\Big\} I_{(z_1,1)}. \end{aligned}$$

The restrictions on our admissible parameter set imply that $\tau(p)^{-k}$ bounded by δ^{-k}. Moreover, since τ, γ, and ζ are linear functions of p, and $p, \dot{p}$, and $\ddot{p}$ are L^∞ functions from Assumptions P1)-P2′), the functions $\dot{\tau}(p), \gamma(p), \zeta(p), \dot{\gamma}(p), \dot{\zeta}(p), \ddot{\gamma}(p)$, and $\ddot{\zeta}(p)$ are in L^∞. We may then conclude that $\ddot{b}$ itself is in L^∞.

A8) The first and second time derivatives, $\dot{h}$ and $\ddot{h}$, of h are in $L^\infty(0,T;L^\infty[0,1])$.

Proof: The coefficient h can be written

$$h(t,z) = \left(\frac{(\dot{\gamma}(p(t,z)) - \dot{\zeta}(p(t,z))}{\tau(p(t,z))} - \frac{(1+\dot{\tau}(p(t,z)))\,(\gamma(p(t,z)) - \zeta(p(t,z)))}{\tau(p(t,z))^2} \right) I_{(z_1,1)}.$$

Its derivatives are given by

$$\begin{aligned}\dot{h}(t,z) &= \Big\{\frac{1}{\tau(p(t,z))}\Big(\ddot{\gamma}(p(t,z))-\ddot{\zeta}(p(t,z))\Big)-\frac{\ddot{\tau}(p(t,z))}{\tau(p(t,z))^2}\times \\ &\Big((\gamma(p(t,z))-\zeta(p(t,z)))+2\dot{\tau}(p(t,z))(\dot{\gamma}(p(t,z))-\dot{\zeta}(p(t,z)))\Big) \\ &+\frac{2\dot{\tau}(p(t,z))}{\tau(p(t,z))^3}\Big(1+\dot{\tau}(p(t,z)))(\gamma(p(t,z))-\zeta(p(t,z))\Big)\Big\}I_{(z_1,1)}\end{aligned}$$

and

$$\begin{aligned}\ddot{h}(t,z) &= \Big\{\frac{1}{\tau(p(t,z))}\Big(\frac{d^3}{dt^3}\gamma(p(t,z))-\frac{d^3}{dt^3}\zeta(p(t,z))\Big)-\frac{\frac{d^3}{dt^3}\tau(p(t,z))}{\tau(p(t,z))^2}\times \\ &\Big((\gamma(p(t,z))-\zeta(p(t,z)))+3\ddot{\tau}(p(t,z))(\dot{\gamma}(p(t,z))-\dot{\zeta}(p(t,z))) \\ &+2\dot{\tau}(p(t,z))(\ddot{\gamma}(p(t,z))-\ddot{\zeta}(p(t,z)))\Big) \\ &+\frac{2\dot{\tau}(p(t,z))}{\tau(p(t,z))^3}\Big(2\ddot{\tau}(p(t,z))(\gamma(p(t,z))-\zeta(p(t,z))) \\ &+3\dot{\tau}(p(t,z)(\dot{\gamma}(p(t,z))-\dot{\zeta}(p(t,z)))+(\dot{\gamma}(p(t,z))-\dot{\zeta}(p(t,z)))\Big) \\ &-\frac{1}{\tau(p(t,z))^4}6\dot{\tau}(p(t,z)^2(1+\dot{\tau}(p(t,z)))(\gamma(p(t,z))-\zeta(p(t,z)))\Big\}I_{(z_1,1)}.\end{aligned}$$

We use condition P2′) and the assumptions on our admissible parameter set to show that the fractional terms in $\dot{h}$ and $\ddot{h}$ are in L^∞. Then we apply P1) and P2′) to verify that the remaining terms are also in L^∞. Combining these results, we have that $\dot{h}$ and $\ddot{h}$ are L^∞ functions.

A9) The first and second derivatives with respect to the first temporal variable, $\frac{d}{dt}G$ and $\frac{d^2}{dt^2}G$, of the kernel function G are in $L^\infty([0,T]\times[0,T];L^\infty[0,1])$.

Proof: The kernel of the Debye function is given by

$$G(t,s,z) =$$

$$\frac{(1+\kappa_\tau \dot{p}(t,z))\,(\gamma_0-\zeta_0+(\kappa_\gamma-\kappa_\zeta)p(s,z))}{(\tau_0+\kappa_\tau p(t,z))^2\,(\tau_0+\kappa_\tau p(s,z))}\exp\left(\int_s^t \frac{-d\xi}{\tau_0+\kappa_\tau p(\xi,z)}\right) I_{(z_1,1)}$$

which can be written

$$G(t,s,z) =$$

$$\Big(\frac{\gamma(p(t,z))-\zeta(p(s,z))}{\tau(p(s,z))}\Big)\Big(\frac{1+\dot{\tau}(p(t,z))}{\tau(p(t,z))^2}\Big)\exp\Big(\int_s^t \frac{-d\xi}{\tau(p(\xi,z))}\Big) I_{(z_1,1)}.$$

Taking the first derivative with respect to t, we have

$$\begin{aligned}\frac{d}{dt}G(t,s,z) &= \Big(\frac{\gamma(p(t,z))-\zeta(p(s,z))}{\tau(p(s,z))}\Big)\exp\Big(\int_s^t \frac{-d\xi}{\tau(p(\xi,z))}\Big)\times \\ &\Big(\frac{\ddot{\tau}(p(t,z))}{\tau(p(t,z))^2}+\frac{-2\dot{\tau}(p(t,z))(1+\dot{\tau}(p(t,z)))}{\tau(p(t,z))^3}-\frac{1+\dot{\tau}(p(t,z))}{\tau(p(t,z))^3}\Big) I_{(z_1,1)}.\end{aligned}$$

The second derivative with respect to t is

$$\begin{aligned}\frac{d^2}{dt^2}G(t,s,z) = &\Big(\frac{\gamma(p(t,z))-\zeta(p(s,z))}{\tau(p(s,z))}\Big)\exp\Big(\int_s^t \frac{-d\xi}{\tau(p(\xi,z))}\Big)\times \\ &\Big(\frac{\frac{d^3}{dt^3}\tau(p(t,z))}{\tau(p(t,z))^2}-\frac{2\dot{\tau}(p(t,z))\ddot{\tau}(p(t,z))}{\tau(p(t,z))^3} \\ &-\frac{2(\ddot{\tau}(p(t,z)(1+\dot{\tau}(p(t,z)))+\dot{\tau}(p(t,z))\ddot{\tau}(p(t,z)))}{\tau(p(t,z))^3} \\ &+\frac{6\dot{\tau}(p(t,z))^2(1+\dot{\tau}(p(t,z)))}{\tau(p(t,z))^4}-\frac{\ddot{\tau}(p(t,z))}{\tau(p(t,z))^3}+\frac{3\dot{\tau}(p(t,z))(1+\dot{\tau}(p(t,z)))}{\tau(p(t,z))^4} \\ &-\frac{\ddot{\tau}(p(t,z))}{\tau(p(t,z))^3}+\frac{2\dot{\tau}(p(t,z))(1+\dot{\tau}(p(t,z)))}{\tau(p(t,z))^4}+\frac{1+\dot{\tau}(p(t,z))}{\tau(p(t,z))^4}\Big) I_{(z_1,1)}.\end{aligned}$$

In Section 3.1.2 we establish that

$$\exp\left(\int_s^t \frac{-d\xi}{\tau(p(\xi,z))}\right)$$

is in $L^\infty([0,T]\times[0,T];L^\infty[0,1])$. Moreover with the linearity in p of τ,γ, and ζ and the use of P2′) and the assumptions on our admissible parameters, it is easy to show that the remaining terms in $\frac{d}{dt}G(t,s,z)$ and $\frac{d^2}{dt^2}G(t,s,z)$ are in L^∞. We may then conclude that the kernel derivatives $\frac{d}{dt}G$ and $\frac{d^2}{dt^2}G$ are L^∞ functions.

If we choose the function J_s appropriately, we may guarantee that A10) holds. In other words, we must select J_s so that the forcing function $F(t,z)=\frac{1}{\epsilon_0}\dot{J}_s(t)$ is in $H^2(0,T,V^*)$ and is of the form $F(t,z)=\tilde{g}(t)\delta(z)$ with $\tilde{g}(t)\in H^2(0,T)$ and $\tilde{g}(0)=\dot{\tilde{g}}(0)=0$.

We have thus shown that the system corresponding to pressure-dependent Debye polarization satisfies Assumptions A7)-A10). We now may conclude that the enhanced regularity results presented in Section 3.2.1 may be applied.

3.2.3 Enhanced regularity of solutions to the Lorentz-based system

In a manner analogous to that of the previous section, we show here that solutions to the system with Lorentz-based pressure-dependent polarization (3.8) have the enhanced regularity guaranteed by Theorem 2. (We have already shown in Section 3.1.3 that solutions to this system are well-posed.) We verify that Assumptions A7)-A10) hold for the coefficients under conditions P1)-P2) (The Lorentz coefficients (3.8), unlike the Debye coefficients, satisfy A7)-A10) without the stronger condition P2′.) and the assumptions on our admissible parameter set Q.

A7) The second time derivative, $\ddot{b}$, of b is in $L^\infty(0,T;L^\infty[0,1])$.

Proof: We recall that $b = \frac{\sigma}{\epsilon_0} I_{(z_1,1)}$ is constant in time; thus $\ddot{b} \equiv 0$ and is in $L^\infty(0,T;L^\infty[0,1])$.

A8) The first and second time derivatives, $\dot{h}$ and $\ddot{h}$, of h are in $L^\infty(0,T;L^\infty[0,1])$.

Proof: We have that

$$\dot{h}(t,z) = \Big(\dot{\alpha}(p(t,z))(\gamma(p(t,z)) - \zeta(p(t,z))) + \alpha(p(t,z))(\dot{\gamma}(p(t,z)) - \dot{\zeta}(p(t,z)))\Big) I_{(z_1,1)}$$

and

$$\begin{aligned}\ddot{h}(t,z) &= \Big(\ddot{\alpha}(p(t,z))(\gamma(p(t,z)) - \zeta(p(t,z))) + \alpha(p(t,z))(\ddot{\gamma}(p(t,z)) - \ddot{\zeta}(p(t,z))) \\ &\quad +2\dot{\alpha}(p(t,z))(\dot{\gamma}(p(t,z)) - \dot{\zeta}(p(t,z)))\Big) I_{(z_1,1)}.\end{aligned}$$

Since α, γ, and ζ are linear functions of p and $p, \dot{p}$ and $\ddot{p}$ are in L^∞, each of the terms in $\dot{h}$ and $\ddot{h}$ are in L^∞. Thus, A8) holds.

A9) The first and second derivatives with respect to the first temporal variable, $\frac{d}{dt}G$ and $\frac{d^2}{dt^2}G$, of the kernel function G are in $L^\infty((0,T)\times(0,T);L^\infty[0,1])$.

Proof: The appropriate derivatives of G are given by

$$\begin{aligned}&\frac{d}{dt}G(t,s,z) = \\ &-\left(\frac{-\dot{\tau}(p(t,z))}{\tau(p(t,z))^2}\Phi_{21}(t,s) + \frac{\dot{\Phi}_{21}(t,s)}{\tau(p(t,z))} + \dot{\alpha}(p(t,z))\Phi_{11}(t,s) + \alpha(p(t,z))\dot{\Phi}(t,s)\right)\times \\ &\left(\alpha(p(s,z))(\gamma(p(s,z)) - \zeta(p(s,z)))\right) I_{(z_1,1)}\end{aligned}$$

and

$$\frac{d^2}{dt^2}G(t,s,z) =$$

$$-\Bigg(\Big(\frac{-\ddot{\tau}(p(t,z))}{\tau(p(t,z))^2}+\frac{2\dot{\tau}(p(t,z))^2}{\tau(p(t,z))^3}\Big)\Phi_{21}(t,s)+\frac{\ddot{\Phi}_{21}(t,s)}{\tau(p(t,z))}+\frac{-2\dot{\tau}(p(t,z))}{\tau(p(t,z))^2}\dot{\Phi}_{21}(t,s)$$

$$+\ddot{\alpha}(p(t,z))\Phi_{11}(t,s)+2\dot{\alpha}(p(t,z))\dot{\Phi}(t,s)+\alpha(p(t,z))\ddot{\Phi}(t,s)\Bigg)\times$$

$$\Big(\alpha(p(s,z))(\gamma(p(s,z))-\zeta(p(s,z)))\Big)I_{(z_1,1)}.$$

As the above expressions involve the derivatives $\dot{\Phi}_{i1}$ and $\ddot{\Phi}_{i1}$, we want to consider their smoothness. We recall that Φ_{ij} are the components of the state transition matrix for equation (3.9). Then $V_1(t) = [\Phi_{11}(t)\Phi_{21}(t)]^T$ and $V_2(t) = [\Phi_{12}(t)\Phi_{12}(t)]^T$ are linearly independent solutions to (3.9). Since the stiffness matrix in (3.9) is continuous under P1) and the assumptions on our admissible parameters, V_1 and V_2 are continuous as well. We want to establish the continuity of $\dot{V}_1$ and $\ddot{V}_1$. Since V_1 is a solution to (3.9), $\dot{V}_1$ is the product of the continuous stiffness matrix and the continuous V_1. Hence $\dot{V}_1$ itself is continuous. Taking derivatives, we see that

$$\ddot{V}_1 = \begin{bmatrix} 0 & 1 \\ -\kappa_\gamma\dot{p} & \frac{\kappa_\tau\dot{p}}{(\tau_0+\kappa_\tau p)^2} \end{bmatrix} V_1 + \begin{bmatrix} 0 & 1 \\ -(\gamma_0+\kappa_\gamma p) & \frac{-1}{\tau_0+\kappa_\tau p} \end{bmatrix} \dot{V}_1.$$

Conditions P1)-P2) and the restrictions on our admissible parameter set imply that the components of both matrices are L^∞-functions. Moreover V_1 and $\dot{V}_1$ are continuous. Thus the components of $\ddot{V}_1$ are in L^∞ and we may conclude that $\dot{\Phi}_{i1}$ and $\ddot{\Phi}_{i1}$ are L^∞-functions.

With this knowlege, we return to consider $\frac{d}{dt}G$ and $\frac{d^2}{dt^2}G$. If we examine $\frac{d}{dt}G$ and $\frac{d^2}{dt^2}G$ term by term in light of conditions P1)-P2) and the assumptions on our admissible parameters, we see each is a combination of sums and products of L^∞-functions. Thus $\frac{d}{dt}G$ and $\frac{d^2}{dt^2}G$ are in L^∞ and A9) holds.

As in Section 3.2.2, we may choose the source current J_s such that A10) holds. Since we have verified Assumptions A7)-A10) for the system with Lorentz-based polarization, we may conclude that the system has the enhanced regularity described in Theorem 2.

3.3 Estimation of parameters

3.3.1 Estimation of parameters in the general variational form

The well-posedness result in Section 3.1 provides a framework in which to formulate parameter estimation problems. As mentioned previously, the general Maxwell system treated by this result arises from a class electromagnetic interrogation problems. The crux of these problems is the estimation of certain parameter values, namely dielectric constants and conductivity coefficients, for the material under interrogation. The estimation problem typically involves finding the parameter values that provide the best fit between the model and data collected from the actual system, using, for example, a least squares criterion. These parameter estimates may then be used to characterize the material.

In practice, the experimental data is compared with finite dimensional numerical approximations to the model. In this section, we examine the relationship between the parameter estimation problems for the original system (3.10) and for a corresponding finite dimensional system. We suppose that the coefficients and sesquilinear form in both (3.10) and its finite dimensional approximation depend on a parameter q in a set Q. If the exact solution to the original system (3.10) were accessible, we would consider the problem of minimizing the least squares cost functional

$$J(q,w) = \sum_{i=1}^{N_t} |\mathcal{O}E(t_i;q) - w_i|^2 \tag{3.41}$$

over $q \in Q$ where $w = \{w_i\}_{i=1}^{N_t}$ is a set of observations taken at times t_i, Q is a set of admissible parameters, and $\mathcal{O}$ is an observation operator. The form of $\mathcal{O}$ depends on the particular application and set of observations. For example, if w_i is a measurement of the electric field taken at a spatial point z at time t_i, then the operator $\mathcal{O}$ entails evaluations of the function $E(t_i,\cdot;q)$ at a point in space. Since we cannot obtain a closed form solution to (3.10), we use the solution $E^N(t;q)$ to the finite dimensional approximating system. The solution $E^N(t;q)$ lies in V^N, a finite dimesional subset of V, and satisfies

$$\begin{gathered} < a(q)\ddot{E}^N(t), \phi >_{V^*,V} + < b(q)\dot{E}^N(t), \phi > + < h(q)E^N(t), \phi > \\ + < \int_0^t G(t,s,\cdot;q)E^N(s,\cdot)\, ds, \phi > \\ +c\dot{E}^N(t,0)\phi(0) + \sigma_1(q)(E^N(t),\phi) =< F(t), \phi >_{V^*,V} \\ E^N(0,z) = \mathcal{P}^N E_0(z) \quad \dot{E}^N(0,z) = \mathcal{P}^N E_1(z) \end{gathered} \tag{3.42}$$

for all $\phi \in V^N$. In particular, we define the piecewise linear basis elements $\{\phi_j^N\}_{j=0}^{N-1}$ with nodal values $\phi_j^N(k/N) = \delta_{kj},\ k = 0,1,\ldots,N$, and let
$V^N =$ span $\{\phi_0^N, \phi_1^N, \ldots, \phi_{N-1}^N\} \subset V$. Then we define $\mathcal{P}^N$ to be the quasi-$L^2(0,1)$ projection (see [40], [7], [20]) of V^* onto V^N defined by

$$< \mathcal{P}^N v^*, v^N >_N =< v^*, v^N >_{V^*,V} \quad \text{for } v^* \in V^* \text{ and for all } v^N \in V^N$$

where

$$< w^N, v^N >_N \equiv \int_0^1 I^N(w^N v^N)(z)\, dz$$

and I^N is the nodal value linear interpolation operator for V^N. It is shown in [40] that the operator $\mathcal{P}^N$ is well-defined and satisfies

$$\begin{aligned} |\mathcal{P}^N\phi|_H &\leq K_1'|\phi|_H \text{ for } \phi \in H \\ |\mathcal{P}^N\phi|_V &\leq K_2'|\phi|_V \text{ for } \phi \in V. \end{aligned} \tag{3.43}$$

As expected, the corresponding cost functional for the finite dimensional system is

$$J^N(q,w) = \sum_{i=1}^{N_t} \left|\mathcal{O}E^N(t_i;q) - w_i\right|^2. \tag{3.44}$$

Again the form of the operator $\mathcal{O}$ is chosen to correspond to the type of data collected. In Section 3.1, we established the well-posedness of (3.10) with solutions E in $L^2(0,T;V)$ and $\dot{E} \in L^2(0,T;H)$, where $V = H_R^1(0,1)$ and $H = L^2(0,1)$, and we also verified that a unique solution to (3.42) exists. These results hold provided that, for each $q \in Q$, Assumptions A1)-A6) are satisfied and the sesquilinear form σ_1 is V-continuous and V-elliptic. Moreover in Section 3.2, we show that the solution E of (3.10) has the enhanced regularity $E \in H^3(0,T;V^*) \cap H^2(0,T;H) \cap H^1(0,T;V)$ under consistency conditions for the initial conditions and the assumptions A7)-A10). We now make the following assumptions about the set of admissible parameters Q, the state space V^N, and the projection operator $\mathcal{P}^N$.

B1) The finite dimensional set Q lies in a metric space $\tilde{Q}$ with a metric $\tilde{d}$ and is compact with respect to this metric.

B2) The finite dimensional subspaces V^N are subsets of V.

B3) For each $\phi \in V$, $|\phi - \mathcal{P}^N\phi|_V \to 0$ as $N \to \infty$.

B4) For each $\phi \in H$, $|\phi - \mathcal{P}^N\phi|_H \to 0$ as $N \to \infty$.

Verifications of B3) and B4) for our particular $\mathcal{P}^N$ are given in [40]. We now make a further assumption on the sesquilinear form σ_1. We assume that $\sigma_1 = \sigma_1(q)$ is defined on Q and satisfies

H1)

$$|\sigma_1(q_1)(\phi,\psi) - \sigma_1(q_2)(\phi,\psi)| \leq \gamma \tilde{d}(q_1,q_2)|\phi|_V|\psi|_V$$

for $q_1, q_2 \in Q$ where γ depends only on Q.

For the electromagnetic system in consideration in this thesis, Assumption H1) is unnecessary since σ_1 is independent of q. However for the purpose of establishing a more general result, we do not assume here that our sesquilinear form is parameter independent.

Furthermore we make the following assumption about our coefficients.

A11) The coefficients depend continuously on q so that as $\tilde{d}(q, q^N) \to 0$, we have

$$i) \qquad |a(q) - a(q^N)|_{L^\infty} \to 0$$

$$ii) \qquad |b(q) - b(q^N)|_{L^\infty} \to 0$$

$$iii) \qquad |h(q) - h(q^N)|_{L^\infty} \to 0$$

$$iv) \qquad |G(q) - G(q^N)|_{L^\infty} \to 0.$$

The above continuity along with the compactness of Q implies that the images $a(Q)$, $b(Q)$, $h(Q)$, and $G(Q)$ are compact. Thus each coefficient can be bounded independently of q. We assume throughout that all bounds on our coefficients do not depend on q.

By solving the parameter estimation problems related to (3.42), (3.44) we obtain a sequence of estimates $\{\bar{q}^N\}$. We wish to demonstrate that under certain conditions this sequence (or a subsequence) converges to the estimate corresponding to the problem related to (3.10), (3.41). In order to do this, we state the following claim, which can be found (along with a proof) as Theorem 5.1 in [19].

Theorem 3: To obtain convergence of at least a subsequence of $\{\bar{q}^N\}$ to a solution $\bar{q}$ of minimizing (3.41) subject to (3.10), it suffices, under assumption B1), to argue

that for arbitrary sequences $\{q^N\}$ in Q with $q^N \to q$ in Q, we have

$$\mathcal{O}E^N(t;q^N) \to \mathcal{O}E(t;q).$$

In [19], the operator $\mathcal{O}$ is general enough to include functions that map functions f such that $f : \mathcal{T} \to \mathcal{V}$ to the space of observations $\mathcal{W}$, where $\mathcal{T}$ is an appropriately chosen (see [19] and [14]) subset of $[0,T]$ that contains the times of observation and $\mathcal{V}$ is a space containing $E(t,\cdot)$. In the numerical examples presented in this paper, the observations correspond to the values of the electric field at the point $z = 0$ at various times, i.e., $\{E(t_i,0)\}$; thus the operator $\mathcal{O}$ involves pointwise evaluation of E at many points in time and one specific point in space.

We suppose that V^N and $\mathcal{P}^N$ satisfy B2)-B4), the sesquilinear form σ_1 satisfies H1), the coefficients satisfy assumptions A1)-A11), and we let $q^N \in Q$ be arbitary such that $q^N \to q$ in Q. Our primary goal is to show that as $N \to \infty$

$$E^N(t,0;q^N) \to E(t,0;q) \tag{3.45}$$

for each $t \in [0,T]$. However, here we verify a more general result. We show that for each $t \in [0,T]$

$$\begin{aligned} E^N(t;q^N) &\to E(t;q) \text{ in the } V \text{ norm} \\ \dot{E}^N(t;q^N) &\to \dot{E}(t;q) \text{ in the } H \text{ norm} \end{aligned} \tag{3.46}$$

as $N \to \infty$, where $E^N, \dot{E}^N$ are the solutions to (3.42) and $E, \dot{E}$ are the solutions to (3.10). We note that we may evaluate these functions pointwise in t due to the enhanced regularity of solutions. Moveover, using the equivalence of norms, we see that (3.46) implies (3.45) and we have the result we need for our computations.

We point out that for a sequence $q^N = q$ for all N, the desired result implies convergence of the finite dimensional approximation to the true solution. This is important

when considering numerical approximations to the solution.

We have established previously that the solution of (3.10) satisfies $E(t) \in V$ and $\dot{E}(t) \in H$ for each t. Since

$$|E^N(t;q^N) - E(t;q)|_V \leq |E^N(t;q^N) - \mathcal{P}^N E(t;q)|_V + |\mathcal{P}^N E(t;q) - E(t;q)|_V$$

and B3) guarantees $|\mathcal{P}^N E(t;q) - E(t;q)|_V \to 0$ as $N \to \infty$, we need only show that

$$|E^N(t;q^N) - \mathcal{P}^N E(t;q)|_V \to 0 \text{ as } N \to \infty$$

for each $t \in [0,T]$. In the same way, it suffices to show that

$$|\dot{E}^N(t;q^N) - \mathcal{P}^N \dot{E}(t;q)|_H \to 0 \text{ as } N \to \infty$$

for each $t \in [0,T]$ to obtain the second result.

We let $E^N = E^N(t;q^N), E = E(t;q)$, and $\Delta^N \equiv E^N(t;q^N) - \mathcal{P}^N E(t;q)$.

Subtracting (3.10) from (3.42), we have for $\phi \in V^N$

$$< a(q^N)\ddot{E}^N - a(q)\ddot{E}, \phi > + < b(q^N)\dot{E}^N - b(q)\dot{E}, \phi >$$

$$+ < h(q^N)E^N - h(q)E, \phi >$$

$$+ < \textstyle\int_0^t (G(q^N)E^N - G(q)E)\ ds, \phi > + c(\dot{E}^N(t,0) - \dot{E}(t,0))\phi(0)$$

$$+\sigma_1(q^N)(E^N, \phi) - \sigma_1(q)(E, \phi) = 0.$$

We add and subtract $\mathcal{P}^N E$ and its derivatives and rearrange terms to obtain

$$< a(q^N)(\ddot{E}^N - \mathcal{P}^N\ddot{E}), \phi > + \sigma_1(q^N)(E^N - \mathcal{P}^N E, \phi)$$

$$+ c(\dot{E}^N(t,0) - \mathcal{P}^N\dot{E}(t,0))\phi(0)$$

$$=< a(q)\ddot{E}, \phi > - < a(q^N)\mathcal{P}^N\ddot{E}, \phi > + \sigma_1(q)(E, \phi) - \sigma_1(q^N)(\mathcal{P}^N E, \phi)$$

$$+ c(\dot{E}(t,0) - \mathcal{P}^N\dot{E}(t,0))\phi(0) + < b(q)\dot{E} - b(q^N)\dot{E}^N, \phi >$$

$$+ < h(q)E - h(q^N)E^N, \phi > + < \textstyle\int_0^t G(q)E - G(q^N)E^N \, ds, \phi > .$$

We choose the test function $\phi = \dot{\Delta}^N \in V^N$ so that

$$< a(q^N)(\ddot{E}^N - \mathcal{P}^N\ddot{E}), \dot{\Delta}^N > + \sigma_1(q^N)(E^N - \mathcal{P}^N E, \dot{\Delta}^N)$$

$$+ c(\dot{E}^N(t,0) - \mathcal{P}^N\dot{E}(t,0))\dot{\Delta}^N(t,0) =$$

$$< a(q)\ddot{E}, \dot{\Delta}^N > - < a(q^N)\mathcal{P}^N\ddot{E}, \dot{\Delta}^N > + \sigma_1(q)(E, \dot{\Delta}^N) - \sigma_1(q^N)(\mathcal{P}^N E, \dot{\Delta}^N)$$

$$+ c(\dot{E}(t,0) - \mathcal{P}^N\dot{E}(t,0))\dot{\Delta}^N(t,0) + < b(q)\dot{E} - b(q^N)\dot{E}^N, \dot{\Delta}^N >$$

$$+ < h(q)E - h(q^N)E^N, \dot{\Delta}^N > + < \textstyle\int_0^t (G(q)E - G(q^N)E^N) \, ds, \dot{\Delta}^N > .$$

We note that

$$2 < a(q^N)(\ddot{E}^N - \mathcal{P}^N\ddot{E}), \dot{\Delta}^N > + 2\sigma_1(q^N)(E^N - \mathcal{P}^N E, \dot{\Delta}^N)$$

$$= \tfrac{d}{dt}\left(< a(q^N)\dot{\Delta}^N, \dot{\Delta}^N > + \sigma_1(q^N)(\Delta^N, \Delta^N)\right) - < \dot{a}(q^N)\dot{\Delta}^N, \dot{\Delta}^N > .$$

Then we have

$$\tfrac{1}{2}\tfrac{d}{dt}\left(< a(q^N)\dot{\Delta}^N, \dot{\Delta}^N > + \sigma_1(q^N)(\Delta^N, \Delta^N)\right) + c(\dot{\Delta}^N(t,0))^2 =$$

$$< a(q)\ddot{E}, \dot{\Delta}^N > - < a(q^N)\mathcal{P}^N\ddot{E}, \dot{\Delta}^N > + < \dot{a}(q^N)\dot{\Delta}^N, \dot{\Delta}^N >$$

$$+\sigma_1(q)(E, \dot{\Delta}^N) - \sigma_1(q^N)(\mathcal{P}^N E, \dot{\Delta}^N)$$

$$+c(\dot{E}(t,0) - \mathcal{P}^N\dot{E}(t,0))\dot{\Delta}^N(t,0) + < b(q)\dot{E} - b(q^N)\dot{E}^N, \dot{\Delta}^N >$$

$$+ < h(q)E - h(q^N)E^N, \dot{\Delta}^N > + < \textstyle\int_0^t (G(q)E - G(q^N)E^N)\ ds, \dot{\Delta}^N > .$$

Integration with respect to t yields

$$< a(q^N)\dot{\Delta}^N(t), \dot{\Delta}^N(t) > + \sigma_1(q^N)(\Delta^N(t), \Delta^N(t))$$

$$+2\textstyle\int_0^t c(\dot{\Delta}^N(\xi,0))^2\ d\xi =$$

$$2\textstyle\int_0^t \Big\{ < a(q)\ddot{E}, \dot{\Delta}^N > - < a(q^N)\mathcal{P}^N\ddot{E}, \dot{\Delta}^N > + < \dot{a}(q^N)\dot{\Delta}^N, \dot{\Delta}^N >$$

$$+\sigma_1(q)(E, \dot{\Delta}^N) - \sigma_1(q^N)(\mathcal{P}^N E, \dot{\Delta}^N)$$

$$+c(\dot{E}(\xi,0) - \mathcal{P}^N\dot{E}(\xi,0))\dot{\Delta}^N(\xi,0) + < b(q)\dot{E} - b(q^N)\dot{E}^N, \dot{\Delta}^N >$$

$$+ < h(q)E - h(q^N)E^N, \dot{\Delta}^N > + < \textstyle\int_0^\xi G(q)E - G(q^N)E^N\ ds, \dot{\Delta}^N > \Big\}\ d\xi$$

$$+ < a(q^N)\dot{\Delta}^N(0), \dot{\Delta}^N(0) > + \sigma_1(q^N)(\Delta^N(0), \Delta^N(0)).$$

We now use the definition of Δ^N to obtain

$$\Delta^N(0) = E^N(0) - \mathcal{P}^N E(0) = E^N(0) - \mathcal{P}^N E_0 = 0$$

$$\dot{\Delta}^N(0) = \dot{E}^N(0) - \mathcal{P}^N\dot{E}(0) = \dot{E}^N(0) - \mathcal{P}^N E_1 = 0.$$

We may then write

$$
\begin{aligned}
&< a(q^N)\dot{\Delta}^N(t), \dot{\Delta}^N(t) > + \sigma_1(q^N)(\Delta^N(t), \Delta^N(t)) \\
&+2\int_0^t c(\dot{\Delta}^N(\xi,0))^2 \, d\xi = \\
&2\int_0^t \Big\{ < a(q)\ddot{E}, \dot{\Delta}^N > - < a(q^N)\mathcal{P}^N\ddot{E}, \dot{\Delta}^N > + < \dot{a}(q^N)\dot{\Delta}^N, \dot{\Delta}^N > \\
&+\sigma_1(q)(E, \dot{\Delta}^N) - \sigma_1(q^N)(\mathcal{P}^N E, \dot{\Delta}^N) \\
&+c(\dot{E}(\xi,0) - \mathcal{P}^N\dot{E}(\xi,0))\dot{\Delta}^N(\xi,0) + < b(q)\dot{E} - b(q^N)\dot{E}^N, \dot{\Delta}^N > \\
&+ < h(q)E - h(q^N)E^N, \dot{\Delta}^N > + < \int_0^\xi G(q)E - G(q^N)E^N \, ds, \dot{\Delta}^N > \Big\} \, d\xi.
\end{aligned}
\tag{3.47}
$$

In order to bound the right side of (3.47), we derive the following estimates:

Estimate 1:

$$
\begin{aligned}
&\int_0^t \Big(2 < a(q)\ddot{E}, \dot{\Delta}^N > -2 < a(q^N)\mathcal{P}^N\ddot{E}, \dot{\Delta}^N > + < \dot{a}(q^N)\dot{\Delta}^N, \dot{\Delta}^N > \Big) \, d\xi \\
= \; &\int_0^t \Big(2 < (a(q) - a(q^N))\ddot{E}, \dot{\Delta}^N > + 2 < a(q^N)(\ddot{E} - \mathcal{P}^N\ddot{E}), \dot{\Delta}^N > \\
&+ < \dot{a}(q^N)\dot{\Delta}^N, \dot{\Delta}^N > \Big) \, d\xi \\
\leq \; &\int_0^t |(a(q) - a(q^N))\ddot{E}|_H^2 + |a(q^N)(\ddot{E} - \mathcal{P}^N\ddot{E})|_H^2 + \tfrac{1}{2}(5 + |\dot{a}(q^N)|_H^2)|\dot{\Delta}^N|_H^2 \, d\xi \\
\leq \; &|a(q) - a(q^N)|_{L^\infty}^2 \int_0^t |\ddot{E}|_H^2 \, d\xi + |a(q^N)|_{L^\infty}^2 \int_0^t |\ddot{E} - \mathcal{P}^N\ddot{E}|_H^2 \, d\xi \\
&+ \tfrac{1}{2}(5 + |\dot{a}(q^N)|_{L^\infty}^2) \int_0^t |\dot{\Delta}^N|_H^2 \, d\xi.
\end{aligned}
$$

Estimate 2:

$$
\begin{aligned}
&2\int_0^t \sigma_1(q)(E, \dot{\Delta}^N) - \sigma_1(q^N)(\mathcal{P}^N E, \dot{\Delta}^N) \, d\xi \\
= \; &2\int_0^t \sigma_1(q^N)(\mathcal{P}^N\dot{E}, \Delta^N) - \sigma_1(q)(\dot{E}, \Delta^N) \, d\xi + 2(\sigma_1(q)(E(t), \Delta^N(t)) \\
&-\sigma_1(q^N)(\mathcal{P}^N E(t), \Delta^N(t)))
\end{aligned}
$$

$$
\begin{aligned}
&= 2\int_0^t \sigma_1(q^N)(\mathcal{P}^N\dot{E}-\dot{E},\Delta^N)+\sigma_1(q^N)(\dot{E},\Delta^N)-\sigma_1(q)(\dot{E},\Delta^N)\ d\xi \\
&\quad +2\Big(\sigma_1(q)(E(t),\Delta^N(t))-\sigma_1(q^N)(E(t),\Delta^N(t)) \\
&\quad +\sigma_1(q^N)(E(t)-\mathcal{P}^N E(t),\Delta^N(t))\Big) \\
&\leq \int_0^t c_1^2|\mathcal{P}^N\dot{E}-\dot{E}|_V^2+\gamma^2(\tilde{d}(q,q^N))^2|\dot{E}|_V^2+2|\Delta^N|_V^2\ d\xi \\
&\quad +\tfrac{c_1^2}{\epsilon}|\mathcal{P}^N E(t)-E(t)|_V^2+\tfrac{\gamma^2}{\epsilon}(\tilde{d}(q,q^N))^2|E(t)|_V^2+2\epsilon|\Delta^N(t)|_V^2,
\end{aligned}
$$

where $\epsilon>0$ is arbitrary.

Estimate 3:

$$
\begin{aligned}
&2c(\dot{E}(\xi,0)-\mathcal{P}^N\dot{E}(\xi,0))\dot{\Delta}^N(\xi,0) \\
\leq\ & c^2|\dot{E}(\xi,0)-\mathcal{P}^N\dot{E}(\xi,0)|^2+|\dot{\Delta}^N(\xi,0)|^2 \\
\leq\ & c^2K_1|\dot{E}-\mathcal{P}^N\dot{E}|_V^2+|\dot{\Delta}^N(\xi,0)|^2.
\end{aligned}
$$

(Here we use the fact that $|\phi|_V^2$ is equivalent to $|\phi'|_H^2+|\phi(0)|^2$ so that $|\phi|_V^2\geq\tilde{K}(|\phi'|_H^2+|\phi(0)|^2)\geq\tilde{K}|\phi(0)|^2$.)

Estimate 4:

$$
\begin{aligned}
&2\int_0^t <b(q)\dot{E}-b(q^N)\dot{E}^N,\dot{\Delta}^N>\ d\xi \\
=\ & 2\int_0^t\{<b(q)(\dot{E}-\mathcal{P}^N\dot{E}),\dot{\Delta}^N>+<(b(q)-b(q^N))\mathcal{P}^N\dot{E},\dot{\Delta}^N> \\
&\quad +<b(q^N)\dot{\Delta}^N,\dot{\Delta}^N>\}\ d\xi \\
\leq\ & \int_0^t |b(q)(\dot{E}-\mathcal{P}^N\dot{E})|_H^2+|b(q^N)\dot{\Delta}^N|_H^2+|(b(q)-b(q^N))\mathcal{P}^N\dot{E}|_H^2+3|\dot{\Delta}^N|_H^2\ d\xi \\
\leq\ & |b(q)|_{L^\infty}^2\int_0^t|\dot{E}-\mathcal{P}^N\dot{E}|_H^2\ d\xi+(|b(q^N)|_{L^\infty}^2+3)\int_0^t|\dot{\Delta}^N|_H^2\ d\xi \\
&\quad +|b(q)-b(q^N)|_{L^\infty}^2\int_0^t|\mathcal{P}^N\dot{E}|_H^2\ d\xi.
\end{aligned}
$$

Estimate 5:

$$
\begin{aligned}
& 2\int_0^t < h(q)E - h(q^N)E^N, \dot{\Delta}^N > \; d\xi \\
= \;& 2\int_0^t \{< h(q)(E - \mathcal{P}^N E), \dot{\Delta}^N > + < (h(q) - h(q^N))\mathcal{P}^N E, \dot{\Delta}^N > \\
& + < h(q^N)\Delta^N, \dot{\Delta}^N >\} \; d\xi \\
\leq \;& \int_0^t \Big(|h(q)(E - \mathcal{P}^N E)|_H^2 + |h(q^N)\Delta^N|_H^2 + 3|\dot{\Delta}^N|_H^2 \\
& + |(h(q) - h(q^N))\mathcal{P}^N E|_H^2 \Big) \; d\xi \\
\leq \;& |h(q)|_{L^\infty}^2 \int_0^t |E - \mathcal{P}^N E|_H^2 \; d\xi + |h(q^N)|_{L^\infty}^2 \int_0^t |\Delta^N|_H^2 \; d\xi + 3\int_0^t |\dot{\Delta}^N|_H^2 \; d\xi \\
& + |h(q) - h(q^N)|_{L^\infty}^2 \int_0^t |\mathcal{P}^N E|_H^2 \; d\xi.
\end{aligned}
$$

Estimate 6:

$$
\begin{aligned}
& 2\int_0^t < \int_0^\xi (G(q)E - G(q^N)E^N) \; ds, \dot{\Delta}^N > \; d\xi \\
= \;& 2\int_0^t < \int_0^\xi G(q)(E - \mathcal{P}^N E) \; ds, \dot{\Delta}^N > + < \int_0^\xi (G(q) - G(q^N))\mathcal{P}^N E \; ds, \dot{\Delta}^N > \\
& + < \int_0^\xi G(q^N)\Delta^N \; ds, \dot{\Delta}^N > \; d\xi \\
\leq \;& \int_0^t \{ | \int_0^\xi G(q)(E - \mathcal{P}^N E) \; ds|_H^2 + | \int_0^\xi (G(q) - G(q^N))\mathcal{P}^N E \; ds|_H^2 \\
& + | \int_0^\xi G(q^N)\Delta^N \; ds|_H^2 + 3|\dot{\Delta}^N|_H^2 \} \; d\xi \\
= \;& \int_0^t \int_0^1 | \int_0^\xi G(q)(E - \mathcal{P}^N E) \; ds|^2 \; dz \; d\xi \\
& + \int_0^t \int_0^1 | \int_0^\xi (G(q) - G(q^N))\mathcal{P}^N E \; ds|^2 \; dz \; d\xi \\
& + \int_0^t \int_0^1 | \int_0^\xi G(q^N)\Delta^N \; ds|^2 \; dz \; d\xi + 3\int_0^t |\dot{\Delta}^N|_H^2 \; d\xi
\end{aligned}
$$

$$
\begin{aligned}
&\leq |G(q)|^2_{L^\infty} \int_0^t \int_0^1 |\int_0^\xi (E - \mathcal{P}^N E)\, ds|^2\, dz\, d\xi \\
&\quad + |G(q) - G(q^N)|^2_{L^\infty} \int_0^t \int_0^1 |\int_0^\xi \mathcal{P}^N E\, ds|^2\, dz\, d\xi \\
&\quad + |G(q^N)|^2_{L^\infty} \int_0^t \int_0^1 |\int_0^\xi \Delta^N\, ds|^2\, dz\, d\xi + 3\int_0^t |\dot{\Delta}^N|^2_H\, d\xi \\
&\leq |G(q)|^2_{L^\infty} T \int_0^t \int_0^1 |E - \mathcal{P}^N E|^2_{L^2(0,\xi)}\, dz\, d\xi \\
&\quad + |G(q) - G(q^N)|^2_{L^\infty} T \int_0^t \int_0^1 |\mathcal{P}^N E|^2_{L^2(0,\xi)}\, dz\, d\xi \\
&\quad + |G(q^N)|^2_{L^\infty} T \int_0^t \int_0^1 |\Delta^N|^2_{L^2(0,\xi)}\, dz\, d\xi + 3\int_0^t |\dot{\Delta}^N|^2_H\, d\xi \\
&\leq |G(q)|^2_{L^\infty} T^2 \int_0^t |E - \mathcal{P}^N E|^2_H\, d\xi + |G(q) - G(q^N)|^2_{L^\infty} T^2 \int_0^t |\mathcal{P}^N E|^2_H\, d\xi \\
&\quad + |G(q^N)|^2_{L^\infty} T^2 \int_0^t |\Delta^N|^2_H\, d\xi + 3\int_0^t |\dot{\Delta}^N|^2_H\, d\xi.
\end{aligned}
$$

Using these estimates, Assumption H1), the V-continuity and V-ellipticity of σ_1, and the fact that $|\phi|^2_H \leq |\phi|^2_V$, we may rewrite (3.47) as

$$
\begin{aligned}
&|\sqrt{a(q^N)}\dot{\Delta}^N(t)|^2_H + c_2|\Delta^N(t)|^2_V + 2\int_0^t c|\dot{\Delta}^N(\xi,0)|^2\, d\xi \\
&\leq \delta_1^N(t) + \delta_2^N(t) + 2\epsilon|\Delta^N(t)|^2_V \\
&\quad + \int_0^t \Big\{ |\dot{\Delta}^N(\xi,0)|^2 + (\tfrac{23}{2} + |b(q^N)|^2_{L^\infty} + \tfrac{1}{2}|\dot{a}(q^N)|^2_{L^\infty})|\dot{\Delta}^N|^2_H \\
&\quad + \big(2 + |h(q^N)|^2_{L^\infty} + T^2|G(q^N)|^2_{L^\infty}\big)\,|\Delta^N|^2_V \Big\}\, d\xi,
\end{aligned}
$$

where

$$\begin{aligned}
\delta_1^N(t) &= \int_0^t \Big\{ |a(q^N)|_{L^\infty}^2 |\ddot{E} - \mathcal{P}^N \ddot{E}|_H^2 \\
&\quad + (c_1^2 + c^2 K_1) |\dot{E} - \mathcal{P}^N \dot{E}|_V^2 + |b(q)|_{L^\infty}^2 |\dot{E} - \mathcal{P}^N \dot{E}|_H^2 \\
&\quad + \left(|h(q)|_{L^\infty}^2 + T^2 |G(q)|_{L^\infty}^2 \right) |E - \mathcal{P}^N E|_H^2 \Big\} \, d\xi \\
&\quad + \frac{c_1^2}{\epsilon} |\mathcal{P}^N E(t) - E(t)|_V^2
\end{aligned}$$

$$\begin{aligned}
\delta_2^N(t) &= |a(q) - a(q^N)|_{L^\infty}^2 \int_0^t |\ddot{E}|_H^2 \, d\xi \\
&\quad + \gamma^2 \tilde{d}(q, q^N) \int_0^t |\dot{E}|_V^2 \, d\xi + |b(q) - b(q^N)|_{L^\infty}^2 \int_0^t |\mathcal{P}^N \dot{E}|_H^2 \, d\xi \\
&\quad + \left(|h(q) - h(q^N)|_{L^\infty}^2 + T^2 |G(q) - G(q^N)|_{L^\infty}^2 \right) \times \\
&\quad \int_0^t |\mathcal{P}^N E|_H^2 \, d\xi + \frac{\gamma^2}{\epsilon} \tilde{d}(q, q^N) |E(t)|_V^2.
\end{aligned}$$

Since $\epsilon > 0$ is arbitrary, we may choose it to be such that $1 > c_2 - 2\epsilon > 0$. Furthermore, the wave speed c satisfies $2c >> 1$. We then use Assumptions A1)-A4) to claim that there exist constants $\nu_1, \nu_2 > 1$ and $1 \geq a_0 > 0$, independent of q, such that

$$\begin{aligned}
&a_0 |\dot{\Delta}^N(t)|_H^2 + (c_2 - 2\epsilon) |\Delta^N(t)|_V^2 + \textstyle\int_0^t (2c - 1) |\dot{\Delta}^N(\xi, 0)|^2 \, d\xi \\
&\leq \delta_1^N(t) + \delta_2^N(t) + \textstyle\int_0^t \nu_1 |\dot{\Delta}^N|_H^2 + \nu_2 |\Delta^N|_V^2 \, d\xi.
\end{aligned}$$

Finally recalling the bounds on ν_1, ν_2, a_0, and $c_2 - 2\epsilon$, we may rewrite the inequality as

$$a_0|\dot{\Delta}^N(t)|_H^2 + (c_2 - 2\epsilon)|\Delta^N(t)|_V^2$$

$$\leq \delta_1^N(t) + \delta_2^N(t) + \int_0^t \left(\frac{\nu_2}{c_2 - 2\epsilon}\right) \nu_1 |\dot{\Delta}^N|_H^2 + \frac{\nu_1\nu_2}{a_0}|\Delta^N|_V^2 \, d\xi$$

$$\leq \delta_1^N(t) + \delta_2^N(t) + \left(\frac{\nu_1\nu_2}{a_0(c_2 - 2\epsilon)}\right) \int_0^t a_0|\dot{\Delta}^N|_H^2 + (c_2 - 2\epsilon)|\Delta^N|_V^2 \, d\xi.$$

In order to apply Gronwall's inequality to obtain uniform convergence of Δ^N and $\dot{\Delta}^N$ in t as $N \to \infty$, we must establish the uniform convergence of δ_1^N and δ_2^N. We have from B3) and B4) that $|\ddot{E}(t) - \mathcal{P}^N\ddot{E}(t)|_H$, $|\dot{E}(t) - \mathcal{P}^N\dot{E}(t)|_V$, and $|E(t) - \mathcal{P}^N E(t)|_V$ converge to zero as $N \to \infty$ for each t. Since this convergence is dominated and $\{E(t)\}_{t\in[0,T]}$ is compact in V, we have that

$$\delta_1^N \to 0 \text{ uniformly in } t \text{ as } N \to \infty.$$

Moreover, the boundedness of $E, \dot{E}$, and $\ddot{E}$ given by the enhanced regularity results and the assumption A8) imply that

$$\delta_2^N \to 0 \text{ uniformly in } t \text{ as } N \to \infty \text{ and } q^N \to q \text{ in } \tilde{Q}.$$

Then we may apply Gronwall's inequality to conclude that

$$\sup_{t\in[0,T]} |\Delta^N(t)|_V^2 \;\; \to \;\; 0 \text{ as } N \to \infty$$

$$\sup_{t\in[0,T]} |\dot{\Delta}^N(t)|_H^2 \;\; \to \;\; 0 \text{ as } N \to \infty$$

which is sufficient to prove the desired result.

3.3.2 Estimation of parameters in the system with pressure-dependent Debye polarization

The general system (3.10) is formulated to accomodate systems arising from a variety of electromagnetic interrogation problems. We are concerned here with a particular system that incorporates a pressure-dependent model for Debye polarization. We demonstrate that this system satisfies Assumptions A11), B1)-B3) and H1) and thus that the results of the previous section apply. (We note that verifications of Assumptions A1)-A10) are given in Section 3.1.2 and Section 3.2.2.)

The system we wish to consider is given by (3.10) with the parameter-dependent coefficients, kernel and forcing functions, and sesquilinear form (3.7).

For this system, the set of admissible parameters Q is a subset of $\mathbb{R}^7$, where seven is the number of parameters to be estimated (in addition to the six polarization parameters from Section 2.3.2, one is often interested in estimating the conductivity coefficient σ). Here we consider $q \in Q \subset \mathbb{R}^7$, where $q = (\sigma, \gamma_0, \zeta_0, \tau_0, \kappa_\gamma, \kappa_\zeta, \kappa_\tau)$. We choose the admissible set Q as described in Section 3.1 to insure that our Debye coefficients are well-defined.

We recall that $q^N \to q$ in the standard Euclidean metric is equivalent to the convergence of each component of q^N. Moreover, any closed and bounded sets Q in $\mathbb{R}^7$ are compact and satisfy the conditions of B1). The conditions B2)-B4) are satisfied by V^N, which is in this case the set of finite dimensional linear piecewise basis elements, and the projection operator $\mathcal{P}^N$. To verify H1), we note that $\sigma_1(q)(\phi, \psi) = c^2 < \phi', \psi' >$ is independent of q and $|\sigma_1(q_1)(\phi, \psi) - \sigma_1(q_2)(\phi, \psi)| = 0$ for any $q_1, q_2 \in Q$.

We next verify A11)i)-iv) for the coefficients in our model. We note that as $q^N \to q$ we have, for a given $p, \dot{p} \in L^\infty$,

$$|\sigma^N - \sigma| \to 0 \tag{3.48}$$

$$\left|\zeta_0^N + \kappa_\zeta^N p - \Big(\zeta_0 + \kappa_\zeta p\Big)\right|_{L^\infty} \to 0 \tag{3.49}$$

$$\left|\gamma_0^N - \zeta_0^N + (\kappa_\gamma^N - \kappa_\zeta^N)p - \Big(\gamma_0 - \zeta_0 + (\kappa_\gamma - \kappa_\zeta)p\Big)\right|_{L^\infty} \to 0 \tag{3.50}$$

$$\left|\tau_0^N + \kappa_\tau^N p - \Big(\tau_0 - \kappa_\tau p\Big)\right|_{L^\infty} \to 0 \tag{3.51}$$

$$\left|(\kappa_\gamma^N - \kappa_\zeta^N)\dot{p} - \Big((\kappa_\gamma - \kappa_\zeta)\dot{p}\Big)\right|_{L^\infty} \to 0 \tag{3.52}$$

and

$$\left|\kappa_\tau^N \dot{p} - \Big(\kappa_\tau \dot{p}\Big)\right|_{L^\infty} \to 0. \tag{3.53}$$

We use (3.49) directly to claim that $|a(q^N) - a(q)|_{L^\infty} \to 0$ whenever $q^N \to q$; thus A11)i) holds.

In demonstrating that A11)ii) holds, we observe that

$$|b(q^N) - b(q)|_{L^\infty} \leq \frac{1}{\epsilon_0}\Big|\sigma^N - \sigma\Big|$$

$$+ \sup_{t\in[0,T]} \sup_{z\in[z_1,1]} \left| \left(\frac{\gamma_0^N - \zeta_0^N + (\kappa_\gamma^N - \kappa_\zeta^N)p(t,z)}{\tau_0^N + \kappa_\tau^N p(t,z)}\right) - \left(\frac{\gamma_0 - \zeta_0 + (\kappa_\gamma - \kappa_\zeta)p(t,z)}{\tau_0 + \kappa_\tau p(t,z)}\right)\right|.$$

Then we may apply equations (3.48), (3.50), and (3.51) and the quotient rule of limits to conclude that $|b(q^N) - b(q)|_{L^\infty} \to 0$ as $q^N \to q$ and A11)ii) is satisfied.

From the definition of h, we have

$$|h(q^N) - h(q)|_{L^\infty} \leq \sup_{t\in[0,T]} \sup_{z\in[z_1,1]} \left\{ \left| \frac{(\kappa_\gamma^N - \kappa_\zeta^N)\dot{p}(t,z)}{\tau_0^N + \kappa_\tau^N p(t,z)} - \frac{(\kappa_\gamma - \kappa_\zeta)\dot{p}(t,z)}{\tau_0 + \kappa_\tau p(t,z)} \right| \right.$$
$$+ \left| \frac{(1+\kappa_\tau\dot{p}(t,z))(\gamma_0 - \zeta_0 + (\kappa_\gamma - \kappa_\zeta)p(t,z))}{(\tau_0 + \kappa_\tau p(t,z))^2} \right.$$
$$\left. \left. - \frac{(1+\kappa_\tau^N\dot{p}(t,z))(\gamma_0^N - \zeta_0^N + (\kappa_\gamma^N - \kappa_\zeta^N)p(t,z))}{(\tau_0^N + \kappa_\tau^N p(t,z))^2} \right| \right\}.$$

From equations (3.52), (3.51), (3.53), and (3.50) and the product and quotient rules of limits, we may conclude that A11)iii) holds.

To show that A11)iv) holds, we argue that

$$|G(q^N) - G(q)|_{L^\infty} \leq \sup_{(t,s)\in[0,T]\times[0,T]} \sup_{z\in[z_1,1]} \left| \exp\left(\int_s^t \frac{-d\xi}{\tau_0^N + \kappa_\tau^N p(\xi,z)} \right) \times \right.$$
$$\left(\frac{(1+\kappa_\tau^N\dot{p}(s,z))(\gamma_0^N - \zeta_0^N + (\kappa_\gamma^N - \kappa_\zeta^N)p(s,z))}{(\tau_0^N + \kappa_\tau^N p(t,z))^2(\tau_0^N + \kappa_\tau^N p(s,z))^2} \right) - \exp\left(\int_s^t \frac{-d\xi}{\tau_0 + \kappa_\tau p(\xi,z)} \right) \times$$
$$\left. \left(\frac{(1+\kappa_\tau\dot{p}(s,z))(\gamma_0 - \zeta_0 + (\kappa_\gamma - \kappa_\zeta)p(s,z))}{(\tau_0 + \kappa_\tau p(t,z))^2(\tau_0 + \kappa_\tau p(s,z))^2} \right) \right|.$$

We note that equation (3.51) coupled with the quotient rule for limits allows us to assert that

$$\exp\left(\int_s^t \frac{-d\xi}{\tau_0^N + \kappa_\tau^N p(\xi,z)} \right) \to \exp\left(\int_s^t \frac{-d\xi}{\tau_0 + \kappa_\tau p(\xi,z)} \right) \tag{3.54}$$

as $q^N \to q$. Thus, we may use equations (3.53), (3.50), (3.51), and (3.54) with the quotient and product rules for limits to verify that

$$|G(q^N) - G(q)|_{L^\infty} \to 0$$

as $q^N \to q$.

We have thus verified that the theory established in Section 3.3.1 can be applied to the system corresponding to pressure-dependent Debye polarization described by the coefficients (3.7).

3.3.3 Estimation of parameters in the system with pressure-dependent Lorentz polarization

Here we show that the results of Section 3.3.1 hold for a Maxwell system with Lorentz-based pressure-dependent polarization. As in Section 3.3.2, we do this by verifying that Assumptions A11), B1)-B3) and H1) hold for the system (3.22) with the parameter-dependent coefficients, kernel and forcing functions, and sesquilinear form (3.8).

For this system, the set of admissible parameters Q is a subset of $\mathbb{R}^9$; the Lorentz system includes all of the same parameters as the Debye as well as the parameters α_0 and κ_α. So we consider $q \in Q \subset \mathbb{R}^9$ where $q = (\sigma, \gamma_0, \zeta_0, \tau_0, \alpha_0, \kappa_\gamma, \kappa_\zeta, \kappa_\tau, \kappa_\alpha)$. As with the Debye coefficients, we choose the admissible set Q as described in Section 3.1 to insure that the Lorentz coefficients are well-defined.

Since the set of admissible parameters Q is a compact and bounded subset of $\mathbb{R}^9$, B1) is satisfied. Moreover, the space V^N, the projection operator $\mathcal{P}^N$, and the sesquilinear form σ_1 are the same as those in Section 3.2.2, we may assume that Assumptions B2)-B4) and H1) are satisfied. We then have that equations (3.48)- (3.53), as well as

$$\left|\alpha_0^N + \kappa_\alpha^N p - \Big(\alpha_0 - \kappa_\alpha p\Big)\right|_{L^\infty} \to 0, \tag{3.55}$$

hold.

Since the coefficient a is the same as that of the Debye-based system, we may use the result of Section 3.3.2 and claim that A11)i) holds.

We may then use (3.48) directly to claim that

$$|b(q) - b(q^N)|_{L^\infty} = \frac{1}{\epsilon_0}|\sigma - \sigma^N| \to 0$$

as $N \to \infty$, and A11)ii) holds.

To verify A11)iii) we note that

$$|h(q) - h(q^N)|_{L^\infty} =$$

$$|(\alpha_0 + \kappa_\alpha p)(\gamma_0 - \zeta_0 + (\kappa_\gamma - \kappa_\zeta)p) - (\alpha_0^N + \kappa_\alpha^N p)(\gamma_0^N - \zeta_0^N + (\kappa_\gamma^N - \kappa_\zeta^N)p)|_{L^\infty}.$$

Then we use (3.50) and (3.55) in conjunction with the limit rule for products to claim that $|h(q) - h(q^N)|_{L^\infty} \to 0$ as $q^N \to q$. Thus A11)iii) holds.

Demonstrating that A11)iv) holds is more complicated. We let

$$\begin{aligned} g_1(t,s,z;q) &= (\alpha_0 + \kappa_\alpha p(t,z))(\alpha_0 + \kappa_\alpha p(s,z))\times \\ &\quad (\gamma_0 - \zeta_0 + (\kappa_\gamma - \kappa_\zeta)p(s,z)) \\ g_2(t,s,z;q) &= \frac{1}{\tau_0 + \kappa_\tau p(t,z)}(\alpha_0 + \kappa_\alpha p(s,z))(\gamma_0 - \zeta_0 + (\kappa_\gamma - \kappa_\zeta)p(s,z)) \end{aligned}$$

and note that

$$\begin{aligned} G(t,s,z;q) &= -\Big(\frac{1}{\tau_0 + \kappa_\tau p(t,z)}\Phi_{21}(t,s) + (\alpha_0 + \kappa_\alpha p(t,z))\Phi_{11}(t,s)\Big) \\ &\quad \times\Big((\alpha_0 + \kappa_\alpha p(s,z))(\gamma_0 - \zeta_0 + (\kappa_\gamma - \kappa_\zeta)p(s,z))\Big)I_{(z_1,1)} \\ &= -\Big(g_1(t,s,z;q)\Phi_{11}(t,s) - g_2(t,s,z;q)\Phi_{21}(t,s)\Big)I_{(z_1,1)}. \end{aligned}$$

We recall that the Φ_{i1} are components of the state transition matrix for a q-dependent ordinary differential equation, so they depend on q. However as we mention in Section 3.1, this dependence is continuous.

Then

$$
\begin{aligned}
&|G(q) - G(q^N)|_{L^\infty} = \\
&\left| g_1(q)\Phi_{11}(q) - g_2(q)\Phi_{21}(q) - g_1(q^N)\Phi_{11}(q^N) + g_2(q^N)\Phi_{21}(q^N) \right|_{L^\infty} = \\
&\Big| g_1(q)\Phi_{11}(q) - g_1(q^N)\Phi_{11}(q) + g_1(q^N)\Phi_{11}(q) - g_1(q^N)\Phi_{11}(q^N) \\
&+ g_2(q^N)\Phi_{21}(q^N) - g_2(q^N)\Phi_{21}(q) + g_2(q^N)\Phi_{21}(q) - g_2(q)\Phi_{21}(q) \Big|_{L^\infty} \leq \\
&\left| g_1(q) - g_1(q^N) \right|_{L^\infty} \left| \Phi_{11}(q) \right|_{L^\infty} + \left| g_1(q^N) \right|_{L^\infty} \left| \Phi_{11}(q) - \Phi_{11}(q^N) \right|_{L^\infty} \\
&+ \left| g_2(q^N) \right|_{L^\infty} |\Phi_{21}(q^N) - \Phi_{21}(q)|_{L^\infty} + \left| g_2(q^N) - g_2(q) \right|_{L^\infty} \left| \Phi_{21}(q) \right|_{L^\infty}.
\end{aligned}
$$

The product and quotient rules for limits and (3.50), (3.51), and (3.55) imply that

$$
\begin{aligned}
|g_1(q) - g_1(q^N)|_{L^\infty} &\to 0 \\
|g_2(q) - g_2(q^N)|_{L^\infty} &\to 0
\end{aligned}
$$

as $q^N \to q$. This and the continuity of the Φ_{i1} allow us to conclude that $|G(q) - G(q^N)|_{L^\infty} \to 0$ as $q^N \to q$ and A11)iv) holds.

We now may apply the theory developed in Section 3.3.1 to the system corresponding to pressure-dependent Lorentz polarization given by (3.8).

Chapter 4

Model simulations

In this chapter, we present numerical methods and solutions for a forward problem related to the model systems presented previously. We describe the numerical approximation methods used, consider the parameter dependence of the models, and give computational results.

4.1 Numerical methods for the model with Debye polarization

In this section, we discuss the numerical methods used to compute forward simulations of the electromagnetic model. Here we only consider the pressure-dependent Debye polarization model. We may then write the model as

$$a(t,z)\ddot{E} + b(t,z)\dot{E} + h(t,z)E + e(t,z)P = c^2E'' + F(t,z), \tag{4.1}$$

where

$$
\begin{aligned}
a(t,z) &= 1 + (\zeta_0 + \kappa_\zeta p - 1) I_{(z_1,1)} \\
b(t,z) &= \left(\frac{\sigma}{\epsilon_0} + \frac{1}{\epsilon_0} \frac{\epsilon_0 \left(\gamma_0 - \zeta_0 + (\kappa_\gamma - \kappa_\zeta) p \right)}{(\tau_0 + \kappa_\tau p)} \right) I_{(z_1,1)} \\
h(t,z) &= \frac{1}{\epsilon_0} \left(\frac{\epsilon_0 (\kappa_\gamma - \kappa_\zeta) \dot{p}}{(\tau_0 + \kappa_\tau p)} - \frac{\epsilon_0 \left(\gamma_0 - \zeta_0 + (\kappa_\gamma - \kappa_\zeta) p \right) (1 + \kappa_\tau \dot{p})}{(\tau_0 + \kappa_\tau p)^2} \right) I_{(z_1,1)} \\
e(t,z) &= \frac{1}{\epsilon_0} \frac{(1 + \kappa_\tau \dot{p})}{(\tau_0 + \kappa_\tau p)^2} I_{(z_1,1)} \\
c^2 &= \tfrac{1}{\epsilon_0 \mu_0} \\
F(t,z) &= -\tfrac{1}{\epsilon_0} \dot{J}_s
\end{aligned}
$$

with

$$
\dot{P} = -\frac{1}{(\tau_0 + \kappa_\tau p)} P + \frac{\epsilon_0 \left(\gamma_0 - \zeta_0 + (\kappa_\gamma - \kappa_\zeta) p \right)}{(\tau_0 + \kappa_\tau p)} E \quad \text{in } [z_1, 1]
$$

and the boundary and initial conditions

$$
\dot{E}(t,0) - cE'(t,0) = 0
$$

$$
E(t,1) = 0
$$

$$
E(0,z) = \dot{E}(0,z) = P(0,z) = 0.
$$

To solve this problem numerically, we use the methodology originally developed for a similar problem which had a standing (as opposed to traveling) pressure wave interface. This problem is discussed in detail in [7]. We look for approximations in $V^N \subset H_R^1(0,1)$, the standard linear finite element space defined on a partition of the interval $(0,1)$ with a set of basis functions $\{w_i\}_{i=0}^N$. We use a finite difference scheme in time to approximate the solution at discrete time points $0 = t_0 < t_1 < \ldots < t_M = T$; we let $\Delta t = t_i - t_{i-1}$, $i = 1, \ldots, M$.

We start with the weak form of equation (4.1)

$$< a\ddot{E}, \phi >_{V^*,V} + < b\dot{E}, \phi > + < hE, \phi > + < eP, \phi > + c\dot{E}(t,0)\phi(0)$$

$$+c^2 < E', \phi' > = < F, \phi >_{V^*,V}$$

which holds for all $\phi \in H_R^1(0,1)$. We define the finite element approximations

$$\begin{aligned} E^n(z) &= \sum_{i=0}^{N-1} \eta_i^n w_i(z) \approx E(t^n, z) \\ P^n(z) &= \sum_{i=0}^{N-1} \nu_i^n w_i(z) \approx P(t^n, z), \end{aligned}$$

and use the following finite difference notation and quotients

$$\begin{aligned} U^{n,\theta} &\equiv \theta(U^{n+1} + 2U^n + U^{n-1}) \\ \delta_{tt}U^n &\equiv \tfrac{1}{\Delta t^2}(U^{n+1} - 2U^n + U^{n-1}) \\ \delta_t U^n &\equiv \tfrac{1}{2\Delta t}(U^{n+1} - U^{n-1}). \end{aligned}$$

The finite difference scheme is selected based on ideas in [25]. The author of [25] discusses Galerkin methods for second order hyperbolic systems. For these problems, the difference scheme has second order accuracy in time. Moreover, the choice of $\theta = 1/4$ in $U^{n,\theta}$ leads to stability independent of δt and N.

Our discretized weak form is then

$$\begin{aligned} &< a\delta_{tt}E^n, \phi_i >_{V^*,V} + < b\delta_t E^n, \phi_i > + < hE^{n,\frac{1}{4}}, \phi_i > \\ &+ < eP^n, \phi_i > + c\delta_t E^n(0)\phi_i(0) + c^2 < (E^{n,\frac{1}{4}})', \phi_i' > \\ &= < F(t^n, \cdot), \phi_i >_{V^*,V} . \end{aligned} \tag{4.2}$$

We note that our notation should indicate the number of spatial elements used, i.e., we should write $E^{n,N}, P^{n,N}$. However since we fix N, we supress this notation for simplification.

This formulation yields a linear system of equations that can be solved for E^{n+1} in terms of E^n, E^{n-1}, and P^n. Generating the components of the system involves computing the values of various inner products at each time step; this is done using Gaussian integration. If we assume that P^n is given exactly and the solution has enough smoothness, the scheme corresponding to the discretization (4.2) to compute E^{n+1} has accuracy [7]

$$|E^n - E(t^n, \cdot)|_{L^2} \leq C\left(\frac{1}{M^2} + \Delta t^2\right).$$

We want a stable scheme with the same accuracy to compute P^n at each time step. Here we use the A-stable Adams Moulton method to write

$$\begin{aligned} P^n &= \frac{1}{1+\frac{\Delta t}{2(\tau_0+\kappa_\tau p^n)}}\Bigg\{P^{n-1} + \frac{\Delta t}{2}\Bigg(\frac{\epsilon_0\left(\gamma_0 - \zeta_0 + (\kappa_\gamma - \kappa_\zeta)p^n\right)}{\tau_0 + \kappa_\tau p^n}E^n \\ &\quad + \frac{\epsilon_0\left(\gamma_0 - \zeta_0 + (\kappa_\gamma - \kappa_\zeta)p^{n-1}\right)}{\tau_0 + \kappa_\tau p^{n-1}}E^{n-1} - \frac{1}{\tau_0 + \kappa_\tau p^{n-1}}P^{n-1}\Bigg)\Bigg\}. \end{aligned} \tag{4.3}$$

where $p^n = p(t^n, \cdot)$ is the acoustic pressure at time t^n.

The initial condtions $E(0,z) = P(0,z) = 0$ give the approximations $E^0 = P^0 = 0$ at $t^0 = 0$. We then use a Taylor series expansion, the model equations, and initial conditions to obtain $E^1 \approx E(t^1, z)$

$$\begin{aligned} E(t^1, z) &= E(0,z) + \Delta t\dot{E}(0,z) + \tfrac{\Delta t^2}{2}\ddot{E}(0,z) + 0(\Delta t^3) \\ &\approx \tfrac{\Delta t^2}{2}\ddot{E}(0,z) \\ &\approx \tfrac{\Delta t^2}{2a}F(0,z). \end{aligned} \tag{4.4}$$

Using (4.2)-(4.4), we prescribe the following algorithm to approximate E and P. First, we use the initial conditions to obtain E^0, P^0. Then we compute E^1 from (4.4). With E^0, E^1, and P^0, in hand, we can compute P^1 from (4.3). Finally we use (4.2) to obtain E^2. The last two steps are then generalized and repeated at each time step to compute E^{n+1} and P^n.

4.2 Numerical simulations

We now use the methods described in Section 4.1 to compute numerical solutions to (4.1). We consider a windowed sine wave pressure input (See Figure 4.1.) Although the pressure wave is traveling to the left, its speed is extremely slow relative to that of the electromagnetic wave. Thus, Figure 4.1 can be thought of as the time snaphot of the pressure wave corresponding to *each* of the snapshots in Figure 4.2.

Figures 4.2(a)-(k) are time snapshots of the electromagnetic wave pulse traveling through a layered medium. (The geometry is as described in Chapter 2, Section 2.1). The solid line at $z = 0.25$ indicates the interface between the air and the dielectric and the dashed lines at $z = 0.5$ and $z = 0.54$ indicate the area occupied by the pressure wave. Each snapshot is shown on the same set of axes so that decreases in wave amplitude can be detected. The pulse is initiated at $z = 0$ and travels to the right. Passing through the medium, it interacts with the air/dielectric interface at $z = z_1$ and an oncoming pressure wave (depicted in Figure 4.1) traveling through the dielectric. As a result of each of these interactions, some of the electromagnetic wave energy is reflected, and wave reflections travel back toward $z = 0$. It is these reflections which return to $z = 0$ that would be observed and used as data in a parameter estimation problem. Figure 4.2(c) illustrates both the air/dielectric reflection which is returning to $z = 0$ and the original wave pulse traveling to the right; in Figure 4.2(d) one can see the air/dielectric reflection being absorbed at the boundary. Likewise, Figure 4.2(g)

clearly shows the reflection from the pressure wave and the original pulse propagating in opposite directions; Figure 4.2(j) depicts the absorption of the electromagnetic reflection from the pressure wave at the boundary. It is interesting to note that when this reflection traveling toward $z = 0$ crosses the air/dielectric interface, some of its energy is again reflected; this phenomena can be seen by looking closely at Figures 4.2(j) and (k).

Unless otherwise stated, the parameter values used in the previous simulations are given in Table 4.1.

$\epsilon_0 = 8.85 \times 10^{-12}$ Coulombs^2/Newton meters^2
$\mu_0 = 4.0\pi \times 10^{-7}$ Newton seconds ^{2}/Coulombs^2
$\epsilon_\infty = 5.5$
$\epsilon_s = 78.2$
$\tau = \tau_0 = 3.162277660168379 \times 10^{-8}$ seconds
$\zeta_0 = 5.5$
$\gamma_0 = 78.2$
$\sigma = 1.0 \times 10^{-5}$ mhos/meter
$\kappa_\tau = 0.05\ \tau_0$ meters^2 seconds/Newtons
$\kappa_\zeta = 0.3\ \zeta_0$ meters^2/Newtons
$\kappa_\gamma = 0.6\ \gamma_0$ meters^2/Newtons
$\omega_{j_s} = 1.0 \times 10^{10}\pi$ radians/second
$\dot{J}_s = \mu_0\ \omega_{j_s} \cos(\omega_{j_s} t)$ Coulombs/meters^2 seconds^2
$\omega_p = 4.0 \times 10^4 \pi$ radians/second
$c_p = 1.5 \times 10^{-3}$ meters/second
$\Delta z = \frac{1}{900}$ meters
$\Delta t = \frac{4.0 \times 10^{-10}}{1600}$ seconds
$z_1 = 0.25$ meters

Table 4.1: Parameter values for computations

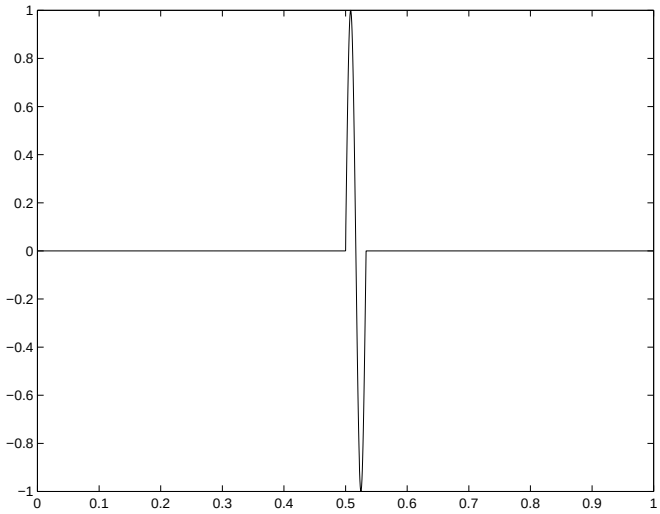

Figure 4.1: Pressure vs depth

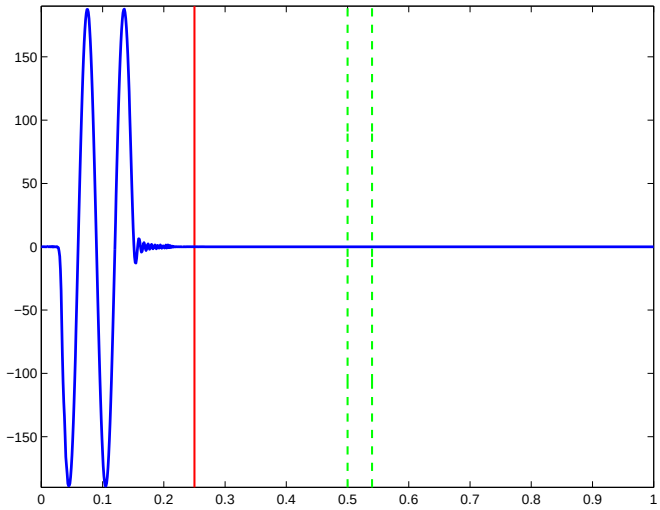

Figure 4.2(a): E field vs depth – t=5.0025e-10

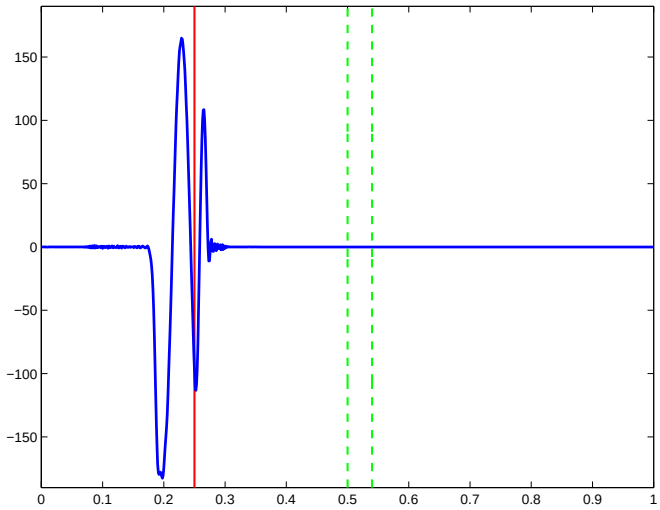

Figure 4.2(b): E field vs depth – t=1.00025e-9

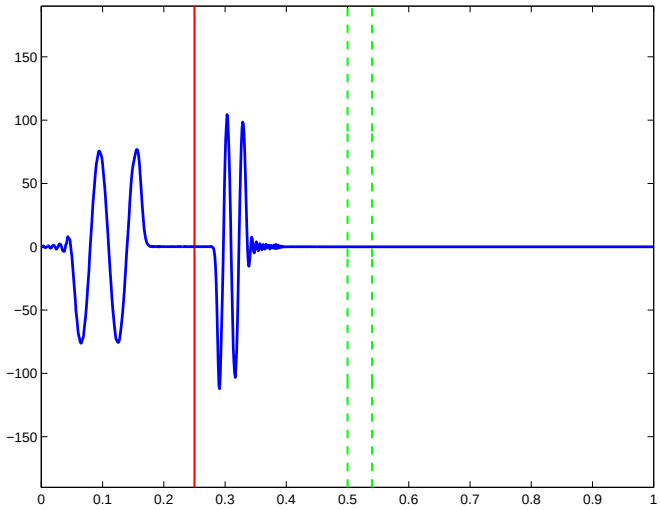

Figure 4.2(c): E field vs depth – t=1.50025e-9

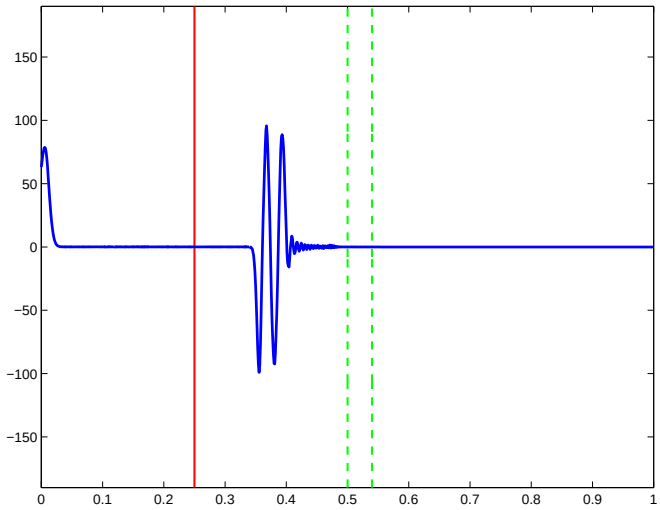

Figure 4.2(d): E field vs depth – t=2.00025e-9

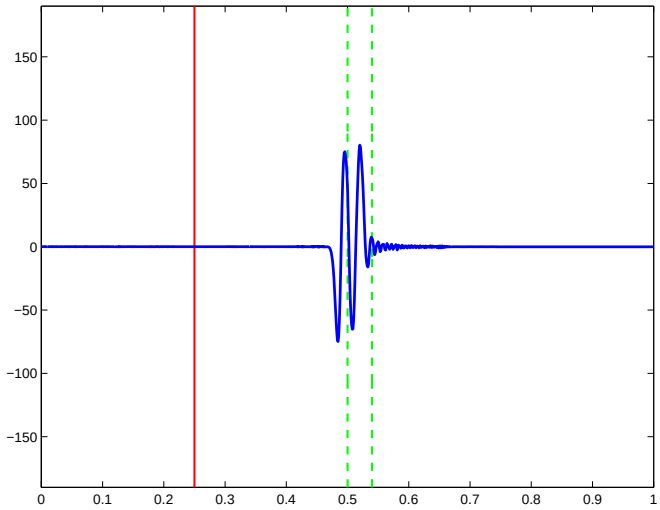

Figure 4.2(e): E field vs depth – t=3.00025e-9

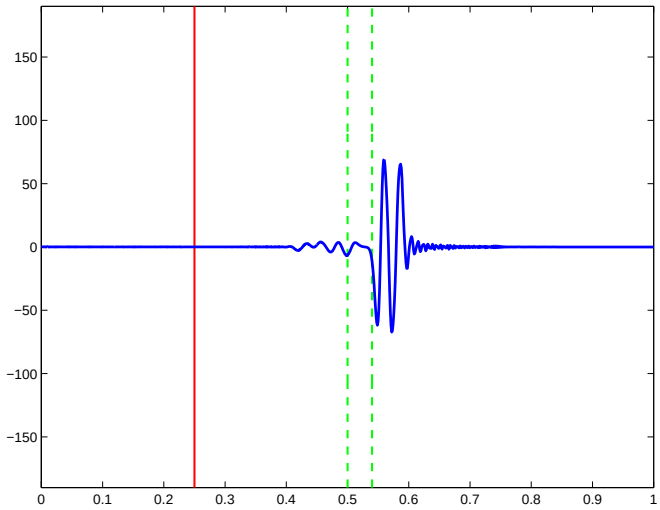

Figure 4.2(f): E field vs depth – t=3.50025e-9

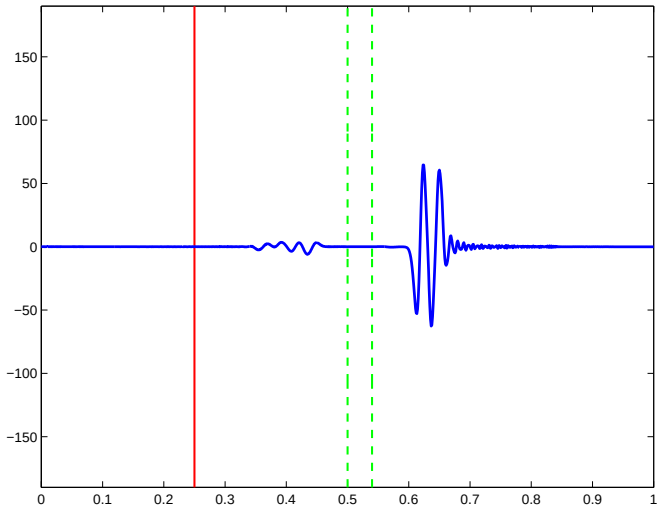

Figure 4.2(g): E field vs depth – t=4.00025e-9

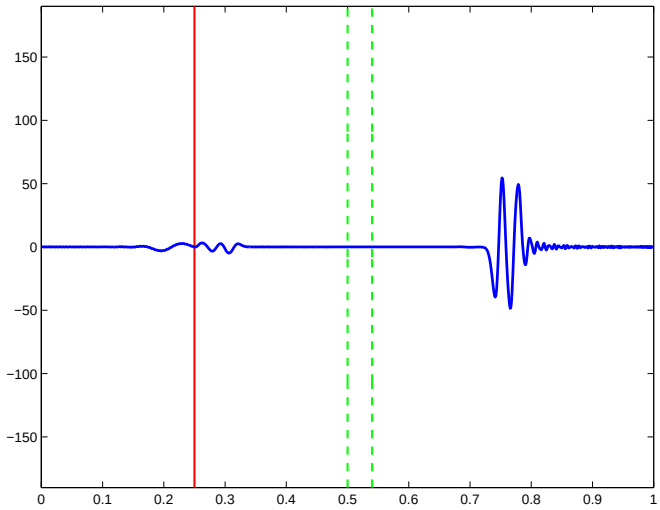

Figure 4.2(h): E field vs depth – t=5.00025e-9

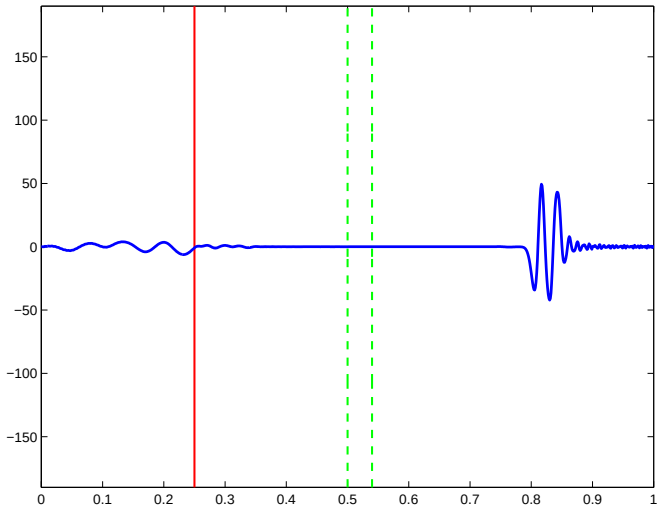

Figure 4.2(i): E field vs depth – t=5.50025e-9

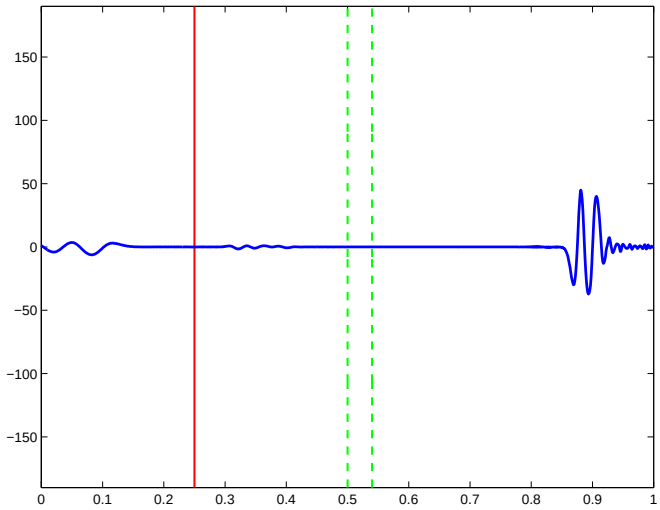

Figure 4.2(j): E field vs depth – t=6.00025e-9

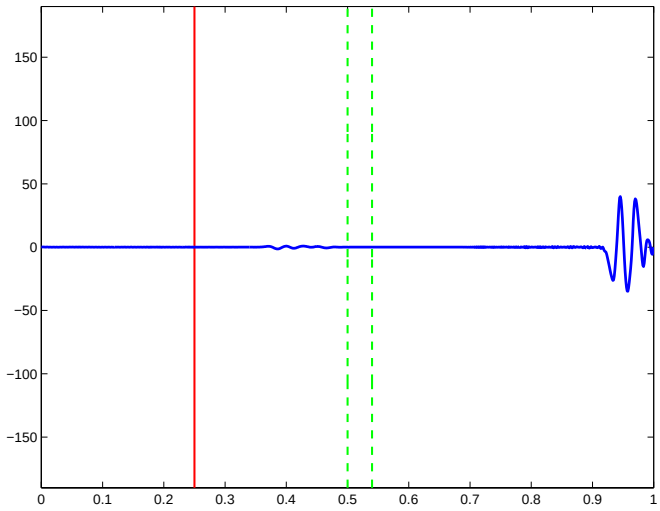

Figure 4.2(k):E field vs depth – t=6.50025e-9

As a test of our numerical methods, we examine the convergence of our simulations as we increase the number of basis elements. Figures 4.3(a)-(e) show time snapshots of the E field versus depth for $N = 900, 1800, 3600$ elements, denoted by "– –", "– · –", and "–" respectively . To focus on the region where numerical error is most

significant, we restrict the axis of each plot to a small spatial interval. This interval includes the leading edge of the E&M pulse, since we expect that our methods would have difficulty capturing this lack of smoothness.

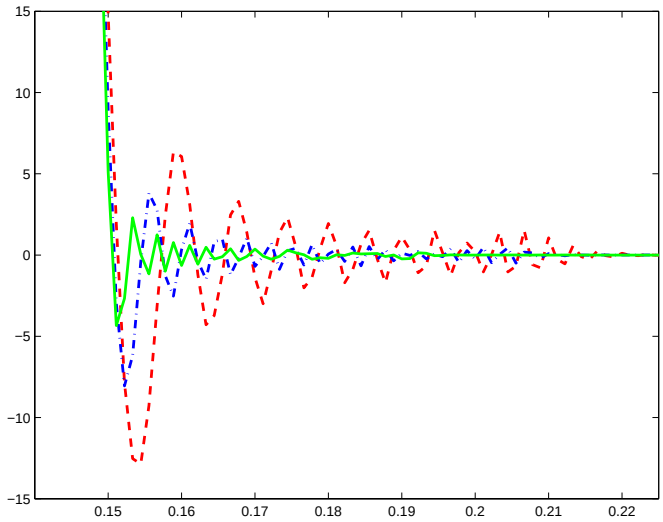

Figure 4.3(a): E field vs depth – t=5.0025e-10

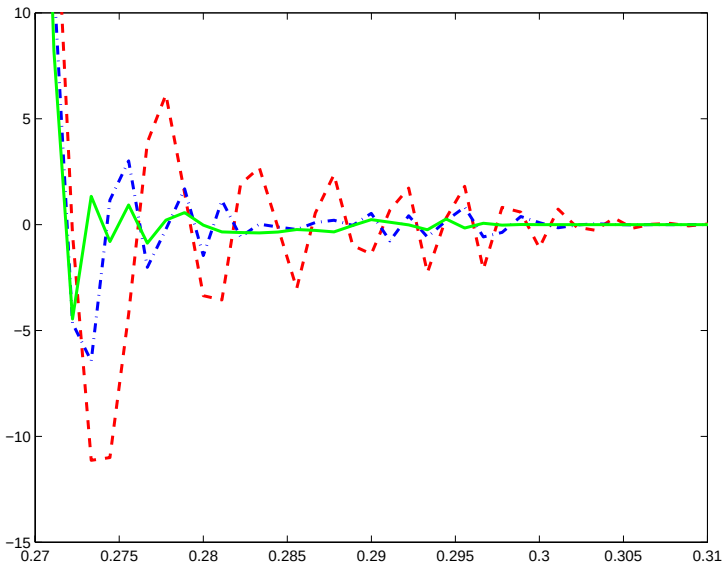

Figure 4.3(b): E field vs depth – t=1.00025e-9

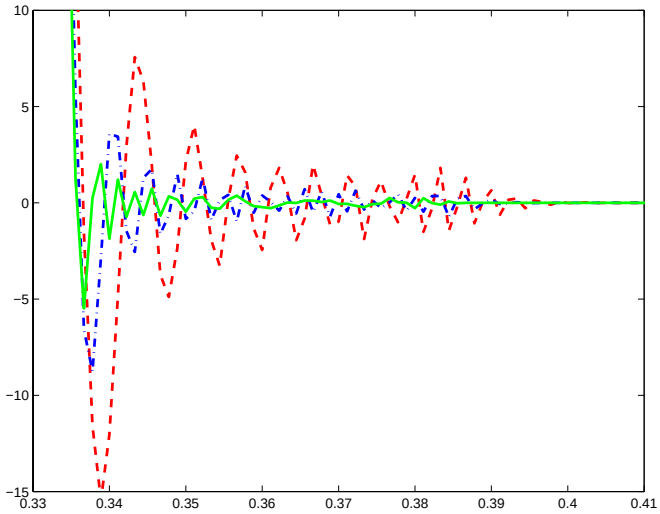

Figure 4.3(c): E field vs depth – t=1.50025e-9

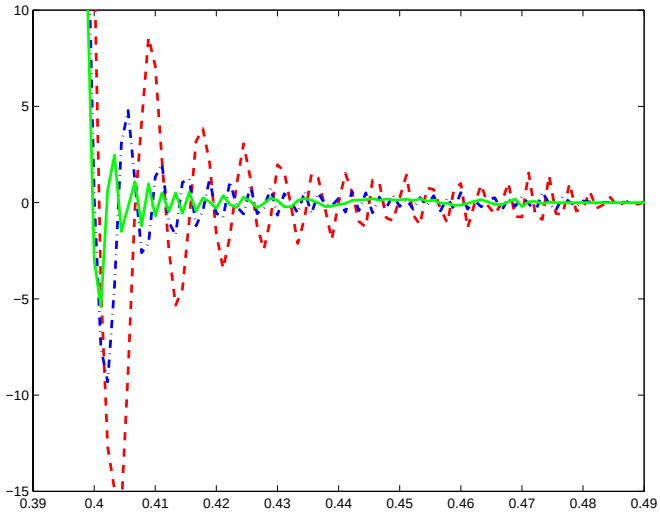

Figure 4.3(d): E field vs depth – t=2.00025e-9

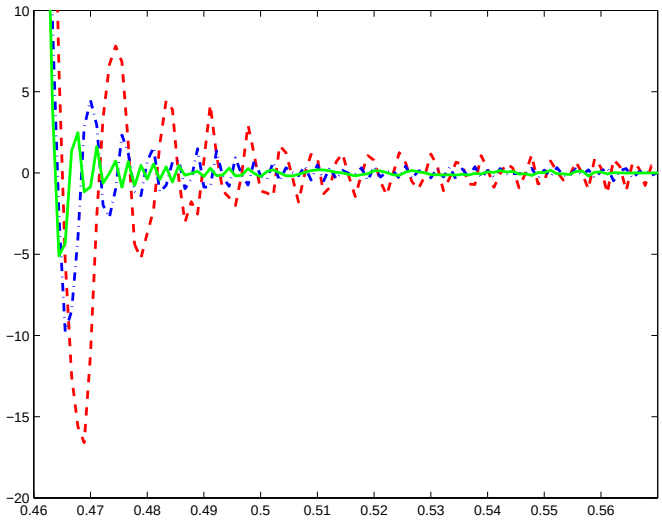

Figure: 4.3(e) E field vs depth – t=2.50025e-9

In addition to the qualitative convergence shown in Figure 4.3, it is useful to measure convergence quantitatively. To this end, we consider the ℓ^∞ and ℓ^2_N norms for each of the snapshots above. We define the norms as follows

$$|f(t) - g(t)|_{\ell^\infty} = sup_k |f(t, z_k) - g(t, z_k)|$$

$$|f(t) - g(t)|_{\ell^2_N} = \frac{1}{N} \left(\sum_k (f(t, z_k) - g(t, z_k))^2 \right)^{\frac{1}{2}}.$$

We consider the difference in norm values as we increase N from 900 to 1800 and from 1800 to 3600. Two incremental increases in N is not enough to make any conclusive statements about rate of convergence, but the results in Table 4.2 indicate that as the number of basis elements double, the ℓ^∞ norm values decrease by a third and the ℓ^2_N decrease by a half.

Snapshot	ℓ^∞ Norm	Value	ℓ^2_N Norm	Value
t=5.0025e-10	$\lvert E^{900}(t) - E^{1800}(t)\rvert$	13.07166	$\lvert E^{900}(t) - E^{1800}(t)\rvert$	3.48134e-2
	$\lvert E^{1800}(t) - E^{3600}(t)\rvert$	8.48205	$\lvert E^{1800}(t) - E^{3600}(t)\rvert$	1.17122e-2
t=1.00025e-9	$\lvert E^{900}(t) - E^{1800}(t)\rvert$	15.71388	$\lvert E^{900}(t) - E^{1800}(t)\rvert$	5.07030e-2
	$\lvert E^{1800}(t) - E^{3600}(t)\rvert$	10.58776	$\lvert E^{1800}(t) - E^{3600}(t)\rvert$	1.60562e-2
t=1.50025e-9	$\lvert E^{900}(t) - E^{1800}(t)\rvert$	15.64256	$\lvert E^{900}(t) - E^{1800}(t)\rvert$	5.90167e-2
	$\lvert E^{1800}(t) - E^{3600}(t)\rvert$	9.01038	$\lvert E^{1800}(t) - E^{3600}(t)\rvert$	1.80095e-2
t=2.00025e-9	$\lvert E^{900}(t) - E^{1800}(t)\rvert$	18.95285	$\lvert E^{900}(t) - E^{1800}(t)\rvert$	7.20012e-2
	$\lvert E^{1800}(t) - E^{3600}(t)\rvert$	10.70232	$\lvert E^{1800}(t) - E^{3600}(t)\rvert$	2.06295e-2
t=2.50025e-9	$\lvert E^{900}(t) - E^{1800}(t)\rvert$	19.42156	$\lvert E^{900}(t) - E^{1800}(t)\rvert$	8.11445e-2
	$\lvert E^{1800}(t) - E^{3600}(t)\rvert$	11.37242	$\lvert E^{1800}(t) - E^{3600}(t)\rvert$	2.17530e-2

Table 4.2 Convergence in norm

4.3 Sensitivity to parameter variation

While we have looked at the behavior of the system as time progresses for a fixed set of parameters, it is also important to examine the system dynamics as the parameters vary. There are many parameters in the model, most of which are material dependent. However the parameters with which we are most concerned are the coefficients of pressure in the polarization model, κ_γ, κ_ζ, and κ_τ.

Figures 4.4-4.7 illustrate the effect of letting each of these coefficients be zero. This is equivalent to assuming that the polarization parameters τ, ϵ_s, and ϵ_∞ are not pressure-dependent. The first three figures show the magnitude of the difference between the boundary data corresponding to the nonzero parameter values $\kappa_\gamma = 0.6\gamma_0$, $\kappa_\zeta = 0.3\zeta_0$, and $\kappa_\tau = 0.05\tau_0$ and the data corresponding to one identically zero parameter.

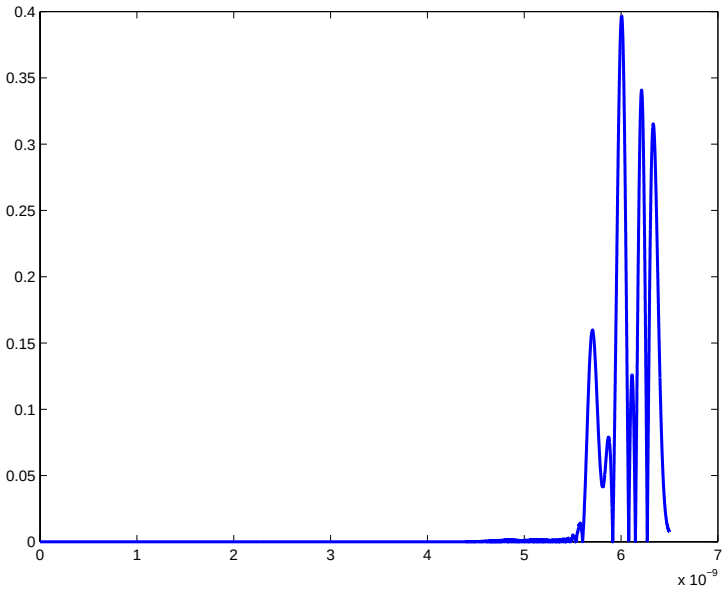

Figure 4.4: Difference in magnitude of E field measured at boundary for $\kappa_\gamma = 0.6\gamma_0$ and $\kappa_\gamma = 0.0$

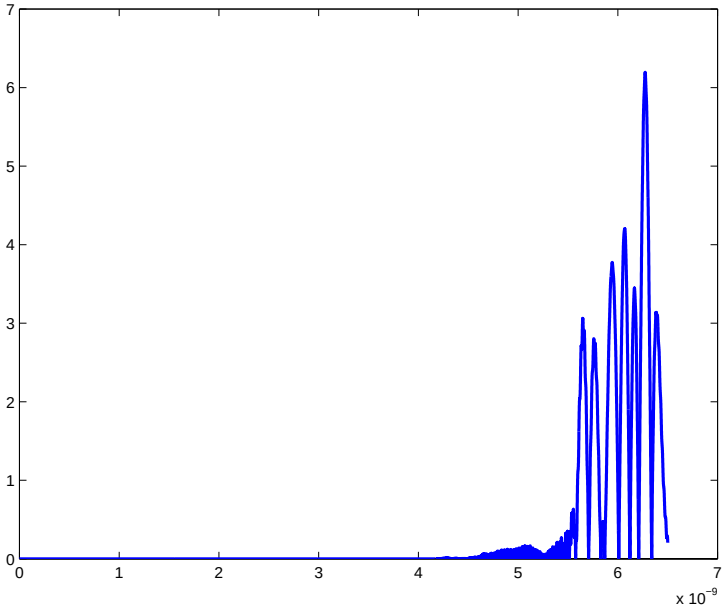

Figure 4.5: Difference in magnitude of E field measured at boundary for $\kappa_\zeta = 0.3\zeta_0$ and $\kappa_\zeta = 0.0$

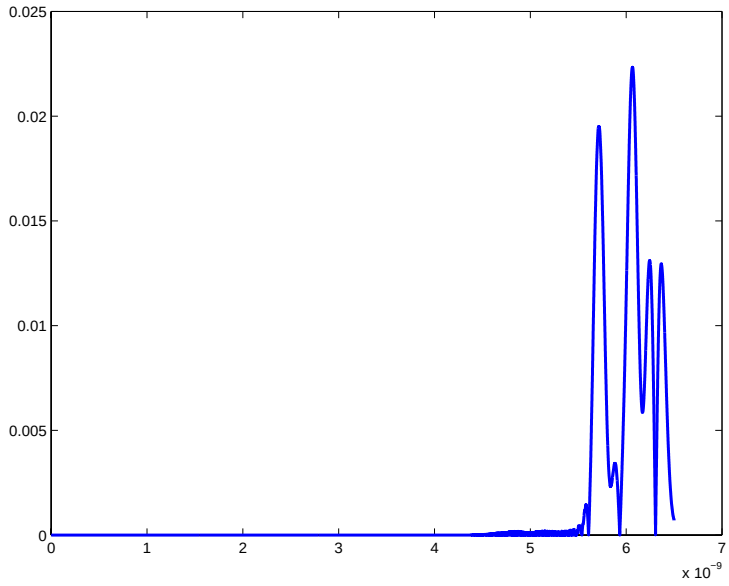

Figure 4.6: Difference in magnitude of E field measured at boundary for $\kappa_\tau = 0.05\tau_0$ and $\kappa_\tau = 0.0$

From Figures 4.4 and 4.6 we see that the difference between the data corresponding to $\kappa_\gamma = 0.6\gamma_0$ and $\kappa_\gamma = 0$ and the difference between data corresponding to $\kappa_\tau = 0.05\tau_0$ and $\kappa_\tau = 0$ are almost neglible. This suggests that the electromagnetic/acoustic interaction does not depend heavily on the pressure-dependence of γ and τ. The amplitude of the peaks in Figure 4.5 however is much larger than those in Figures 4.4 and 4.6. This suggests that ζ may have a more significant impact on the interaction. In order to better observe this impact, we directly compare the boundary data corresponding to $\kappa_\zeta = 0.3\zeta_0$, denoted with a solid line, with the boundary data corresponding to $\kappa_\zeta = 0.0$, denoted with a dashed line. (Due to the small amplitude peaks in Figures 4.4 and 4.6, comparisons of this type for κ_γ and κ_τ are superfluous.) The comparison is shown in Figure 4.7. The axes are restricted to show only the interval where the data sets are different. In this plot, we clearly see that the electromagnetic reflections from the pressure wave interaction are nearly nonexistent when $\kappa_\zeta = 0.0$. Again this implies that ζ, and hence ϵ_∞, has the most effect on the

electromagnetic/acoustic interaction.

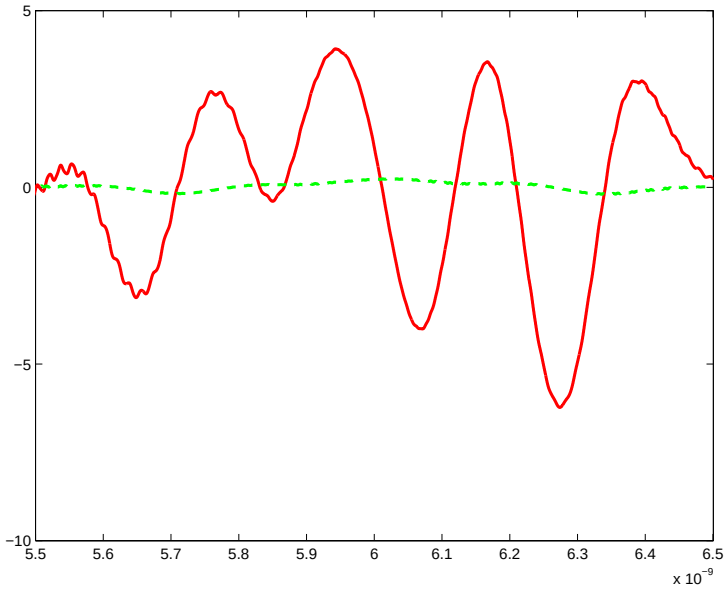

Figure 4.7: E field measured at boundary for $\kappa_\zeta = 0.3\zeta_0$ and $\kappa_\zeta = 0.0$

We have observed the effects of completely removing pressure-dependence from each parameter. Now we want to examine gradiations within the supposition of pressure-dependence. To this end, we assume that κ_γ, κ_ζ, and κ_τ are all non-zero and vary their magnitudes. Figures 4.8-11 show that there is little difference as we raise or lower the magnitudes of κ_γ and κ_τ. On the other hand, a noticeable increase in the amplitude of the pressure wave reflection with an increase in κ_ζ can be seen in Figure 4.12; $\kappa_\zeta = 0.4\zeta_0$ is denoted by "$- \cdot -$," $\kappa_\zeta = 0.3\zeta_0$ is denoted by "$- \ -$," and $\kappa_\zeta = 0.2\zeta_0$ is denoted by "–." This again supports the hypothesis that $\zeta(p) = \epsilon_\infty(p)$ is the most influential in the wave interaction.

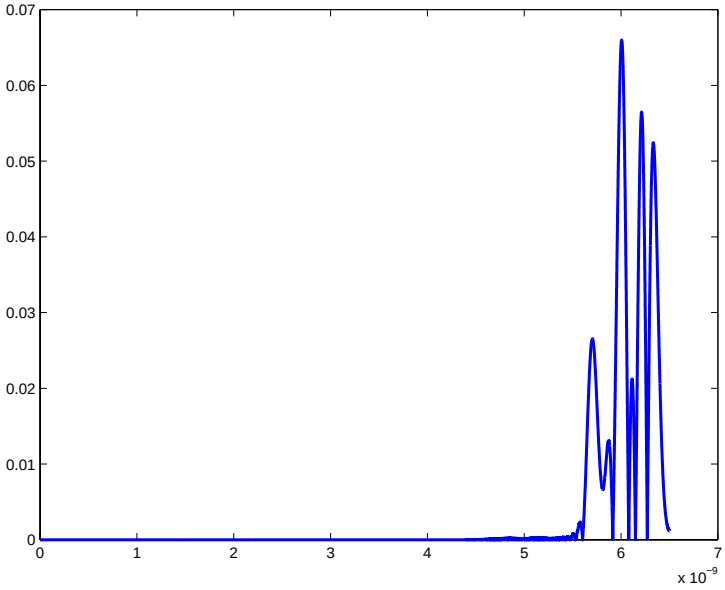

Figure 4.8: Difference in magnitude of E field measured at boundary for $\kappa_\gamma = 0.6\gamma_0$ and $\kappa_\gamma = 0.5\gamma_0$

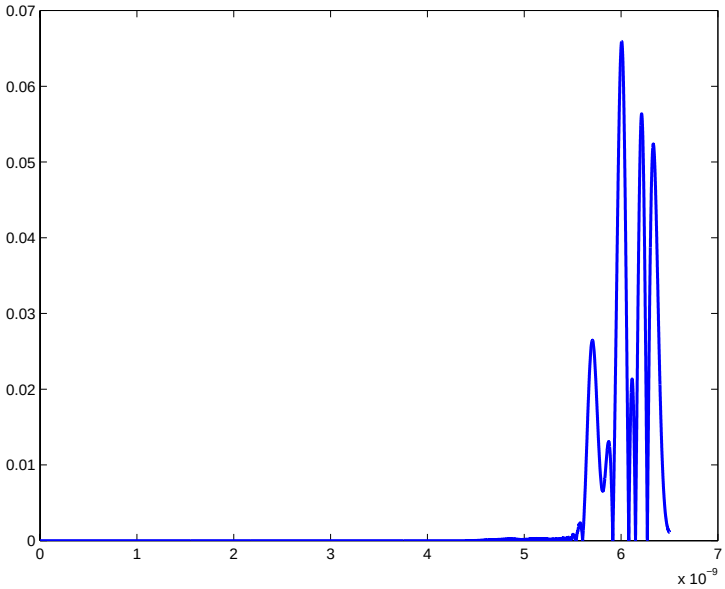

Figure 4.9: Difference in magnitude of E field measured at boundary for $\kappa_\gamma = 0.7\gamma_0$ and $\kappa_\gamma = 0.6\gamma_0$

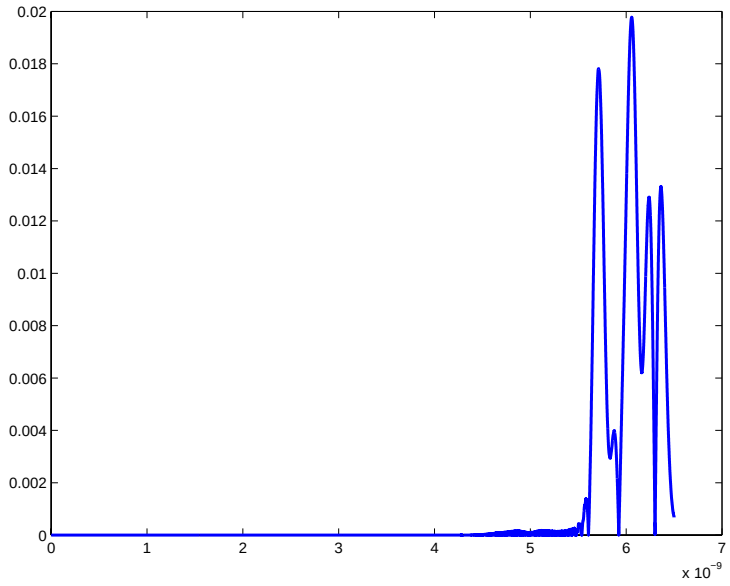

Figure 4.10: Difference in magnitude of E field measured at boundary for $\kappa_\tau = 0.1\tau_0$ and $\kappa_\tau = 0.05\tau_0$

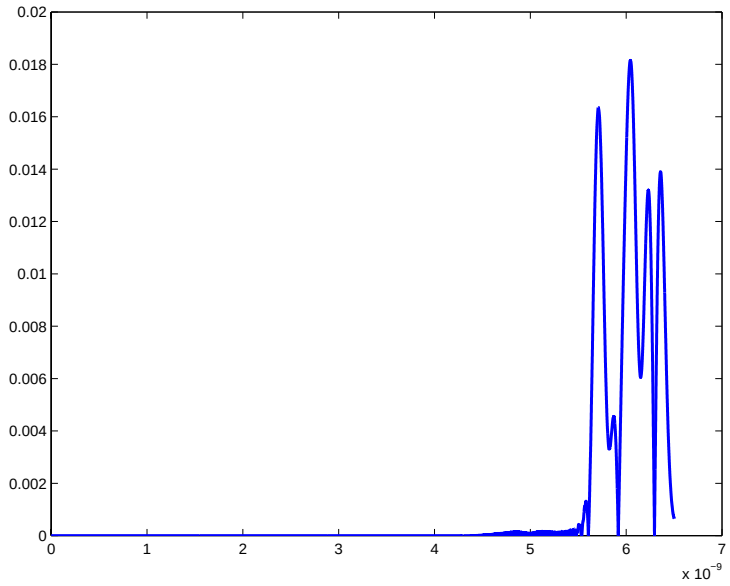

Figure 4.11: Difference in magnitude of E field measured at boundary for $\kappa_\tau = 0.15\tau_0$ and $\kappa_\tau = 0.1\tau_0$

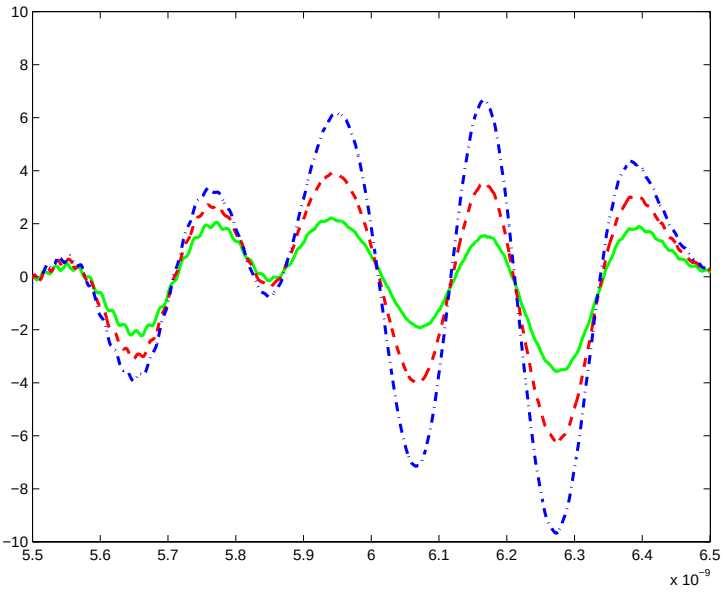

Figure 4.12: E field measured at boundary for $\kappa_\zeta = 0.4\zeta_0$, $\kappa_\zeta = 0.3\zeta_0$, and $\kappa_\zeta = 0.2\zeta_0$

Finally, we are interested in studying the effect of the acoustic pressure wave speed on the electromagnetic/acoustic interaction. We recall that the acoustic wave speed is very small relative to the speed of the E&M pulse. In the time snapshots shown in Figure 4.2, the spatial movement of the pressure wave is indiscernible. We wonder if this slowly varying acoustic pressure wave is essentially a standing wave. To evaluate the effect of a traveling wave, we look at the boundary data corresponding to different acoustic wave speeds. Figure 4.13 shows the boundary data corresponding to wave speeds $c_p = 2.5$ denoted by "$- \cdot -$," $c_p = 2.0$ denoted by "$- \ -$," and $c_p = 1.5$ denoted by "$-$." We restrict the axes to show just the pressure wave reflection data. We see that *as we increase wave speed we increase the amplitude of the reflection.* This suggests that the spatial dependence of the pressure wave is not a superfluous characteristic of the model.

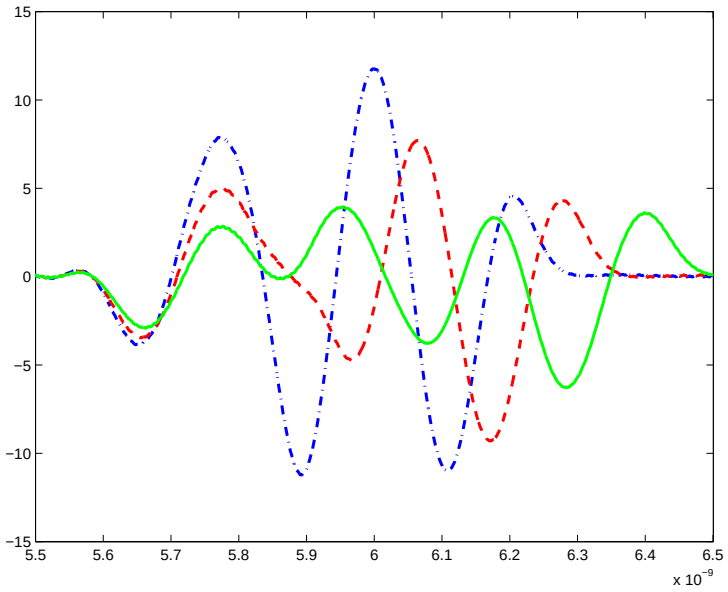

Figure 4.13: E field measured at boundary for different acoustic wave speeds

We can obtain a similar increase in amplitude of reflections by fixing the acoustic wave speed and increasing the acoustic frequency. This is illustrated in Figure 4.14 where $c_p = 1.5$ is fixed and "$-\cdot-$" denotes an acoustic frequency of $6.5\pi e04$, "$-\ -$"denotes an acoustic frequency of $5.5\pi e04$, and "$-$." denotes a frequency of $4\pi e04$. Again, the axes are restricted to show just the pressure wave reflection data. We note how alike Figures 4.13 and Figures 4.14 are.

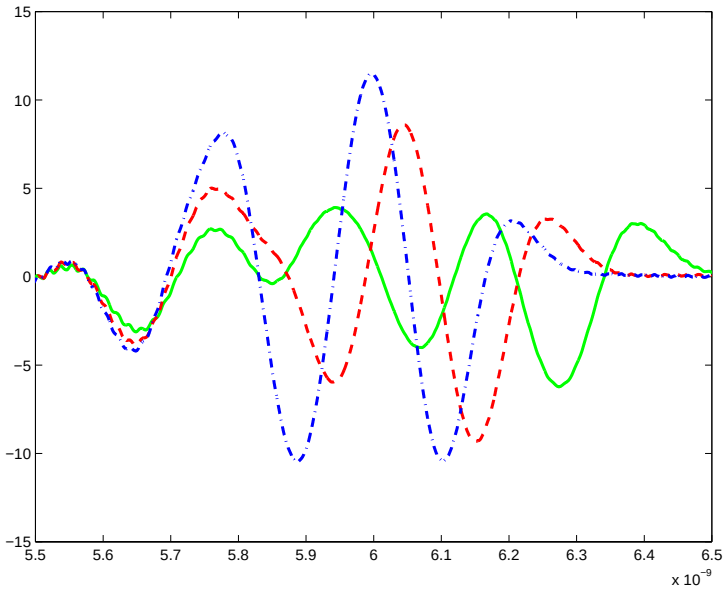

Figure 4.14: E field measured at boundary for different acoustic frequencies

These increases in amplitude are due to constructive interference of the electromagnetic wave reflections. The Bragg condition for optimal interference effects for light is given by (page 817, [39]; page 311, [22])

$$\sin\theta = \frac{\Lambda}{2\lambda},$$

where θ is the angle of incidence of the electromagnetic waves, Λ is the wavelength of the incident light, and λ is the wavelength of the acoustic wave. Since the wavelength is the wave velocity divided by the frequency of the wave, both of these parameters, speed and frequency, may have an effect on the level of constructive interference and hence the amplitude of the electromagnetic wave reflections.

The similarities between Figure 4.13, where we increase acoustic wave speed, and Figure 4.14, where we increase acoustic frequency, can also be explained through the Doppler effect. To understand this effect, we think of the dielectric as a stationary medium through which the acoustic wave travels at a speed c_p and the electromagnetic

wave as an observer moving at speed c. From its frame of reference, the electromagnetic wave "sees" the acoustic wave speed as $c_p - c$ and hence its frequency as $\frac{c_p - c}{\lambda}$ where λ is the wavelength of the acoustic wave (page 699, [39]). If we change the acoustic wave speed to $\tilde{c}_p$, we change the frequency "seen" by the electromagnetic wave to $\frac{\tilde{c}_p - c}{\lambda}$ since the wavelength remains the same. Thus, a modification of the acouctic wave speed results in an change of the acoustic wave frequency as "seen" by the electromagnetic wave.

Chapter 5

Parameter estimation

As we mention throughout, the crux of any electromagnetic interrogation problem is the identification of material parameters. The identification process generally involves comparing experimental data to observations from a mathematical model to determine which parameter values minimize the difference between the two.

In Chapter 3, we demonstrated that a (sub)sequence of minimizers $\{\bar{q}^N\}$ of the cost functionals (3.44) converges to a minimizer $\bar{q}$ of (3.41). In this chapter, we present computational results for the problem of finding $\bar{q}^N$ for a fixed N. (We attempt to choose N large so that $\bar{q}^N$ is close to $\bar{q}$.)

This problem is equivalent to our main objective, estimating the polarization and conductivity parameters of a dielectric by comparing numerical solutions of the model with experimental data. We recall from Chapter 2 that our polarization model has six material-dependent parameters, $\tau_0, \zeta_0, \gamma_0, \kappa_\tau, \kappa_\zeta$, and κ_γ in the equation

$$(\tau_0 + \kappa_\tau p)\,\dot{P} + P = \epsilon_0\,(\gamma_0 - \zeta_0 + (\kappa_\gamma - \kappa_\zeta)p)\,E,$$

and the conductivity coefficient σ.

We want to test the feasibilty of estimating them from experimental data. At this time, we do not yet have data from experiments (an experimental device to obtain

such data is currently being constructed); instead we create simulated data from our computations. The simulated data consists of the boundary data from a numerical approximation to the solution of the system with added noise. (See Chapter 4 for sample numerical solutions to the forward problem.) We compute this approximate solution with fixed parameters values. These values are then thought of as our "unknown" true material parameters. The goal is to estimate these values. We appraise our ability to solve the problem by comparing the estimates with the true fixed values. If we cannot accurately approximate the parameter values in this context, we cannot expect to be able to estimate them in an experimental setting.

We let q generically denote the set of parameters we wish to estimate in the examples presented below; these may include the mean values in the polarization model, τ_0, γ_0, and ζ_0, the coefficients of pressure in the polarization model, κ_τ, κ_γ, and κ_ζ, and/or the conductivity coefficient σ. We let q^* denote the true values of the corrsponding "unknown" parameters. We leave the values of all other parameters fixed.

There are two sets of electromagnetic reflections that reach the boundary. The first, after the initial signal, are the reflections from the air/dielectric interface and the second are from the virtual interface produced by the acoustic pressure wave. (Figure 5.1 depicts each set of reflections separately.) In some scenarios, using data that contains only one set of reflections may be advantageous. For example, one may use the data from the initial signal and the reflections from the air/dielectric interface (i.e., the first section of data in Figure 5.1) to refine the initial parameter estimates and then use these refinements with the data from the acoustic interface reflections to obtain final estimates. In another approach, one may use just the data from the acoustic interface reflections to estimate the parameters. In any case, the cost functional for the examples given here is of the form

$$J(q) = \sum_{i \in I} (E^i_{data} - E(t_i, 0; q))^2.$$

where I corresponds to an appropriately chosen data set. (Since here we consider exclusively the finite dimensional system for a fixed N, we drop the N for ease of notation.)

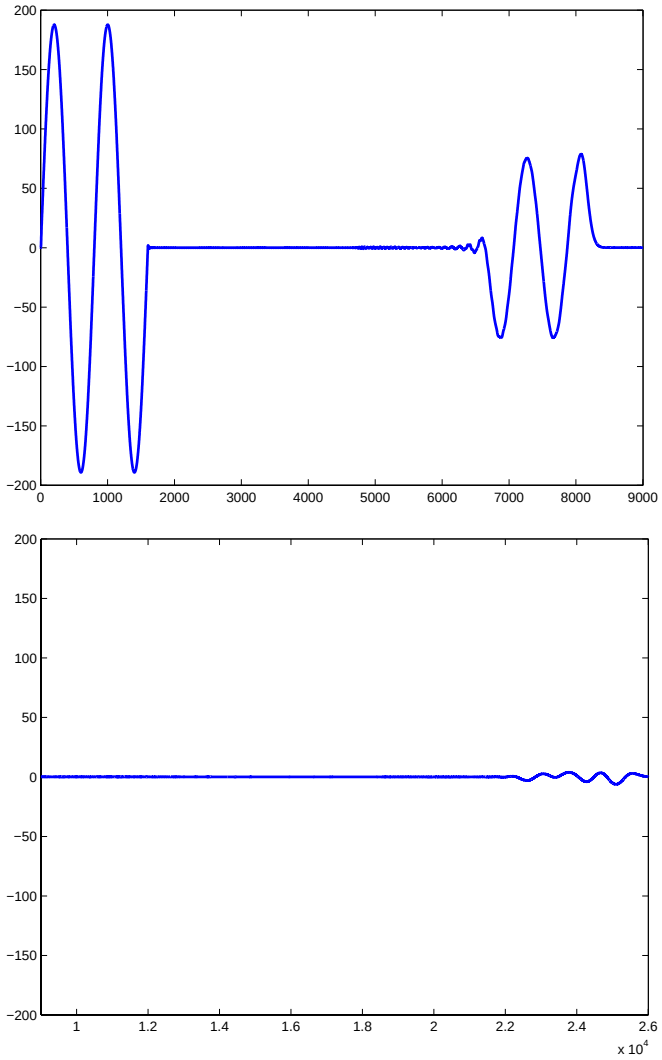

Figure 5.1: The two sets of reflections that reach the boundary

We used a Nelder Mead optimization routine [33] to find the parameter values that minimize the cost function. This optimization method is a gradient-free, simplex search method. The use of a gradient-based method to solve this problem is impractical due to computational time. The particular routine used requires an initial simplex of estimates and a termination tolerance for the difference between subsequent function evaluations. We choose the initial estimates to have varying levels of error in relation to the true parameter values. For these computations, we set the termination tolerance at 1e-09.

As already noted, we created simulated data to test our algorithms. The data set without noise is simply observations at the boundary taken from a forward simulation of the model using the parameter set q^*. The data sets with error were created by adding an appropriate amount of normally distributed relative random noise to the original data set. The random noise was generated by the MATLAB command *randn* which creates normally distributed noise with mean 0 and variance 1 and was scaled and shifted appropriately. Because the noise is relative, the magnitude of noise is greater in the intervals of data that contain the initial interrogating impulse and the reflections.

We next present sample results for specific parameter estimation problems. We first consider the problem of estimating $q^* = [\gamma_0^*, \zeta_0^*, \lambda^* = \frac{1}{\sqrt{\mu_0 \epsilon_0} \tau_0^*}]$
$= [78.2, 5.5, 0.10545728042059]$ from data with varying levels of noise. Here τ_0^* is so small that it is advantageous to estimate λ^*, a scaled function of τ_0^*; an estimated value of τ_0^* may be computed from an estimation of λ^*. We use the data containing the initial signal and the reflections from the air/dielectric interface to refine the initial parameter estimates q_0 and the data containing the reflections from the acoustic interface to obtain final estimates. We present the results in the following table.

Initial estimate q_0	Final estimate for data without noise $\bar{q}$
$q_0 = 1.0q^*$	[78.2, 5.5, 0.10545728042059]
$q_0 = 0.95q^*$	[78.190631, 5.499999, 0.105462]
$q_0 = 1.05q^*$	[78.197841, 5.500000, 0.105458]
$q_0 = 0.9q^*$	[77.128609, 5.499937, 0.107040]
$q_0 = 1.1q^*$	[70.763992, 5.499504, 0.117540]
	Final estimate for data with 1% noise
$q_0 = 0.95q^*$	[78.210472, 5.499997, 0.105444]
$q_0 = 1.05q^*$	[77.260485, 5.499940, 0.106852]
$q_0 = 0.9q^*$	[78.198944, 5.499998, 0.105461]
$q_0 = 1.1q^*$	[78.482467, 5.500010, 0.105052]
	Final estimate for data with 5% noise
$q_0 = 0.95q^*$	[74.876211, 5.499764, 0.110559]
$q_0 = 1.05q^*$	[77.975797, 5.499939, 0.105722]
$q_0 = 0.9q^*$	[78.337467, 5.500010, 0.105186]
$q_0 = 1.1q^*$	[78.405972, 5.499987, 0.105175]

Table 5.1: Parameter estimation results for
$q^* = [\gamma_0^*, \zeta_0^*, \lambda^* = \frac{1}{\sqrt{\mu_0 \epsilon_0} \tau_0^*}] = [78.2, 5.5, 0.10545728042059]$

These results illustrate that it is possible to recover accurate approximations of γ_0^*, ζ_0^*, and λ^* in the presence of noise and with error up to 10% in the initial estimates. A few of the results are unexpected, for instance the ability to approximate the values better in the presence of 5% noise with an initial guess with -10% error than with an initial guess with -5% error. We suspect these anomalies are due to the simplex search nature of the optimization routine.

The results in the table clearly indicate that we can recover q^* without much error.

However it is often illustrative to compare the solutions calculated with the estimates with the solutions calculated with q^*. To do this, we plot the absolute value of the error for the solutions computed at the boundary, i.e.,

$$|E(t_i, 0; \bar{q}) - E(t_i, 0; q^*)|,$$

where $\bar{q}$ is the final estimate (given in the table). As an example, Figure 5.2 depicts this error for the estimation problem with 5% noise and an initial guess with -10% error. We see that overall the magnitude of error is small and that, as expected, the most error occurs in approximating the material and acoustic interface reflections.

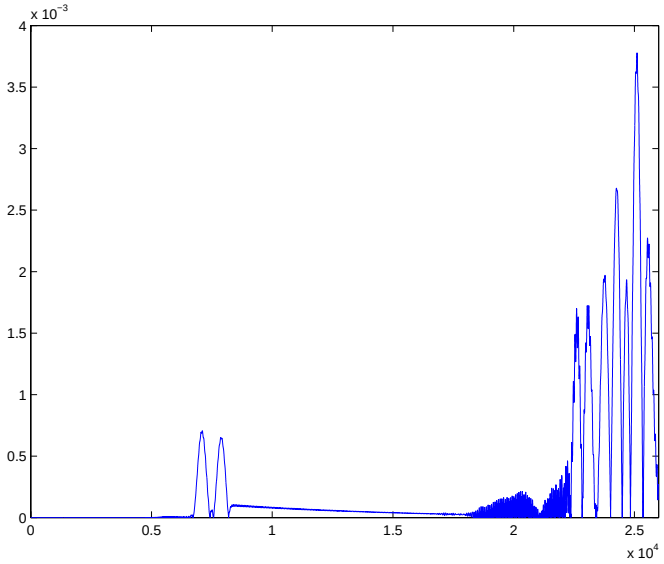

Figure 5.2: $|E(t_i, 0; \bar{q}) - E(t_i, 0; q^*)|$ vs t_i –
Absolute error for the parameter estimation problem
with 5% noise and an initial guess with -10% error

We next consider the estimation of $q^* = [\kappa_\gamma^*, \kappa_\zeta^*, \kappa_\tau^*] = [46.92, 1.65, 1.581139e - 09]$ from the previous data sets. Since these parameters are the coefficients of pressure, they are irrelevant and undeterminable until the electromagnetic/acoustic interaction

occurs. Thus we include only the second section of data in the cost functional. We present the results below.

Initial estimate q_0	Final estimate for data without noise $\bar{q}$
$q_0 = 0.99q^*$	[46.450800, 1.633500, 3.16174e-09]
$q_0 = 1.01q^*$	[46.92, 1.65, 1.58114e-09]
$q_0 = 0.95q^*$	[44.574000, 1.567500, 5.52700e-09]
$q_0 = 1.05q^*$	[49.266000, 1.732500, 0]
$q_0 = 0.9q^*$	[42.228000, 1.485000, 0]
$q_0 = 1.1q^*$	[51.61200, 1.815000, 0]
	Final estimate for data with 1% noise
$q_0 = 0.99q^*$	[46.450800, 1.633500, 3.17078e-09]
$q_0 = 1.01q^*$	[47.389200, 1.666500, -7.2435e-10]
$q_0 = 0.95q^*$	[44.574000, 1.567500, 5.53493e-09]
$q_0 = 1.05q^*$	[49.266000, 1.732500, -1.064074e-08]
$q_0 = 0.9q^*$	[42.228000, 1.485000, 6.01095e-09]
$q_0 = 1.1q^*$	[51.612000, 1.814500, -1.712928e-08]
	Final estimate for data with 5% noise
$q_0 = 0.99q^*$	[46.450800, 1.633500, 3.22126e-09]
$q_0 = 1.01q^*$	[47.389200, 1.666500, -6.6658e-10]
$q_0 = 0.95q^*$	[44.574000, 1.567500, 5.56261e-09]
$q_0 = 1.05q^*$	[49.266000, 1.732500, -1.061871e-08]
$q_0 = 0.9q^*$	[42.228000, 1.485000, 6.02759e-09]
$q_0 = 1.1q^*$	[51.612000, 1.815000, -1.712024e-08]

Table 5.2: Parameter estimation results for

$q^* = [\kappa_\gamma^*, \kappa_\zeta^*, \kappa_\tau^*] = [46.92, 1.65, 1.581139e-09]$

We are able to obtain reasonable estimates for the parameters, especially κ_γ^* and κ_ζ^*.

We have difficulty estimating the value of κ_τ^*, most likely because the value is small. In general, the estimation error increases with the error in the initial guess. However, increasing the noise level in the data does not significantly effect the estimation accuracy.

We note that we obtain better estimates for the mean values (γ_0^*, ζ_0^*, and τ_0^*) than for the pressure coefficients ($\kappa_\gamma^*, \kappa_\zeta^*$, and κ_τ^*). This is understandable, as the mean values are more influential in the system dynamics. They are also more important in identifying and characterizing the material.

In an electromagnetic interrogation parameter estimation problem, an estimate is sufficient if it can be used to classify the material. We consider the results for estimating $q^* = [\kappa_\gamma^*, \kappa_\zeta^*, \kappa_\tau^*] = [46.92, 1.65, 1.581139e-09]$ using data with 5% relative normal noise and an initial guess with -10% error. After solving the parameter estimation problem, we obtain the result $\bar{q} = [42.228000, 1.485000, 6.02759e-09]$. If parameter values within the hypothetical range, $40 < \kappa_\gamma < 50$, $1.4 < \kappa_\zeta < 1.8$, and $1e-09 < \kappa_\tau < 9e-09$ are characteristic of the material under interrogation, we are successful in our attempt to solve the estimation problem. On the other hand, if the characteristic material parameters fall within the (hypothetical) range $45 < \kappa_\gamma < 47$, $1.6 < \kappa_\zeta < 1.7$, and $1e-09 < \kappa_\tau < 2e-09$, we are unable to characterize the material with our estimates and our attempt is unsuccessful. Ranges of these parameter values for different materials have not been experimentally determined, so we have no concrete measure as yet to assess our ability to solve the problem.

We now turn our attention to estimating the conductivity coefficient σ. We recall that the material conductivity is described by Ohm's law, $J_c = \sigma E$.

Knowing the value of the conductivity coefficient can be very useful in characterizing a material. Therefore we also want to assess our ability to estimate σ with the process described above. Since our model does not specify pressure-dependent conductivity, we do not expect the acoustic interaction to modulate the value of σ. Thus we use

all of the data simultaneously in the estimation process. The results are presented in Table 5.3.

Initial iterate	Final estimate for data without noise
0.99 σ^*	0.990000e-05
1.01 σ^*	1.010000e-05
0.95 σ^*	0.950000e-05
1.05 σ^*	1.050000e-05
$0.9\sigma^*$	0.900000e-05
1.1 σ^*	1.100000e-04
	Final estimate for data with 1% noise
0.99 σ^*	0.990000e-05
1.01 σ^*	1.010000e-05
0.95 σ^*	1.180000e-05
1.05 σ^*	1.050000e-05
0.9 σ^*	1.280000e-05
1.1 σ^*	1.100000e-05
	Final estimate for data with 5% noise
0.99 σ^*	2.140000e-05
1.01 σ^*	2.120000e-05
$0.95\sigma^*$	2.140000e-05
1.05 σ^*	2.160000e-05
0.9 σ^*	2.160000e-05
1.1 σ^*	2.130000e-05

Table 5.3: Parameter estimation results for $\sigma^* = 1.0e-05$

Although our final estimates for σ^* are reasonable, we see that often, especially when the data is without noise, our initial estimate, even with inherent error, is deemed

sufficient by the optimization routine. This indicates that small changes in the value of σ do not significantly affect the system behavior. This makes finding the true value of the conduction coefficient more difficult because many values of σ nearly minimize the cost functional.

The results in this chapter indicate that we can successfully estimate material parameters from noisy simulated data. We obtain the most accurate estimates for the mean values in the pressure-dependent polarization model. Because in practice these values (the mean relaxation time and permittivities) are known for various materials and can be compared with the estimated values for identification purposes, this is a satisfying result.

Chapter 6

Hypothesis testing

The foundation of our electromagnetic interrogation technique rests on the idea that the system polarization is pressure-dependent and the parameters characterizing this dependence can be identified. We base our polarization model on the systemic physics and dynamics and believe the pressure is significant. We wish to investigate the significance of the pressure-dependent terms from a statistical perspective.

To do this, we follow [9] and compare the cost functional values obtained by minimizing over two different sets of admissible parameters. One set is the admissible set described in Chapter 5; the other is restricted to omit the pressure-dependence from the model. We minimize the cost functional over both parameter sets using data from a pressure-dependent model and using data from a pressure-independent model to test the significance of the pressure-dependence.

Specifically, if we consider the problem of estimating the parameters in the polarization relaxation function $\tau(p) = \tau_0 + \kappa_\tau p$, we want to study the significance of the $\kappa_\tau p$ term. We let Q be the set of admissible values of (τ_0, κ_τ) (see Chapter 5) and Q_0 be the set of admissible values of $(\tau_0, 0)$. We note that the values in Q_0 have a fixed value $\kappa_\tau = 0$ and thus the parameter estimation problem has less freedom. We solve the parameter estimation problem over Q and Q_0 and compare the resulting values

of the cost functional. We use pressure-dependent and pressure-independent data to test the significance of the pressure terms in each. (In the case where the model is fitted to pressure-independent data, the coefficients of pressure not being estimated, κ_γ and κ_ζ, are set to zero.) We consider the problems of estimating the parameters in the permittivity functions $\gamma(p) = \gamma_0 + \kappa_\gamma p$ and $\zeta(p) = \zeta_0 + \kappa_\zeta p$ in an analogous manner.

We compare the cost function values via the test statistic

$$U_n^N = n\frac{J_n^N(\hat{q}_n^N) - J_n^N(\bar{q}_n^N)}{J_n^N(\bar{q}_n^N)} \tag{6.1}$$

where $\hat{q}_n^N$ is the minimizer of J_n^N over Q_0 and $\bar{q}_n^N$ is the minimizer of J_n^N over Q. Here n is the number of observations in the data and N is the number of spatial basis elements in the numerical approximation. The theory detailed in [9] states that under certain assumptions we have consistency of estimators

$$\bar{q}_n^N \to q^*$$

as N and n tend to infinity, where q^* is the parameter value used to generate the data. Moreover the theory establishes the convergence

$$U_n^N \to \chi^2(1)$$

for $q^* \in Q_0$ where $\chi^2(1)$ is a chi-squared distributed random variable with one degree of freedom. The first result assures us that as the number of observations increases and the approximate solutions approach the true solution our parameter estimate approaches the true value. As theoretically important as this result is, the second is more useful. It says that as the number of observations and level of approximation increase, the behavior of our test statistic U_n^N approaches that of a $\chi^2(1)$ distributed random variable.

We employ this result in the following way. If $q^* \notin Q_0$, we expect $J_n^N(\hat{q}_n^N)$ to be larger than $J_n^N(\bar{q}_n^N)$, with a greater difference giving more weight to the assumption $q^* \notin Q_0$. Thus, in order to reject the hypothesis $q^* \in Q_0$ we need to be confident that U_n^N is sufficiently large. Since the limiting value of U_n^N is a random variable with a $\chi^2(1)$ distribution, we use the $\chi^2(1)$ distribution to define what it means for U_n^N to be "large". For example, there is a probability of 0.9 that a randomly $\chi^2(1)$ distributed variable X is less than 2.70554, so we may choose to say that U_n^N is "large" if $U_n^N > 2.70554$. In this case, we would say that we reject the the hypothesis $q^* \in Q_0$ with ninety percent certainty.

The following results were obtained using the test statistic (6.1). In these examples, the number of observations is $n = 26002$ and the number of basis elements is $N = 900$. We use the two-step process mentioned in Chapter 5 in the minimization process; thus the values of J_n^N shown here are weighted sums of the cost functional values from each minimization. The simulated data has 1% normally distributed relative noise added to it, and we start our minimization processes with $\pm 5\%$ error in the initial guess.

The first example involves testing the hypothesis $H_0 : \kappa_\tau = 0$ *for simulated data from the pressure-dependent model*. As in our hypothetical example, we want to compare the test statistic U_n^N with the $\chi^2(1)$ distribution. The rejection criteria with 99.5% certainty for the $\chi^2(1)$ distribution is 7.87944. As we see in Table 6.1 both of the test statistic values for this first example are greater than the rejection criteria. Thus we reject the hypothesis. This indicates that one should use a pressure-dependent relaxation term to successfully model pressure-dependent data.

The natural example to consider next is testing the hypothesis $H_0 : \kappa_\tau = 0$ *for simulated data from the model without pressure-dependence*. However due to limitations in our optimization routine we are unable to find minimizers (τ_0, κ_τ) when the data is pressure-independent (see Table 6.2). We suspect that this is due to the fact that κ_τ^* is nearly zero.

Degrees of freedom	Initial iterate	Intermediate costs	Final total cost	Test statistic
1	$0.95\tau_0^*$	3.940324e-02 1.533029	1.015872	2.789816e+02
2	$0.95\tau_0^*$ $0.95\kappa_\tau^*$	3.940324e-02 1.516533	1.005088	
1	$1.05\tau_0^*$	3.940324e-02 1.533029	1.015872	2.650209e+02
2	$1.05\tau_0^*$ $1.05\kappa_\tau^*$	3.940324e-02 1.517351	1.005622	

Table 6.1: Results for testing the hypothesis $H_0 : \kappa_\tau = 0$ *for simulated data from the pressure-dependent model*

Degrees of freedom	Initial iterate	Intermediate costs
1	$0.95\tau_0^*$	3.940324e-02 1.538113
2	$0.95\tau_0^*$ $0.05\kappa_\tau^*$	3.153384e-08 minimization failure
1	$1.05\tau_0^*$	3.940324e-02 1.538113
2	$1.05\tau_0^*$ $0.05\kappa_\tau^*$	3.940324e-02 minimization failure

Table 6.2: Results for testing the hypothesis $H_0 : \kappa_\tau = 0$ *for simulated data from the model without pressure-dependence*

We now turn our attention to the function describing permittivity at infinite frequencies $\epsilon_\infty = \zeta(p) = \zeta_0 + \kappa_\zeta p$ and test the hypothesis $H_0 : \kappa_\zeta = 0$ *for simulated data from the pressure-dependent model*. Since we are again comparing our test statistics with the $\chi^2(1)$ distribution, we use the same rejection criteria. The test statistic values given in Table 6.3 are greater than the rejection criteria, so we may again reject the hypothesis. This is further evidence that pressure-dependence is necessary to fit pressure-dependent data.

For this permittivity function, we are successful in our attempts to test the hypothesis $H_0 : \kappa_\zeta = 0$ *for simulated data from the model without pressure-dependence*. (The difference here is attributed to the fact that $\kappa_\zeta^* >> \kappa_\tau^*$.) The test statistics for this problem, given in Table 6.4, are greater than the rejection criteria, so we must reject the hypothesis. We know that $\kappa_\zeta^* = 0$ for pressure-independent data, so this is contrary to our expectation. We suspect that this contradiction to our expected results is due to the noise in our data.

Degrees of freedom	Initial iterate	Intermediate costs	Final total cost	Test statistic
1	0.95 ζ_0^*	3.940135e-02 1.557529	1.031888	3.450000e02
2	$0.95\zeta_0^*$ $0.95\kappa_\zeta^*$	3.940135e-02 1.536861	1.018376	
1	$1.05\zeta_0^*$	3.940135e-02 1.557529	1.031889	3.450000e02
2	$1.05\zeta_0^*$ $1.05\kappa_\zeta^*$	3.940135e-02 1.536861	1.018376	

Table 6.3: Results for testing the hypothesis $H_0 : \kappa_\zeta = 0$ *for simulated data from the pressure-dependent model*

Degrees of freedom	Initial iterate	Intermediate costs	Final total cost	Test statistic
1	0.95 ζ_0^*	3.940135e-02 1.538114	1.019195	2.470169e02
2	0.95 ζ_0^* 0.05 κ_ζ^*	3.940135e-02 1.523442	1.009604	
1	1.05 ζ_0^*	3.940135e-02 1.538114	1.019195	2.470169e02
2	1.05 ζ_0^* 0.05 κ_ζ^*	3.940135e-02 1.523442	1.009604	

Table 6.4: Results for testing the hypothesis $H_0 : \kappa_\zeta = 0$ *for simulated data from the model without pressure-dependence*

Lastly we consider the significance of the pressure-dependent term in the static permittivity $\epsilon_s = \gamma(p) = \gamma_0 + \kappa_\gamma p$. We begin by testing the hypothesis $H_0 : \kappa_\gamma = 0$ *for simulated data from the pressure-dependent model*. Comparing the test statistics in Table 6.5 with the rejection criteria used previously, we reject this hypothesis. This indicates that the pressure-dependence of the static permittivity is significant.

We now test the final hypothesis $H_0 : \kappa_\gamma = 0$ *for simulated data from the model without pressure-dependence*. The resulting test statistics given in Table 6.6 exceed the rejection criteria, so we reject the hypothesis H_0. This again contradicts our expectation but may be an unavoidable artifact of the noise in our data.

Degrees of freedom	Initial iterate	Intermediate costs	Final total cost	Test statistic
1	$0.95\gamma_0^*$	3.940323e-02 1.5190312	1.006721 0.995530	2.923008e02
2	$0.95\gamma_0^*$ $0.95\kappa_\gamma^*$	3.940323e-02 1.501913		
1	$1.05\gamma_0^*$	3.940323e-02 1.519031	1.006721	2.923008e02
2	$1.05\gamma_0^*$ $1.05\kappa_\gamma^*$	3.940323e-02 1.501913	0.995530	

Table 6.5: Results for testing the hypothesis $H_0 : \kappa_\gamma = 0$ *for simulated data from the pressure-dependent model*

Degrees of freedom	Initial iterate	Intermediate costs	Final total cost	Test statistic
1	$0.95\gamma_0^*$	3.940323e-02 1.538113	1.019196	5.189145e02
2	$0.95\gamma_0^*$ $0.95\kappa_\gamma^*$	3.940323e-02 1.507610	0.999254	
1	$1.05\gamma_0^*$	3.940323e-02 1.538113	1.019196	5.189145e02
2	$1.05\gamma_0^*$ $1.05\kappa_\gamma^*$	3.940323e-02 1.507610	0.9992542	

Table 6.6: Results for testing the hypothesis $H_0 : \kappa_\gamma = 0$ *for simulated data from the model without pressure-dependence*

The previous results suggest that the pressure-dependent terms are in fact significant

when developing a model to describe data with inherent pressure-dependent polarization. This provides additional justification for our use of pressure-dependent terms in the polarization model. If there is pressure-dependence in the system polarization, a model that omits pressure-dependent terms will not adequately represent the dynamics.

The results also indicate that when the pressure-dependence is not present in the data, hypothesis testing does not necessarily validate the assumption that the pressure coefficients are zero. We believe this is due to the noise in the data; although the pressure-induced system dynamics are significant, they are small and may not be easily detected in the presence of noise.

Chapter 7

The acoustic system

7.1 Introduction and problem motivation

In all of our work until this point, we let the acoustic pressure be a given function, dependent on space and time but independent of electric field and polarization. In other words, we tacitly assume that the effect of the electromagnetic fields and polarization on the pressure wave is negligible. This assumption is reasonable (page 810, [39]), but perhaps not completely physical. Thus in future work we may want to model the behavior of the pressure wave and its modulation as a result of electromagnetic fields. In this chapter, we make a step in this direction by first solving the acoustic wave equation in the absense of any electromagnetic fields. We investigate impulse generated pressure waves in a heterogeneous medium. In particular, we consider an acoustic pressure wave initiated by a windowed sine wave impulse traveling through a layered medium and formulate the equations and boundary conditions describing the system. We explore several approaches to solving the problem with the finite element method and settle on a (somewhat nonstandard) fully Galerkin scheme. We then present solutions obtained with this method.

7.2 Problem formulation

In this section, we present the system under consideration. First, we write the equations that describe the behavior of the traveling acoustic wave in strong form. Then we develop a variational formulation for the system and discuss difficulties that arise while doing so.

We consider the wave equation for acoustic pressure in a material consisting of three homogeneous layers. We assume that in the left and right layers of the material the wave propagates with the same wave speed, but that the wave travels at a different speed in the middle layer. The boundary conditions are given by the input of windowed sine wave at $z = 1$ and a no reflection, or total absorbing, condition at $z = 0$. A schematic of the geometry is given in Figure 7.1. We suppose that the system is initially at rest. Then the equations that govern this system are given by

$$\ddot{\tilde{p}} - c^2(z)\tilde{p}'' = 0 \tag{7.1}$$

$$\begin{aligned} \tilde{p}(0,z) &= 0 \qquad & \tilde{p}(t,1) &= f(t) \\ \dot{\tilde{p}}(0,z) &= 0 \qquad & \dot{\tilde{p}}(t,0) - c(0)\tilde{p}'(t,0) &= 0 \end{aligned}$$

where

$$c(z) = \begin{cases} c_1 & 0 \le z < z_1 \\ c_2 & z_1 \le z \le z_2 \\ c_1 & z_2 < z \le 1, \end{cases} \qquad f(t) = \begin{cases} 0 & 0 \le t \le \tau, t \ge 2\tau \\ \sin(\frac{2\pi}{\tau}(t-\tau)) & \tau < t < 2\tau. \end{cases}$$

for $0 \le z_1 \le z_2 < 1$ and $0 < \tau$.

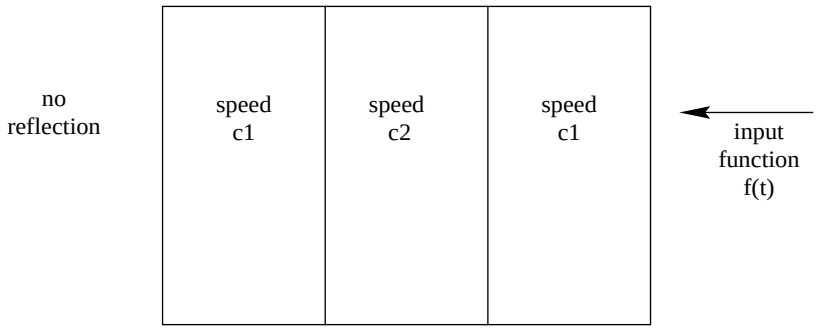

Figure 7.1: Schematic diagram of geometry

Since finding a solution to the wave equation is normally an easy exercise in solving partial differential equations, computing a numerical solution to this system would appear to be a simple chore. However, unique characteristics of this system make solving it a somewhat more challenging task.

To treat the nonhomogeneous time dependent Dirichlet boundary condition at $z = 1$, we make a change of variables which facilitates finite element solutions. To obtain a new equation with a homogeneous boundary condition at $z = 1$, we introduce a new state variable p defined by

$$p(t, z) = \tilde{p}(t, z) - zf(t). \tag{7.2}$$

In this new state our system is

$$\ddot{p} - c^2(z)p'' + z\ddot{f}(t) = 0 \tag{7.3}$$

$$\begin{aligned} p(0,z) &= 0 \qquad & p(t,1) &= 0 \\ \dot{p}(0,z) &= 0 \qquad & \dot{p}(t,0) - c_1 p'(t,0) - c_1 f(t) &= 0 \end{aligned} \tag{7.4}$$

$$\begin{aligned} p(t,z_1-) &= p(t,z_1+) \qquad & c^2(z_1-)p'(t,z_1-) &= c^2(z_1+)p'(t,z_1+) \\ p(t,z_2-) &= p(t,z_2+) \qquad & c^2(z_2-)p'(t,z_2-) &= c^2(z_2+)p'(t,z_2+) \end{aligned} \tag{7.5}$$

where $c(z)$ and $f(t)$ are as defined above. We observe that this change of variable does provide the desired boundary condition at $z = 1$. Since discontinuities (at z_1 and z_2) are present in the propagating medium, we also must introduce interface conditions. We do this by requiring continuity of $p(t,\cdot)$ and $c^2p'(t,\cdot)$ at $z = z_1$ and $z = z_2$. (We note that these conditions *should* be applied to the original equation for $\tilde{p}$, but to simplify the computations we require the conditions of p after changing variables.) The continuity on p will be an essential condition while the continuity of c^2p' will be a natural condition in our weak formulation below.

Since $c(z)$ is only piecewise continuous in z, we do not expect solutions to the above equation in strong form in space (i.e., C^2 or even only H^2 in z). Therefore, for both theoretical and computational purposes, it is useful to write the system in weak or variational form in the spatial variable. This approach is standard. However, we note that in our change of variables, we have introduced the term $\ddot{f}(t)$ into the wave equation. If we recall that the function f is a windowed sine wave, we realize that its second derivative $\ddot{f}(t)$ includes a delta impulse in time (see Figure 7.2). One thus observes that we also may not be able to expect solutions in strong form in time. Thus, we may expect distributional derivatives in both time and space.

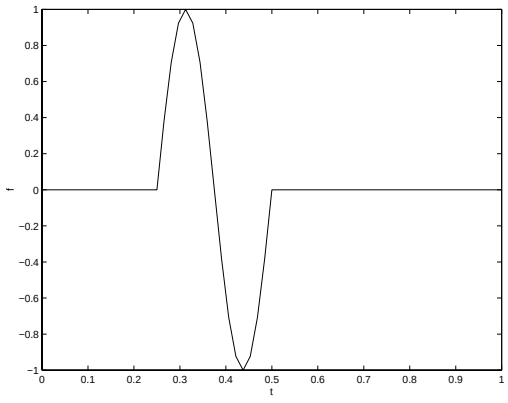

Figure 7.2(a): f(t)

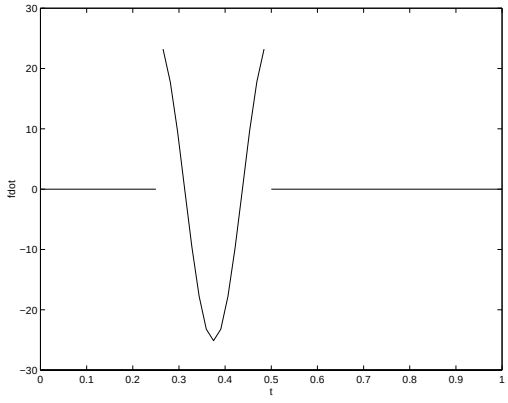

Figure 7.2(b): First derivative of f(t)

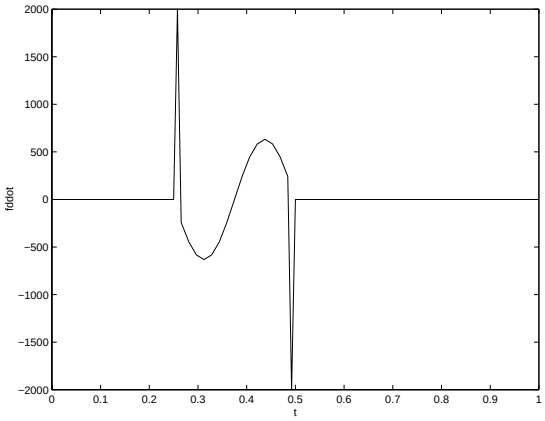

Figure 7.2(c): Second derivative of f(t)

We tried two different approaches to deal with potential difficulties due to lack of smoothness of solutions. First, we ignored the lack of smoothness of $\ddot{f}$ and proceeded with a standard semi-Galerkin finite element method. Since we know that our solution should be a traveling sine wave (at least if we assume $c_1 = c_2$), it was clear from the resulting simulations that this solution technique was not adequate. For our second approach, we used mollifiers to smooth the "windowing" of the function f and again continued in the traditional way using a standard semi-Galerkin finite element method. However, this approach led to solutions that failed to converge to

the known solution. We concluded that an appropriate way to solve the problem might be to use a fully Galerkin finite element scheme. For further discussion of fully Galerkin methods, see, for example, [28], [36].

We let $< \cdot, \cdot >$ denote the usual L^2 inner product on $(0,1)$, i.e.,
$< f, g >= \int_0^1 f(z)g(z)\ dz$, and we let $< \cdot, \cdot >_{(a,b)}$ denote the L^2 inner product on the specified interval (a,b). We define the spaces $H^1_R(a,b) = \{\phi \in H^1(a,b) | \phi(b) = 0\}$ and $H^1_L(a,b) = \{\phi \in H^1(a,b) | \phi(a) = 0\}$. Moreover, we use the notation $f \in \mathcal{H}(X)$ where $X = (a,b) \cup (b,c) \cup (c,d)$ to denote that f restricted to each of the open intervals is H^2 on that interval.

We suppose that p satisfies (7.3), (7.4) and the following hold:

$$\begin{aligned} &p \in H^1_L(0,T; H^1_R(0,1)) \\ &p(\cdot, z) \in H^2(0,T) \text{ almost everywhere in } (0,1) \\ &p(t, \cdot) \in \tilde{H} \equiv \{\phi \in C(0,1) : \phi \in H^2(\tilde{\Omega})\} \text{ almost everywhere in } (0,T), \\ &\quad \text{where } \tilde{\Omega} \equiv (0, z_1) \cup (z_1, z_2) \cup (z_2, 1). \end{aligned} \tag{7.6}$$

Then

$$\int_0^T < \ddot{p}, \phi > \psi\ dt\ - \int_0^T < c^2(z)p'', \phi > \psi\ dt\ + \int_0^T \ddot{f}\psi\ dt < z, \phi >= 0$$

holds for all $\phi \in H^1_R(0,1)$ and for all $\psi \in H^1_R(0,T)$.

Integrating by parts, we have

$$- \int_0^T < \dot{p}, \phi > \dot{\psi} \; dt$$

$$+ \int_0^T \left(c_1^2 < p', \phi' >_{(0,z_1)} \; + c_2^2 < p', \phi' >_{(z_1,z_2)} \; + c_1^2 < p', \phi' >_{(z_2,1)} \right) \psi \; dt$$

$$- \int_0^T \dot{f}\dot{\psi} \; dt < z, \phi > + < \dot{p}, \phi > \psi|_0^T \; - \; \int_0^T \left(c_1^2 p'\phi|_0^{z_1-} + c_2^2 p'\phi|_{z_1+}^{z_2-} + c_1^2 p'\phi|_{z_2+}^1 \right) \psi \; dt$$

$$+ < z, \phi > \dot{f}\psi|_0^T = 0.$$

We may then substitute our boundary, interface, and initial conditions (7.4), as well as the conditions on ϕ and ψ, into the above equation to obtain

$$- \int_0^T < \dot{p}, \phi > \dot{\psi} \; dt$$

$$+ \int_0^T \left(c_1^2 < p', \phi' >_{(0,z_1)} \; + c_2^2 < p', \phi' >_{(z_1,z_2)} \; + c_1^2 < p', \phi' >_{(z_2,1)} \right) \psi \; dt$$

$$- \int_0^T \dot{f}\dot{\psi} \; dt < z, \phi > + c_1 \int_0^T \dot{p}(\cdot, 0)\phi(0)\psi \; dt - c_1^2 \int_0^T f(\cdot)\phi(0)\psi \; dt = 0.$$

This implies

$$- \int_0^T < \dot{p}, \phi > \dot{\psi} \; dt \; + \int_0^T < c^2(z)p', \phi' > \psi \; dt \; - \int_0^T \dot{f}\dot{\psi} \; dt < z, \phi >$$

$$+ c_1 \int_0^T \dot{p}(\cdot, 0)\phi(0)\psi \; dt - c_1^2 \int_0^T f(\cdot)\phi(0)\psi \; dt = 0.$$

This suggests that our weak solution with $p(0, z) = 0$ and $p(t, 1) = 0$ should satisfy

$$- \int_0^T < \dot{p}, \phi > \dot{\psi} \; dt \; + \int_0^T < c^2(z)p', \phi' > \psi \; dt \; - \int_0^T \dot{f}\dot{\psi} \; dt < z, \phi >$$

$$+ c_1 \int_0^T \dot{p}(\cdot, 0)\phi(0)\psi \; dt - c_1^2 \int_0^T f(\cdot)\phi(0)\psi \; dt = 0$$

for all $\phi \in H_R^1(0, 1)$ and for all $\psi \in H_R^1(0, T)$.

Thus, we seek solutions $p \in H_L^1(0, T; V)$, where $V \equiv H_R^1(0, 1)$, that satisfy

$$\begin{gathered} -\int_0^T <\dot{p},\phi>\dot{\psi}\ dt\ +\int_0^T <c^2(z)p',\phi'>\psi\ dt\ -\int_0^T \dot{f}\dot{\psi}\ dt<z,\phi> \\ +c_1\int_0^T \dot{p}(\cdot,0)\phi(0)\psi\ dt - c_1^2\int_0^T f(\cdot)\phi(0)\psi\ dt = 0 \end{gathered} \tag{7.7}$$

for all $\phi \in H_R^1(0,1)$ and for all $\psi \in H_R^1(0,T)$.

If we assume that our solutions have enough smoothness, i.e., $p(t,\cdot) \in \tilde{H}$ and $p(\cdot,z) \in H^2(0,T)$, we can verify that this is, in fact, a desired weak form of our equation. Assuming this smoothness and integrating the weak form by parts, we find

$$\int_0^T <\ddot{p},\phi>\psi\ dt$$

$$-\int_0^T \left(c_1^2 <p'',\phi>_{(0,z_1)} + c_2^2 <p'',\phi>_{(z_1,z_2)} + c_1^2 <p'',\phi>_{(z_2,1)}\right)\psi\ dt$$

$$+<z,\phi>\int_0^T \ddot{f}\psi\ dt + c_1\int_0^T \dot{p}(\cdot,0)\phi(0)\psi\ dt - c_1^2\int_0^T f(\cdot)\phi(0)\psi\ dt$$

$$-<\dot{p},\phi>\psi|_0^T - <z,\phi>\dot{f}\psi|_0^T$$

$$+\int_0^T \left(c_1^2 p'\phi|_0^{z_1-} + c_2^2 p'\phi|_{z_1+}^{z_2-} + c_1^2 p'\phi|_{z_2+}^1\right)\psi\ dt = 0$$

for all $\phi \in H_R^1(0,1)$ and for all $\psi \in H_R^1(0,T)$ with $p(0,z) = 0$ and $p(t,1) = 0$.

Then

$$\begin{aligned}
&\int_0^T < \ddot{p}, \phi > \psi \; dt - \int_0^T < c^2(z)p'', \phi > \psi \; dt + < z, \phi > \int_0^T \ddot{f}\psi \; dt \\
&+c_1 \int_0^T \dot{p}(\cdot, 0)\phi(0)\psi \; dt - c_1^2 \int_0^T f(\cdot)\phi(0)\psi \; dt + < \dot{p}(0, \cdot), \phi > \psi(0) \\
&- \int_0^T c_1^2 p'(\cdot, 0)\phi(0)\psi \; dt \\
&+ \int_0^T \left[\phi(z_1) \left(c_1^2 p'(\cdot, z_1-) - c_2^2 p'(\cdot, z_1+)\right)\right. \\
&\left.-\phi(z_2) \left(c_1^2 p'(\cdot, z_2+) - c_2^2 p'(\cdot, z_2-)\right)\right] \psi \; dt \\
&= 0
\end{aligned} \tag{7.8}$$

for all $\phi \in H_R^1(0,1)$ and for all $\psi \in H_R^1(0,T)$ with $p(0,z) = 0$ and $p(t,1) = 0$.

If we choose $\phi \in H_I^1(0,1) = \{\phi \in H^1(0,1) | \phi(0) = \phi(1) = 0, \; \phi(z_1) = \phi(z_2) = 0\} \subset H_R^1(0,1)$ and $\psi \in H_0^1(0,T) = \{\psi \in H^1(0,T) | \psi(0) = \psi(T) = 0\} \subset H_R^1(0,T)$, then we have

$$\int_0^T < \ddot{p}, \phi > \psi \; dt - \int_0^T < c^2(z)p'', \phi > \psi \; dt + < z, \phi > \int_0^T \ddot{f}\psi \; dt = 0$$

for all $\phi \in H_I^1(0,1)$ and for all $\psi \in H_0^1(0,T)$.

Since $\psi \in H_0^1(0,T)$ is arbitrary, this implies that

$$< \ddot{p}, \phi > - < c^2(z)p'', \phi > + \ddot{f} < z, \phi >= 0$$

for all $\phi \in H_I^1(0,1)$.

Hence, since $H_I^1(0,1)$ is dense in $L^2(0,1)$,

$$\ddot{p} - c^2(z)p'' + \ddot{f}z = 0$$

in the L^2 sense and hence almost everywhere.

We thus have that (7.8) reduces to

$$
\begin{aligned}
&c_1 \int_0^T \dot{p}(\cdot,0)\phi(0)\psi \; dt - c_1^2 \int_0^T f(\cdot)\phi(0)\psi \; dt + < \dot{p}(0,\cdot), \phi > \psi(0) \\
&- \int_0^T c_1^2 p'(\cdot,0)\phi(0)\psi \; dt \\
&+ \int_0^T \left[\phi(z_1)\left(c_1^2 p'(\cdot,z_1-) - c_2^2 p'(\cdot,z_1+)\right)\right. \\
&\left. -\phi(z_2)\left(c_1^2 p'(\cdot,z_2+) - c_2^2 p'(\cdot,z_2-)\right)\right]\psi \; dt \\
&= 0
\end{aligned}
\tag{7.9}
$$

for all $\phi \in H_R^1(0,1)$ and for all $\psi \in H_R^1(0,T)$.

Using standard arguments, we obtain from (7.9) the initial and boundary conditions

$$\dot{p}(0,z) = 0$$

$$\dot{p}(t,0) - c_1 p'(t,0) - c_1 f(t) = 0,$$

as well as the interface conditions

$$c_1^2 p'(t,z_1-) = c_2^2 p'(t,z_1+)$$

$$c_1^2 p'(t,z_2+) = c_2^2 p'(t,z_2-)$$

almost everywhere.

Hence, we have shown that if $p \in H^1(0,T;V)$ (which implies $p(t,\cdot)$ is continuous at z_1 and z_2) satisfies the weak form (7.7) and p possesses the additional smoothness $p(t,\cdot) \in \tilde{H}$ and $p(\cdot,z) \in H^2(0,T)$, then

$$\ddot{p} - c^2(z)p'' + z\ddot{f}(t) = 0 \text{ almost everywhere}$$

$$
\begin{array}{ll}
p(0,z) = 0 & \dot{p}(0,z) = 0 \text{ almost everywhere} \\
p(t,1) = 0 & \dot{p}(t,0) - c_1 p'(t,0) - c_1 f(t) = 0 \text{ almost everywhere} \\
 & \\
p(t,z_1-) = p(t,z_1+) & c^2(z_1-)p'(t,z_1-) = c^2(z_1+)p'(t,z_1+) \text{ almost everywhere} \\
p(t,z_2-) = p(t,z_2+) & c^2(z_2-)p'(t,z_2-) = c^2(z_2+)p'(t,z_2+) \text{ almost everywhere.}
\end{array}
$$

Thus the variational form (7.7) has been verified with the pointwise interface conditions at $z = z_1$ and $z = z_2$ being weakly satisfied whenever p is a solution of (7.7).

7.3 An approximate system with computational examples

In view of the weak formulation of the previous section for the system, we develop a dual finite element approximation to the solution. Since we have written the equations weakly in both time and space, it is natural to use a fully (time and space) Galerkin scheme.

Since we seek solutions $p \in H_L^1(0,T;V)$ with $V \equiv H_R^1(0,1)$ that satisfy the weak form, it is also natural to approximate p by a linear combination of piecewise linear basis elements in both time and space. That is,

$$p(t,z) \approx p^{MN}(t,z) = \sum_{i=1}^{M} \sum_{j=0}^{N-1} a_{ij} \psi_i(t) \phi_j(z), \tag{7.10}$$

where $\psi_i \in H_L^1(0,T)$ and $\phi_j \in H_R^1(0,1)$ are the standard piecewise linear spline functions.

We may substitute this approximation into our weak form to obtain defining equations for the coefficients a_{ij} given by

$$\sum_{i=1}^{M}\sum_{j=0}^{N-1} a_{ij}\Big\{ -\int_0^T \dot{\psi}_i\dot{\psi}\ dt < \phi_j, \phi > + \int_0^T \psi_i\psi\ dt < c^2(z)\phi_j', \phi' >$$

$$+c_1\int_0^T \dot{\psi}_i\psi\ dt\ \phi_j(0)\phi(0)\Big\} - \Big\{ < z, \phi > \int_0^T \dot{f}\dot{\psi}\ dt + c_1^2\int_0^T f\psi\ dt\ \phi(0)\Big\} = 0$$

for all $\phi \in H_R^1(0,1)$ and for all $\psi \in H_R^1(0,T)$. However this results in too many equations, but as usual, one restricts the families of ϕ and ψ for which we require the system to hold. In particular, we require it for $\phi = \phi_l \in H_R^1(0,1), l = 0, 1, \ldots, N-1$ and for $\psi = \psi_m(t) \in H_R^1(0,T), m = 0, \ldots, M-1$, where ϕ_l and ψ_m are piecewise linear spline functions. This yields the reduced system of equations

$$\sum_{i=1}^{M}\sum_{j=0}^{N-1} a_{ij}\Big\{ -\int_0^T \dot{\psi}_i\dot{\psi_m}\ dt < \phi_j, \phi_l > + \int_0^T \psi_i\psi_m\ dt < c^2(z)\phi_j', \phi_l' >$$

$$+c_1\int_0^T \dot{\psi}_i\psi_m\ dt\ \phi_j(0)\phi_l(0)\Big\} - \Big\{ < z, \phi_l > \int_0^T \dot{f}\dot{\psi_m}\ dt + c_1^2\int_0^T f\psi_m\ dt\ \phi_l(0)\Big\}$$

$$= 0$$

for each $l = 0, \ldots, N-1$, and for each $m = 0, \ldots, M-1$.

For each $j = 0, \ldots, N-1$, for each $i = 1, \ldots, M$, for each $l = 0, \ldots, N-1$, and for each $m = 0, \ldots, M-1$, we define

$$G_{lm}^{ij} = -\int_0^T \dot{\psi}_i\dot{\psi_m}\ dt < \phi_j, \phi_l > + \int_0^T \psi_i\psi_m\ dt < c^2(z)\phi_j', \phi_l' >$$

$$+c_1\int_0^T \dot{\psi}_i\psi_m\ dt\ \phi_j(0)\phi_l(0)$$

and for each $l = 0, \ldots, N-1$, and $m = 0, \ldots, M-1$, we define

$$H_{lm} = < z, \phi_l > \int_0^T \dot{f}\dot{\psi_m}\ dt + c_1^2\int_0^T f\psi_m\ dt\ \phi_l(0).$$

Thus, we can write our algebraic system of defining equations as

$$\sum_{i=1}^{M}\sum_{j=0}^{N-1} a_{ij}G_{lm}^{ij} = H_{lm}$$

for each $l = 0, \ldots, N-1$, $m = 0, \ldots, M-1$.

Next, for all $i = 1, \ldots, M$, we let

$$\vec{a}_i = [a_{i0} \quad a_{i1} \quad \cdots \quad a_{iN-1}],$$

and for all $i = 1, \ldots, M$; $l = 0, \ldots, N-1$; and $m = 0, \ldots, M-1$, we let

$$\vec{G}_{lm}^{i} = \begin{bmatrix} G_{lm}^{i0} \\ G_{lm}^{i1} \\ \vdots \\ G_{lm}^{iN-1} \end{bmatrix}.$$

Then for all $i = 1, \ldots, M$; $l = 0, \ldots, N-1$; and $m = 0, \ldots, M-1$,

$$\sum_{j=0}^{N-1} a_{ij}G_{lm}^{ij} = \vec{a}_i\vec{G}_{lm}^{i}.$$

So, for all $l = 0, \ldots, N-1$ and $m = 0, \ldots, M-1$,

$$\begin{aligned} \sum_{i=1}^{M}\sum_{j=0}^{N-1} a_{ij}G_{lm}^{ij} &= \sum_{i=1}^{M} \vec{a}_i\vec{G}_{lm}^{i} \\ &= \vec{a}_1\vec{G}_{lm}^{1} + \vec{a}_2\vec{G}_{lm}^{2} + \ldots + \vec{a}_M\vec{G}_{lm}^{M} \\ &= H_{lm}. \end{aligned}$$

Furthermore, we define

$$\alpha = [\vec{a}_1 \quad \vec{a}_2 \quad \cdots \quad \vec{a}_{M-1}]$$

$$\mathcal{G} = \begin{bmatrix} \vec{G}^1_{00} \cdots \vec{G}^1_{N-10} & \vec{G}^1_{01} \cdots \vec{G}^1_{N-11} & \cdots & \vec{G}^1_{0M-1} \cdots \vec{G}^1_{N-1M-1} \\ \vec{G}^2_{00} \cdots \vec{G}^2_{N-10} & \vec{G}^2_{01} \cdots \vec{G}^2_{N-11} & \cdots & \vec{G}^2_{0M-1} \cdots \vec{G}^2_{N-1M-1} \\ & \vdots & & \\ \vec{G}^M_{00} \cdots \vec{G}^M_{N-10} & \vec{G}^M_{01} \cdots \vec{G}^M_{N-11} & \cdots & \vec{G}^M_{0M-1} \cdots \vec{G}^M_{N-1M-1} \end{bmatrix}$$

and

$$\mathcal{H} = \begin{bmatrix} H_{00} \cdots H_{N-10} & H_{01} \cdots H_{N-11} & \cdots & H_{0M-1} \cdots H_{N-1M-1} \end{bmatrix}.$$

Thus we find that our finite element scheme can be written

$$\alpha \mathcal{G} = \mathcal{H} \tag{7.11}$$

and hence

$$\alpha = \mathcal{H}\mathcal{G}^{-1}.$$

As usual in finite element approximations, if we choose N, M sufficiently large, we expect that by computing α from (7.11), we can obtain coefficients a_{ij} such that

$$p^{MN}(t, z) = \sum_{i=1}^{M} \sum_{j=0}^{N-1} a_{ij} \psi_i(t) \phi_j(z)$$

is a good approximation for p on the time interval $[0, T]$. Thus the corresponding $\tilde{p}$ defined via (7.2) sufficiently approximates the behavior of the solution to (7.1). However, we find that in practice it is difficult to accurately approximate p over a given interval $[0, T_F]$ in one step due to the conditioning of the system (7.11) whenever T_F is large. (We discuss the details of the implementation later in this section.) Instead we first approximate p over a shorter interval $[0, t_1]$, where $t_1 < T_F$ and the windowed sine wave is *entirely within the material by the time* $t = t_1$. Note that we can change the time T in the weak form to accommodate any interval over which

we wish to solve. Then, since we can find a sufficient approximation for p over this smaller interval, we are able to accurately approximate $\tilde{p}$ and describe the pressure over the interval $[0, t_1]$.

In order to determine the behavior of the pressure on the entire given interval $[0, T_F]$, we need to describe the pressure on the interval $(t_1, T_F]$. This is equivalent to considering the original wave equation for pressure with boundary conditions given by a zero input at $z = 1$ and a no reflection condition at $z = 0$ but now initially there is a windowed sine wave already propagating through the material. The equations that govern this system are given by

$$\ddot{\tilde{y}} - c^2(z)\tilde{y}'' = 0$$

$$\begin{aligned} &\tilde{y}(0,z) = g(z) && \tilde{y}(t,1) = 0 \\ &\dot{\tilde{y}}(0,z) = h(z) && \dot{\tilde{y}}(t,0) - c_1\tilde{y}'(t,0) = 0 \end{aligned}$$

$$\begin{aligned} &\tilde{y}(t,z_1-) = \tilde{y}(t,z_1+) && c^2(z_1-)\tilde{y}'(t,z_1-) = c^2(z_1+)\tilde{y}'(t,z_1+) \\ &\tilde{y}(t,z_2-) = \tilde{y}(t,z_2+) && c^2(z_2-)\tilde{y}'(t,z_2-) = c^2(z_2+)\tilde{y}'(t,z_2+), \end{aligned}$$

where

$$g(z) = \tilde{p}(t,z)|_{t=t_1}, \qquad h(z) = \dot{\tilde{p}}(t,z)|_{t=t_1}.$$

Observe that we have a nonhomogeneous initial condition at $t = 0$. When using a semi-Galerkin finite element scheme, nonhomogeneous initial conditions are of little consequence, but this is not the case for fully Galerkin schemes. To treat this case, it is desirable to make another change of variables. To this end, we let

$$y(t,z) = \tilde{y}(t,z) + (t-1)g(z),$$

and the resulting equations for y are

$$\ddot{y} - c^2(z)y'' + c^2(z)(t-1)g''(z) = 0$$

$$\begin{aligned} &y(0,z) = 0 && y(t,1) = 0 \\ &\dot{y}(0,z) = h(z) + g(z) && \dot{y}(t,0) - c_1 y'(t,0) = 0 \end{aligned}$$

with the appropriate interface conditions and where $c(z)$, $g(z)$, and $h(z)$ are as defined previously, and we use that fact that $g'(0) = g(1) = g(0) = 0$ due to the location of the pressure impulse entirely within the material at $t = t_1$.

Using similar notation and techniques as before, we find that the weak form of our equation is

$$\begin{aligned} &- \int_0^T < \dot{y}, \phi > \dot{\psi} \; dt \; + \int_0^T < c^2(z) y', \phi' > \psi \; dt \\ &- \int_0^T (t-1)\psi \; dt < c^2(z) g', \phi' > - < h+g, \phi > \psi(0) \\ &+ \int_0^T c_1 \dot{y}(\cdot, 0) \phi(0) \psi \; dt = 0 \end{aligned} \tag{7.12}$$

for all $\phi \in H_R^1(0,1)$ and for all $\psi \in H_R^1(0,T)$ where $T = T_F - t_1$ with $y(0,z) = 0$ and $y(t,1) = 0$.

Thus, we seek solutions $y \in H_L^1(0,T;V)$, where $V \equiv H_R^1(0,1)$, that satisfy (7.12).

Given the weak form (7.12) of our equation, we can again approximate y by a linear combination of basis elements in time and space

$$y(t,z) \approx y^{MN}(t,z) = \sum_{i=1}^{M} \sum_{j=0}^{N-1} \gamma_{ij} \psi_i(t) \phi_j(z),$$

where $\psi_i \in H_L^1(0,T)$ and $\phi_j \in H_R^1(0,1)$ are piecewise linear spline functions. We note that in our computations M, N need not be the same as those for the approximation of p on the interval $[0, t_1]$, although we use the same notation here for ease of exposition.

Following the same procedure as before, we substitute the approximation into the weak form of our equation, finding that

$$\begin{aligned} &\sum_{i=1}^{M} \sum_{j=0}^{N-1} \gamma_{ij} \Big\{ - < \phi_j, \phi_l > \int_0^T \dot{\psi}_i \dot{\psi}_m \; dt \\ &+ \; < c^2(z) \phi_j', \phi_l' > \int_0^T \psi_i \psi_m \; dt + c_1 \phi_j(0) \phi_l(0) \int_0^T \dot{\psi}_i \psi_m \; dt \Big\} \\ &= \int_0^T (t-1) \psi_m \; dt < c^2(z) g', \phi_l' > + \; < h+g, \phi_l > \psi_m(0) \end{aligned}$$

holds for the piecewise linear spline functions $\psi_m \in H_R^1(0,T),\ m = 0,\ldots,M-1$, and $\phi_l \in H_R^1(0,1),\ l = 0,\ldots,N-1$. Then, as before, we can write these equations as a system

$$\Gamma\mathcal{G} = \mathcal{K}$$

where Γ contains the coefficients γ_{ij}, $\mathcal{G}$ is as defined previously, and $\mathcal{K}$ is analogous to the previously defined $\mathcal{H}$. This equation can be solved for the coefficient vector Γ, and the coefficients can in turn be used to determine approximations for y and $\tilde{y}$. Summarizing, we use

$$\begin{aligned} p(t,z) &\approx p^{M_pN_p}(t,z) = \sum_{i=1}^{M_p}\sum_{j=0}^{N_p-1} a_{ij}\psi_i(t)\phi_j(z) \quad \text{for } z\in[0,1],\quad t\in[0,t_1] \\ y(t,z) &\approx y^{M_yN_y}(t,z) = \sum_{i=1}^{M_y}\sum_{j=0}^{N_y-1} \gamma_{ij}\psi_i(t)\phi_j(z) \quad \text{for } z\in[0,1],\quad t\in[0,T_F-t_1] \end{aligned}$$

and

$$\begin{aligned} \tilde{p}^{M_pN_p}(t,z) &= p^{M_pN_p}(t,z) + zf(t) \quad \text{for } z\in[0,1],\ t\in[0,t_1] \\ \tilde{y}^{M_yN_y}(t,z) &= y^{M_yN_y}(t,z) - (t-1)g(z) \quad \text{for } z\in[0,1],\ t\in[0,T_F-t_1] \\ \tilde{p}^{M_pN_p}(t,z) &= \tilde{y}^{M_yN_y}(t-t_1,z) \quad \text{for } z\in[0,1],\ t\in[t_1,T_F] \end{aligned}$$

to define an appropriate approximation to the behavior of the wave on the spatial interval $[0,1]$ and the entire given time interval $[0,T_F]$.

Prior to presenting some solutions obtained from this approximation, we discuss briefly the implementation of these approximation techniques. The calculations were performed using code written in MATLAB, version 5.3 (The MathWorks, Inc., Natick, MA), and the computations were carried out on a Sun Sparc Ultra 10 workstation.

The coefficient vectors α and Γ were computed with MATLAB's *slash* command, which finds solutions by Gaussian elimination. We recall that the elements in $\mathcal{K}$ are

$$\int_0^T (t-1)\psi_m \, dt < c^2(z)g', \phi_l' > + \ < h+g, \phi_l > \psi_m(0).$$

Here, g represents $\tilde{p}^{M_p N_p}(t, \cdot)$ at a specified time t_1. As a result, we only have access to values of g at the nodal points, z_k. Furthermore, $h(z)$ represents $\dot{\tilde{p}}^{M_p N_p}(t, z)$ at t_1, but these values must be approximated at the appropriate spatial nodes. So, in order to compute the terms in $\mathcal{K}$, we must first numerically approximate $\dot{g}$ (which is the same as h) and g' from the known data points and then calculate the inner products. We use a centered difference method to approximate g' at the nodal points and a backward difference method to approximate $\dot{g}$ at the same points. Then we use linear interpolation via the MATLAB command *interp1* to obtain values for $g(z), g'(z)$, and $\dot{g}(z)$ at intermediate values z between the nodes. With these "enhanced" data sets, we can use the trapezoidal method, via MATLAB's *trapz* command, to compute the inner products.

Finally, we show plots to illustrate the behavior of the wave as it passes through the layered medium. Each of the plots in Figure 7.3 is a snapshot in time of the pressure in the medium for the parameters given in Table 7.1 with $M = N = 256$ basis elements. Looking at the snapshots sequentially, we can see the pressure wave move through the layers. The noise in front of and behind the wave is a result of approximation error and should not have significant impact on the electromagnetic interrogation process when used in the applications described in this thesis.

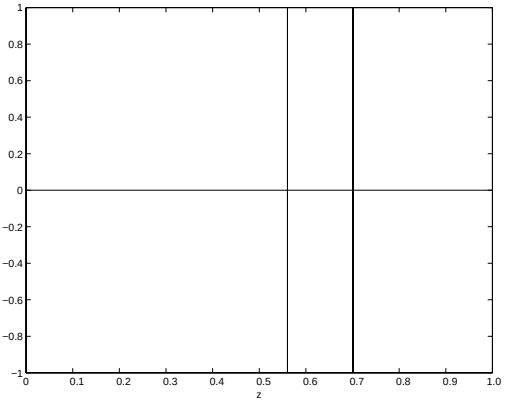

Figure 7.3(a):

Pressure vs depth – t=0

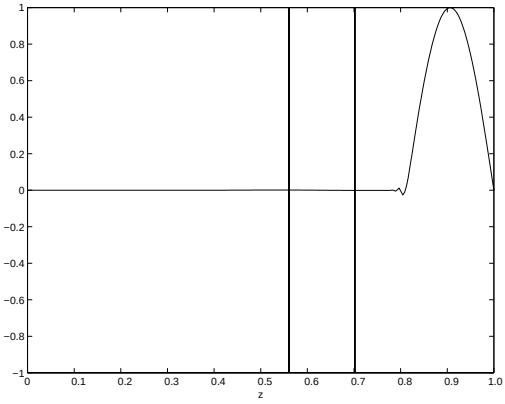

Figure 7.3(b):

Pressure vs depth – t=0.375

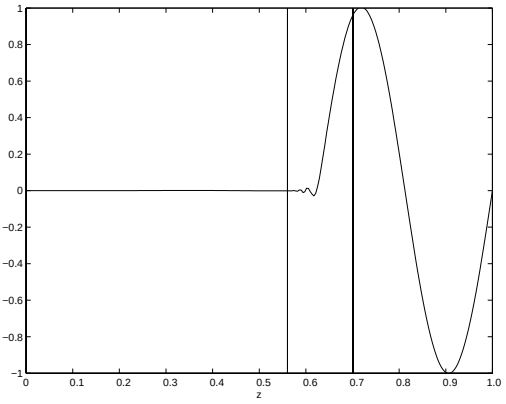

Figure 7.3(c):

Pressure vs depth – t=0.5

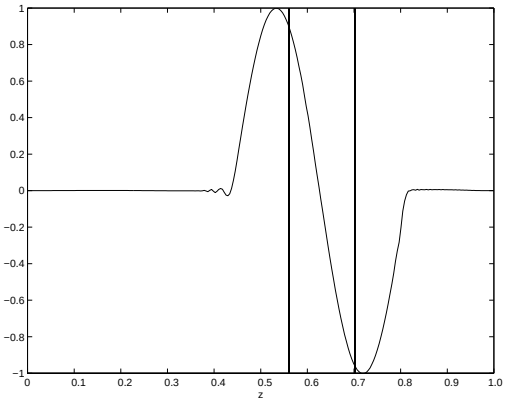

Figure 7.3(d):

Pressure vs depth – t=0.625

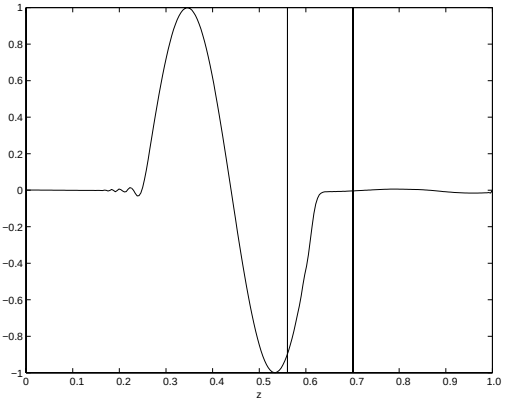

Figure 7.3(e):

Pressure vs depth – t=0.75

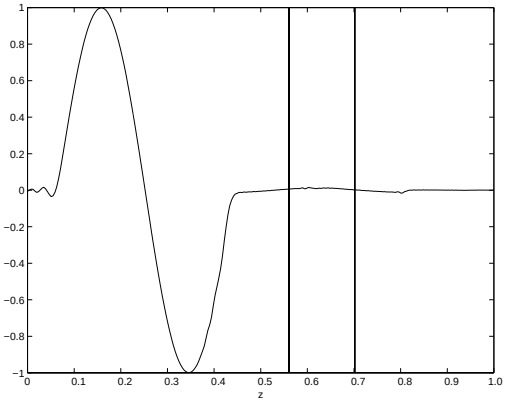

Figure 7.3(f):

Pressure vs depth – t=0.875

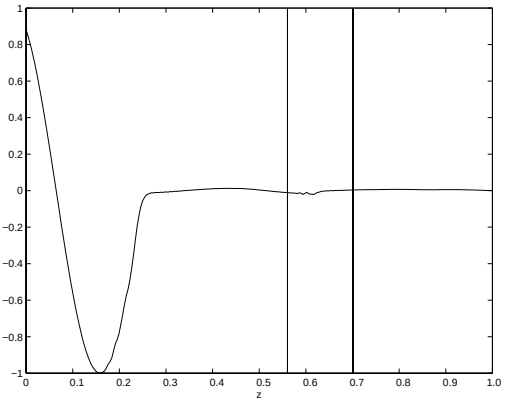

Figure 7.3(g):

Pressure vs depth – t=1.0

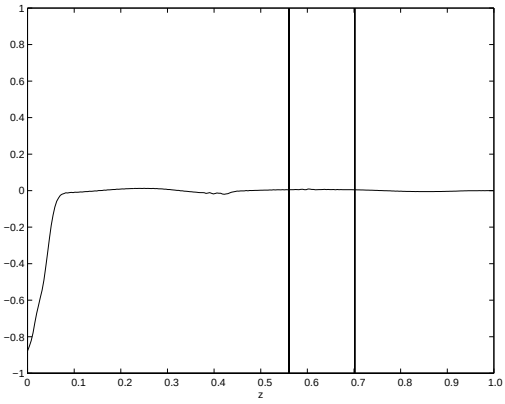

Figure 7.3(h):

Pressure vs depth – t=1.125

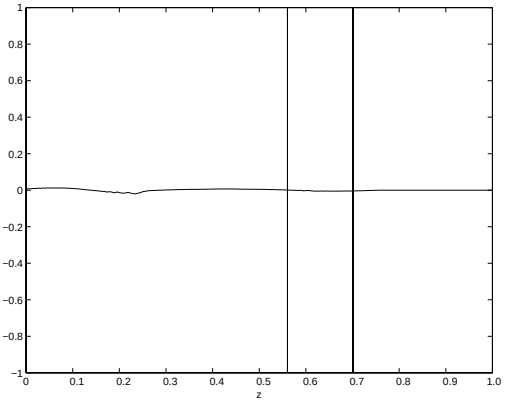

Figure 7.3(i):

Pressure vs depth – t=1.25

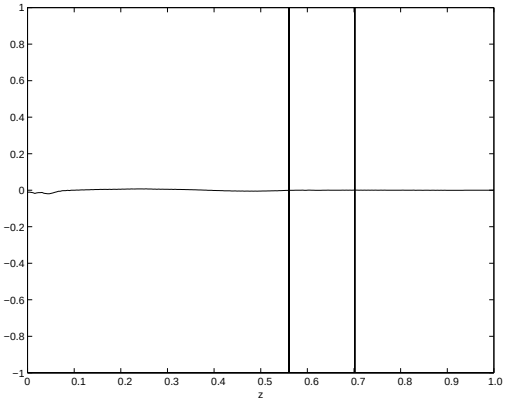

Figure 7.3(j):

Pressure vs depth – t=1.375

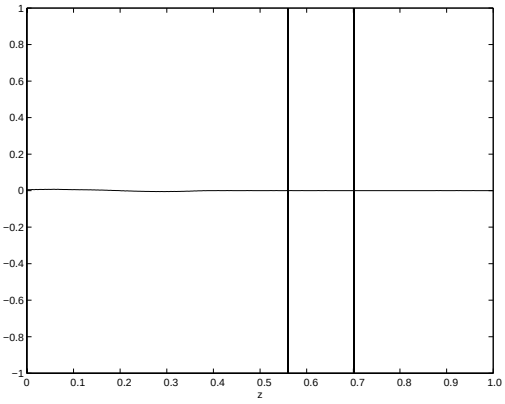

Figure 7.3(k):

Pressure vs depth – t=1.5

Parameter	Value
c_1	1.5
c_2	1.485
z_1	0.5605
z_2	0.7012
τ	0.25
t_1	0.5
T_F	1.5

Table 7.1: Parameter values for computations in Figure 7.3

To address approximation error, we compare solutions as the number of basis elements increases. In Figure 7.4, we see the solutions of pressure versus depth for a fixed time computed with varying number of basis elements. We see that as the number of basis elements increases from $N = M = 64$ (denoted by $\circ$) to $N = M = 128$ (denoted by $\times$) to $N = M = 256$ (denoted by $*$), the solutions appear to converge. Figure 7.5 gives the corresponding plots for solutions of pressure versus time at a fixed depth. Again, we see apparent convergence as the number of basis elements increases. This suggests that any error in the approximate solution is due to approximation error. The values of parameters used in these computations are given in Table 7.2. Moreover, Table 7.3 illustrates the convergence in norm we see as we increase the number of basis elements. The norms used to obtain the results given in the table are defined as follows

$$\begin{aligned} |f-g|_{l^\infty} &= \sup_k \sup_l |f(t_k,z_l)-g(t_k,z_l)| \\ |f-g|_{l^2} &= \left(\frac{1}{N_k N_l}\sum_k\sum_l (f(t_k,z_l)-g(t_k,z_l))^2\right)^{\frac{1}{2}}, \end{aligned}$$

where (t_k, z_l) are the nodal points of the piecewise linear elements $\{\psi_i\}, \{\phi_j\}$ of the

approximation (7.10) and N_k, N_l are the number of nodal points.

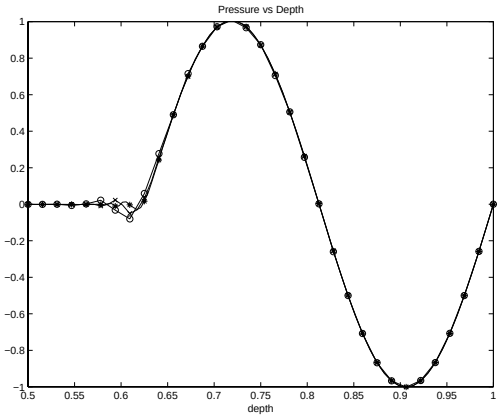

Figure 7.4(a):

Convergence of elements in depth

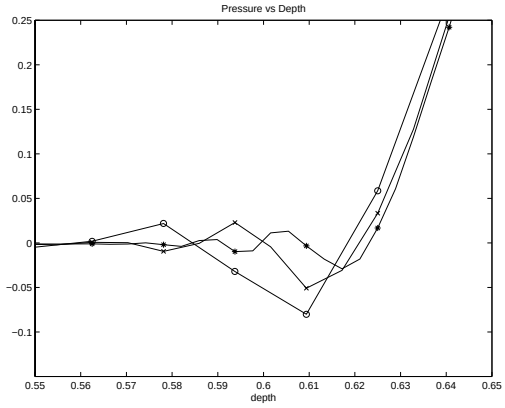

Figure 7.4(b):

A close-up of Figure 7.4(a)

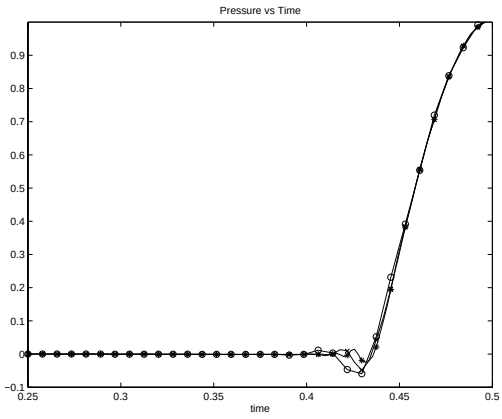

Figure 7.5(a):

Convergence of elements in time

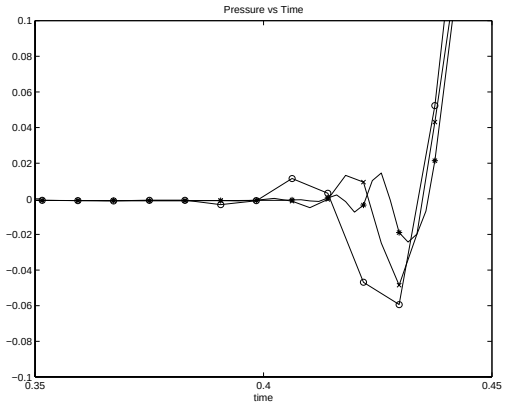

Figure 7.5(b):

A close-up of Figure 5(a)

Parameter	Value
c_1	1.5
c_2	1.485
z_1	0.5605
z_2	0.7480
τ	0.25
t_1	0.5
T_F	0.5

Table 7.2: Parameter values for computations in Figures 7.4 and 7.5

Norm	Value	Norm	Value
$\lvert\tilde{p}^{32,32} - \tilde{p}^{16,16}\rvert_{l^\infty}$	0.119126	$\lvert\tilde{p}^{32,32} - \tilde{p}^{16,16}\rvert_{l^2}$	0.048853
$\lvert\tilde{p}^{64,64} - \tilde{p}^{32,32}\rvert_{l^\infty}$	0.080170	$\lvert\tilde{p}^{64,64} - \tilde{p}^{32,32}\rvert_{l^2}$	0.032970
$\lvert\tilde{p}^{128,128} - \tilde{p}^{64,64}\rvert_{l^\infty}$	0.069472	$\lvert\tilde{p}^{128,128} - \tilde{p}^{64,64}\rvert_{l^2}$	0.025776
$\lvert\tilde{p}^{256,256} - \tilde{p}^{128,128}\rvert_{l^\infty}$	0.048119	$\lvert\tilde{p}^{256,256} - \tilde{p}^{128,128}\rvert_{l^2}$	0.021199

Table 7.3: Convergence in norm

Chapter 8

Concluding remarks and future directions

8.1 Concluding remarks

The focus of this thesis is an electromagnetic interrogation technique in which an acoustic pressure wave traveling within a target material acts as a virtual reflector for the interrogating microwave pulse. We consider this interrogation technique from several different perspectives, including physical, analytical, computational, and statistical, in an attempt to better understand its capabilities and limitations.

We first develop a physics-based mathematical model to describe the behavior of the electromagnetic/acoustic system underlying the interrogation technique. We use a one-dimensional form of Maxwell's equations to model the general electromagnetic dynamics and couple to it a polarization model which incorporates the electromagnetic/acoustic interaction. In the process of formulating this interaction model, we give a brief survey of some of the many models for electromagnetic/acoustic interaction found in the literature. In addition, we give an abbreviated discussion of the mechanisms behind electric polarization. We then present our choice of models, a Debye model for orientational polarization modified to incorporate pressure-dependence, and provide the rationale for this choice.

The resulting mathematical system can be generalized to include a wider class of electromagnetic systems. We examine this general system from a theoretical point of view and prove results regarding the well-posedness of the system and the convergence of approximating solutions to the system. These results are critical in developing a framework for the inverse problem related to the interrogation technique and in establishing confidence for the numerical simulations for the system with pressure-dependent Debye polarization.

With the theoretical results as a foundation, we construct numerical approximations to the solutions for the pressure-dependent Debye system. They provide a visual understanding of the systemic behavior over time, the sensitivity of the system to the polarization parameters, and the nature of the "data" that would be collected in an experiment. This newfound understanding is then applied to the problem of estimating the dielectric parameters from simulated data from the model (because true experimental data is not yet available). We find that we are able to successfully estimate many of the characteristic parameters from the dielectric, in particular the mean polarization parameters, from noisy data and with error in our initial guesses. Finally, we use statistical methods to verify that the pressure-dependence in the polarization model we have developed is in fact significant to the model. We test the null hypothesis that the model is pressure-independent using pressure-dependent data and pressure-independent data. In the case where the data does depend on pressure, we find that we cannot accept the null hypothesis. That is, we must reject the hypothesis that pressure-dependent data can be adequately predicted by a model without pressure-dependence. Our results using pressure-independent data, however, are less conclusive.

8.2 Future directions

There are numerous and varied directions in which the research presented here can be taken in the future. In this section, we propose some of the most feasibile, necessary, and, in our opinion, interesting.

8.2.1 Experimental design

The most imminent and eminant next step related to this research involves the construction of a laboratory experiment designed to demonstrate the scattering of electromagnetic waves by acoustic disturbances. The experimental configuration includes a guiding wave structure, or transmission line, within which electromagnetic waves will propagate. These waves will be launched at one end by a fast-rise-time pulse generator; meanwhile acoustic waves will be launched at the opposite end by an ultrasonic source. The proposed medium through which the waves will travel is an agar-agar gel, chosen due to its properties for electromagnetic and acoustic wave propagation as well as its commonalities with living tissue (as some potential applications involve biological imaging). Funds have already been procured to build this experiment, and the construction should commence shortly.

8.2.2 Acoustic pressure system

In Chapter 7, we present a system describing the dynamics of an acoustic pressure wave as it propagates through a layered medium. We derive a weak formulation for the system, suggest a computational approach to obtaining numerical solutions, and display results. We believe this system is well-posed, but these issues still need to be addressed.

8.2.3 A coupled electromagnetic/acoustic interaction model

For the electromagnetic system with pressure-dependent Debye polarization discussed in this paper, the polarization, and hence the electromagnetic field, depends on acoustic pressure. The pressure wave is given here *a priori* and is assumed to be invariant in the presence of the electric field. We believe that this assumption is reasonable in a first step in model development (such as is presented here). However, this assumption may not accurately describe the physics of the system; the pressure wave is likely modulated by the electromagnetic field and the polarization, and these effects should be taken into account. Thus it would be useful to develop a model for coupled electromagnetic/acoustic interaction. Not only would the development of a model for mutual interaction be an interesting and challenging task in understanding the physics of the system, but the coupled model would pose new analytical and computational issues as well (Is the coupled system well-posed? What is the best way to compute the electric field, the polarization, and the pressure wave simultaneously?).

8.2.4 Extension to higher dimensions

The problem presented here is one-dimensional. In order to formulate the problem in only one dimension, we must make several simplifying assumptions including assuming the homogeneity of the material in two directions. Since this is not a very practical supposition, the problem is more realistic when formulated in two or three dimensions. In our 1-D problem, we enforce an aborbing condition $\dot{E} - cE' = 0$ at the boundary $z = 0$ to prevent wave reflections from traveling back through the domain of interest. Boundary conditions of this type are not as easily implemented in more than one dimension. In [6], the authors solve a similar problem, one in which the electromagnetic waves are reflected from a perfectly-conductive backing, in two dimensions using perfectly-matched layers (PML) to absorb wave reflections from the

boundaries. A similar approach may be applicable to the electromagnetic/acoustic problem if one wanted to solve it in higher dimensions.

8.2.5 Reduced order models

Adding to the dimension or complexity of the current model will undoubtably result in an increase in computational time and storage. Thus it may be advantageous to explore methods of increasing computational efficiency. A possible approach is to use ideas from the Karhunan-Loeve or Proper Orthogonal Decomposition reduced order methodology. This methodology involves approximating the solution using only the basis functions that are most important in describing the system dynamics; thus it requires less basis functions than traditional methods. Approximations using this methodology have been successful in eddy current based electromagnetic interrogation techniques [12], [11], [10], and control design [8], [24], [34], [37].

List of References

[1] R. A. Albanese, J. Penn, and R. Medina, "Short-rise-time microwave pulse propagation through dispersive biological media", *J. Optical Society of America A* **6** (1989), pp. 1441-1446.

[2] J. C. Anderson, *Dielectrics*, Reinhold Publishing Company, New York, 1964.

[3] P. J. Antsaklis and A. N. Michel, *Linear Systems*, The McGraw-Hill Companies, Inc., New York, 1997.

[4] C. A. Balanis, *Advanced Engineering Electromagnetics*, John Wiley & Sons, New York, 1989.

[5] H. T. Banks, "Necessary conditions for control problems with variable time lags, *SIAM J. Control*, **6** (1968), pp. 9-47.

[6] H. T. Banks and B. L. Browning, "Time domain electromagnetic scattering using perfectly matched layers", in preparation.

[7] H. T. Banks, M. W. Buksas, and T. Lin, *Electromagnetic Material Interrogation Using Conductive Interfaces and Acoustic Wavefronts*, SIAM Frontiers in Applied Mathematics, Philadelphia, 2000.

[8] H. T. Banks, R. C. del Rosario, and R. C. Smith, "Reduded Order Model Feedback Control Design: Numerical Implementation in a Thin Shell Model", CRSC-TR98-27, NCSU, July 1998; *IEEE Trans. Auto. Control*, **45** (2000), pp. 1312-1324.

[9] H. T. Banks and B. G. Fitzpatrick, "Statistical methods for model comparison in parameter estimation problems for distributed systems", *Journal of Mathematical Biology*, **28** (1990), pp. 501-527.

[10] H.T. Banks, M.L. Joyner, B. Wincheski, and W.P. Winfree , "Electromagnetic interrogation techniques for damage detection", CRSC-TR01-15, NCSU, June 2001; *Proceedings Electromagnetic Nondestructive Evaluation 2001*, Kobe, Japan, May 18-19, 2001, IOS Press, Amsterdam, (2002), to appear.

[11] H.T. Banks, M.L. Joyner, B. Wincheski, and W.P. Winfree , "Real time computational algorithms for eddy current based damage detection", CRSC-TR01-16, NCSU, June 2001; *Inverse Problems*, to appear.

[12] H.T. Banks, M.L. Joyner, B. Wincheski, and W.P. Winfree, "Nondestructive evaluation techniques using a reduced order computational methodology", ICASE Technical Report 2000-10, NASA Langley Research Center, March 2000; *Inverse Problems*, **16** (2000), pp. 929-945.

[13] H. T. Banks and T. Lin, "Determining the structure of a biological medium using acousto-optic probes", *J. Inv. Ill-Posed Problems*, **7** (1999), pp. 61-82.

[14] H. T. Banks, C. J. Musante, and J. K Raye, "Approximate methods for inverse problems governed by nonlinear parabolic systems", *Numerical Functional Analysis and Optimization*, **21** (2000), pp 791-816.

[15] H. T. Banks and J. K. Raye, "Well-posedness for systems representing electromagnetic/ acoustic wavefront interaction", CRSC-TR01-34, December 2001; *ESIAM: Control, Optimization, and Calculus of Variations*, to appear

[16] H. T. Banks, J. K. Raye, and R. A. Albanese, "Non-Destructive Evaluation of Materials Using Pulsed Microwave Interrogating Signals and Acoustic Wave Induced Reflections", in preparation.

[17] H. T. Banks and J. K. Raye, "Computational methods for nonsmooth acoustic systems", CRSC-TR01-02, NCSU, January 2001; *Computational and Applied Mathematics*, to appear.

[18] H. T. Banks and J. K. Raye, "Computational methods for nonsmooth acoustic systems arising in an electromagnetic hysteresis identification problem", *Proceedings of the 18th ASME Biennial Conference on Mechanical Vibration and Noise*, Pittsburgh, PA, September 9-12, 2001, to appear.

[19] H. T. Banks, R. C. Smith, and Y. Wang, *Smart Material Structures: Modeling, Estimation, and Control*, J. Wiley & Sons, Chichester, 1996.

[20] H. T. Banks and J. Zhou, "Regularity and approximation of systems arising in electromagnetic interrogation of dielectric materials", *Num. Func. Analysis and Optimization*, **20** (1999), pp. 609-627.

[21] G. K. Batchelor, *An Introduction to Fluid Dynamics*, Cambridge University Press, Cambridge, 1967.

[22] R. W. Boyd, *Nonlinear Optics*, Academic Press, San Diego, 1992.

[23] S. R. deGroot and P. Mazur, *Non-equilibrium Thermodynamics*, North-Holland Publishing Company, Amsterdam, 1962.

[24] R. C. del Rosario, *Computational Methods for Feedback Control in Structural Systems*, Ph.D. Thesis, North Carolina State University, 1998.

[25] T. Dupont, "L^2 estimates for Galerkin methods for second order hyperbolic systems", *SIAM Journal on Numerical Analysis*, **10** (1973), pp. 880-889.

[26] R. S. Elliott, *Electromagnetics: History, Theory, and Applications*, IEEE Press, New York, 1993.

[27] L. C. Evans, *Partial Differential Equations*, American Mathematical Society, Providence, 1998.

[28] C. A. J. Fletcher, *Computational Galerkin Methods*, Springer-Verlag, Berlin, 1984.

[29] F. Franks, *Water A Comprehensive Treatise*, Plenum Press, New York, 1972.

[30] E. H. Grant, R. J. Sheppard, and G. P. South, *Dielectric Behavior of Biological Models in Solution*, Clarendon Press, Oxford, 1978.

[31] J. B. Hasted, *Aqueous Dielectrics*, Chapman and Hall, London, 1973.

[32] J. D. Jackson, *Classical Electrodynamics*, John Wiley & Sons, New York, 2nd edition, 1975.

[33] C. T. Kelley, *Iterative Methods for Optimization*, SIAM Frontiers in Applied Mathematics, Philadelphia, 1999.

[34] G. M. Kepler, H. T. Tran, and H. T. Banks, "Reduced Order Model Compensator Control of Species Transport in a CVD Reactor," CRSC-TR99-15, April 1999; *Optimal Control: Applications and Methods*, **21** (2000), pp. 143-160.

[35] D. K. Kondepudi and I. Prigogine, *Modern Thermodynamics From Heat Engines to Dissipative Structures*, John Wiley & Sons, New York, 1998.

[36] J. Lund and K. L. Bowers, *Sinc Methods for Quadrature and Differential Equations*, SIAM, Philadelphia, 1992.

[37] H. V. Ly and H. T. Tran, "Proper Orthogonal Decomposition for Flow Calculations and Optimal Control in a Horizontal CVD Reactor", CRSC-TR98-13, March 1998; *Quart. Applied Math*, submitted.

[38] N. H. March and M. P. Tosi, *Atomic Dynamics in Liquids*, Dover, New York, 1976.

[39] P. M. Morse and K. U. Ingard, *Theoretical Acoustics*, The McGraw-Hill Companies, Inc., New York, 1968.

[40] R. H. Nochetto and C. Verdi, "Approximations of degenerate parabolic problems using numerical integration, *SIAM Journal on Numerical Analysis*, **25** (1988), pp. 784-814.

[41] J. A. Stratton, *Electromagnetic Theory*, The McGraw-Hill Companies, Inc., New York, 1941.

[42] J. H. Van Vleck, *The Theory of Electric and Magnetic Susceptibilities*, Oxford University Press, London, 1931.